Tomas Bata University in Zlín
Faculty of Technology

Doctoral thesis

Engineering of Polymer Magnetic Composites with Controlled Electromagnetic Properties

Inženýrství polymerních magnetických kompozitů s regulovatelnými elektromagnetickými vlastnostmi

Vladimir Babayan

December 2012

Zlín, Czech Republic

Doctoral study programme: P2808 Chemistry and Materials Technology
2808V006 Technology of Macromolecular Substances

Supervisor: Assoc. Prof. Natalia Kazantseva, Ph.D.

Consultants: Assoc. Prof. Jarmila Vilčaková, Ph.D., Ing. Robert Moučka, Ph.D.

CONTENTS

ABSTRACT

The present doctoral thesis is devoted to the development of magnetic materials with controlled electromagnetic properties in the radiofrequency band with a view to design radio absorbing materials.

The objects of investigation are polymer magnetic composites based on magnetic particles with «core-shell» structure. These materials are synthesized by oxidative polymerization of aniline in the presence of multi-domain MnZn ferrite particles using strong and weak oxidants. In this case, polyaniline film grows on the surface of ferrite during the synthesis, and its structure is formed under the influence of magnetic interactions of paramagnetic aniline oligomers and ferrite. It is shown that the electromagnetic properties of MnZn–PANI composites can be controlled by changing the properties of polyaniline coating (thickness, density, and conductivity) through the choice of the reaction conditions and the post-polymerization treatment of PANI overlayer. Magnetoelastic stresses in ferrite particles, which cause the growth of the magnetic anisotropy and thereby lead to an increase in coercivity and thermomagnetic stability and a shift of the magnetic dispersion region toultra-high frequency band, are the main factor providing a controllable variation in properties. As a result, single-layer radio absorbers with different range of operating frequencies are proposed.

The magnetic properties of polyaniline in different oxidation and protonation states are also investigated. The ferromagnetic properties of protonated pernigraniline, which is characterized by high content of spins, are established and analyzed with a view to finding a possible mechanism of magnetic ordering in polyaniline. The last results are important for the development of organic magnets.

Keywords: polymer magnetic composites, conducting polymers, ferrites, core-shell particle structure, organic magnets, radio absorbers.

SOUHRN

Předkládaná doktorská práce je věnována vývoji magnetických materiálů s regulovatelnými elektromagnetickými vlastnostmi v radiofrekvenční oblasti, jež našly uplatnění jako radioabsorpční materiály.

Předmětem výzkumu jsou polymerní magnetické kompozity na bázi magnetických částic se strukturou «jádro-slupka». Syntéza těchto materiálů mechanismem oxidační polymerizace anilínu v přítomnosti multi-doménových částic MnZn feritu pomocí silných a slabých oxidantů. Během syntézy roste vrstva polyanilínu přednostně na povrchu feritu a její struktura se vytváří vlivem magnetických interakcí mezi paramagnetickými anilínovými oligomery a feritem. Dále je v práci ukázáno, že elektromagnetické vlastnosti kompozitů MnZn-PANI lze kontrolovat obměnou parametrů polynilínové vrstvy (tloušťka, hustota, vodivost), jež se dá dosáhnout změnou reakčních podmínek či post-polymerizačním úpravou vrstvy PANI. Jsou to především magnetoelastická napětí uvnitř částic feritu, která způsobují nárůst magnetické anisotropie a takto vedou ke zvýšení koercitivity, termomagnetické stability a posuvu magnetické disperzní oblasti do vysokých frekvencí, jež umožňují kontrolovatelně měnit vlastnosti kompozitu. Výsledkem jsou pak návrhy jednovrstvých absorbérů s různými rozsahy operačních frekvencí.

Stejně tak se práce zabývá magnetickými vlastnostmi polyanilínu v jeho různých oxidačních a protonovaných stavech. Jsou zavedeny a s ohledem na nalezení možného mechanismu magnetické organizace v polyanilínu také analyzovány feromagnetické vlastnosti protonovaného pernigranilinu, pro nějž je charakteristický vysoký obsah spinů. Tyto výsledky jsou přínosné pro vývoj organických magnetů.

Klíčová slova: polymerní magnetické kompozity, vodivé polymery, ferity, částice se strukturou jádro-supka, organické magnety, radioabsorbéry

ACKNOWLEDGEMENTS

Here is my chance to extend immense gratitude to those who made this work possible.

First and foremost, I owe a debt of gratitude to my supervisor assoc. prof. Natalia Kazantseva for providing me the tremendous opportunity to join her research group and for her invaluable guidance, willingness to share knowledge and experience, constant support and encouragement during the entire period of my Ph.D. studies.

I am greatly indebted to my consultants assoc. prof. Jarmila Vilčáková and Dr. Robert Moučka for their time, interest and invaluable technical assistance throughout the course of the work. I am deeply grateful to prof. Yuri Kazantsev whose extraordinary support, guidance and conclusive remarks had a remarkable impact on my research.

I would like to express my sincere gratitude to prof. PetrSáha for giving me the opportunity to pursue my studies at Polymer Centre and for creating an excellent research environment. The help and support of the colleagues from Polymer Centre is also highly appreciated.

Furthermore I would like to thank the coauthors of my publications, in particular Dr. Irina Sapurina and Dr. Jaroslav Stejskal for their cooperation as well as the reviewers of this doctoral thesis and Dr. Ivan Nikitin for proofreading of my manuscripts.

I cannot finish without acknowledging how eternally grateful and thankful I am to my exceptionally loving family whose blessings and nurture pave every step of my way.

ABBREVIATIONS AND SYMBOLS

AC	Alternating Current
BAR	Bruggeman Asymmetric Rule
BM	Bergman-Milton
BSR	Bruggeman Symmetric Rule
CI	Carbonyl Iron
DC	Direct Current
DW	Domain Wall
EMT	Effective Medium Theory
HO	High-oriented
LE	Liquid Elastomer
LLL	Landau-Lifshitz-Looyenga
MBAR	Modified Bruggeman Asymmetric Rule
MG	Maxwell-Garnet
MR	Magnetization Rotation
MU	Musal
NFR	Natural Ferromagnetic Resonsnce
PANI	Polyaniline
PMC	Polymer Magnetic Composite
PPy	Polypyrole
PU	Polyurethane
PVS	Polder-van-Santen
RA	Radio absorber
RAM	Radio absorbing material
TP	Thermoplastic
TS	Thermoset
UHF	Ultra High Frequency
μ_0	Magnetic constant (permeability of vacuum)

μ	Complex magnetic permeability
μ'	Real part of complex magnetic permeability
μ''	Imaginary part of complex magnetic permeability
μ_{eff}	Effective magnetic permeability of composite
μ_i	Magnetic permeability of inclusion particles
μ_h	Permeability of host matrix
μ_a	Absolute magnetic permeability
μ_r	Relative magnetic permeability
χ_{eff}	Effective magnetic susceptibility of composite
χ_i	Magnetic susceptibility of inclusion particles
ε	Complex dielectric permittivity
ε_{eff}	Effective dielectric permittivity of composite
γ	Gyromagnetic ratio
σ	Tensile strength
ρ	Density
ε_b	Elongation at break
$tan\delta$	Dissipation factor
$B(n)$	Spectral function
c	Velocity of light
C_P	Percolation threshold
d_0	Matching thickness of radio absorber
f	Frequency of electromagnetic field
f_0	Matching frequency of radio absorber
f_r	Resonance frequency
H	Strength of magnetic field
H_C	Coercive field
H_{DC}	DC magnetizing field
H_A	Magnetic anisotropy field

H_θ	Out of plane magnetic anisotropy
H_φ	In plane magnetic anisotropy
H_d	Demagnetizing field
H_e	Strength of the magnetic component of the applied electromagnetic field
H_i	Strength of the magnetic component of internal field acting on magnetic composite
L	Loading factor
n_0	Shape factor of inclusion particles
p	Volume fraction of filler particles
$\widehat{N}_\mathrm{M}$	Tensor of demagnetization factors
N_d	Shape demagnetization factor
N_ex	External demagnetization factor
N_i	Inner demagnetization factor
R	Reflection coefficient
T	Temperature
T_g	Glass transition temperature
ΔT	Operating temperature range
Z_0	Impedance of free space
Z	Input impedance

LIST OF FRAMING PAPERS

PAPER I

BABAYAN, V., KAZANTSEVA, N. E., MOUCKA, R., SAPURINA, I., SPIVAK, Y.M., MOSHNIKOV, V.A. Combined effect of demagnetizing field and induced magnetic anisotropy on the magnetic properties of manganese–zinc ferrite composites. *J. Magn. Magn.Mater.*2012, vol. 324, no. 2, p. 161-172.

PAPER II

BABAYAN, V., KAZANTSEVA, N. E., SAPURINA, I., MOUCKA, R., VILCAKOVA, J., STEJSKAL, J. Magnetoactive feature of in-situ polymerized polyaniline film developed on the surface of manganese–zinc ferrite. *Appl. Surf. Sci*. 2012, vol. 258, no. 19, p. 7707–7716.

PAPER III

BABAYAN, V., KAZANTSEVA, N. E., SAPURINA, I., MOUCKA, R., STEJSKAL, J., SÁHA, P. Increasing the high-frequency magnetic permeability of MnZn ferrite in polyaniline composites by incorporating silver. Submitted for publication to *J. Magn.Magn.Mater*. (manuscript number MAGMA-D-12-00986R1).

PAPER IV

KOMPAN, M. E., SAPURINA, I. Yu., BABAYAN, V., KAZANTSEVA, N. E. Electrically conductive polyaniline–molecular magnet with the possibility of chemically controlling the magnetic properties. *Phys. Solid State* 2012, vol. 54, no. 12, p. 2412-2418.

1. INTRODUCTION

Magnetic composite materials, usually prepared with ferro- and ferrimagnetic particles embedded in a polymer matrix, are widely used in electronic devices and systems, such as magnetic substrates for microwave antennas, microwave inductors, radio-absorbing materials, etc. [1-7]. A field of application of a polymer magnetic composite (PMC) determines the requirements on the initial permeability (μ_i), the level of magnetic losses, and the operating frequency range. Thus, the desirable properties for PMCs used in high-frequency devices are high initial permeability (μ_i~ 10-100) and low losses in a wide frequency range. In contrast, PMCs used as radio absorbing materials (RAMs) should have high permeability and high magnetic losses in the operating frequency range.

PMCs offer a significant advantage over bulk magnetic materials because of the possibility to design materials with high values of permeability in an ultrahigh frequency (UHF) band. The unique property of PMCs is that one can control the values of complex permeability and the position of the permeability dispersion region on the frequency scale by choosing the type of magnetic filler, its concentration in a polymer and also by varying the shape, size and microstructure of particles. Attempts are also made to control the magnetic properties of the composites through its microstructure. The main problem with the development of PMCs is the necessity to maintain the physical and mechanical properties of a PMC, which restricts the volume content of the magnetic filler. Hence, new methods that would allow one to obtain enhanced values of high-frequency permeability in highly-filled PMCs are necessary.

There are a few techniques that permit to obtain higher values of permeability in a PMC: the use of multicomponent filler [8-13]; the use of multicomponent magnetic particles [14-17]; and the formation of magnetic texture in a composite by orienting shape-anisotropic magnetic particles by an external magnetic field, or during forge rolling (magnetic elastomers), or by orientational drawing (magnetic fibers) [18, 19].

A remarkable advantage of PMCs filled with multicomponent (core-shell) magnetic particles, such as low-anisotropy spinel-type ferrites coated by conducting polymers (polyaniline, PANI, or polypyrrole, PPy), is that they allow one to regulate the frequency dependence of permeability and permittivity by changing the conductivity and the thickness of the conducting polymer overlayer (shell) [17, 18, 20]. From the practical viewpoint, it is important that the thickness of the polymer shell and its conductivity can be controlled by altering

the reaction conditions, in particular, the concentration of the reactants in the reaction medium and its temperature [21-23]. For instance, in [23], the pH of the reaction medium is considered to be the most important parameter of the synthesis, which has a decisive influence on both the molecular and supramolecular structure of PANI and, consequently, on its conductivity.

Although the main factors influencing the electromagnetic parameters of composites containing ferrite particles with conducting coating are known (the thickness and the conductivity of polymer shell), the physical mechanisms responsible for the changes in their magnetic properties have not yet been fully understood. Being aware of these issues is an important step towards the development of methods for the controlled synthesis of multicomponent magnetic particles and composites with desired electromagnetic properties.

2. BASIC COMPONENTS OF POLYMER MAGNETIC COMPOSITES: MATERIALS SELECTION

The design of PMCs, especially highly filled ones, requires that one should achieve a particular balance between the processing ability and the properties of composites for a given range of applications. The primary purpose of the polymer matrix in magnetic composites is to bind the filler particles together owing to its cohesive and adhesive characteristics, while the filler particles are responsible for the electromagnetic properties of the composite. The physical, mechanical, and electromagnetic properties of a composite significantly depend on how uniformly the filler particles are distributed in a polymer. There are two main factors that influence the particles distribution in a polymer, namely, the filler–filler and the filler–matrix interactions. Thus, the selection of materials and their compatibility are crucial for the design of PMCs.

Polymers can generally be classified as thermoplastics and thermosets. In order to fabricate polymer-based composites, melted thermoplastics are mixed with filler and then processed into a final product, whereas filled thermosets must undergo further polymerization to complete crosslinking reactions of composite solidification. Many factors influence the processing operation, namely, viscosity, the orientation of heterogeneous phases, and the rate of the reactions. Among these factors, viscosity is the most crucial one for processing. Viscosity strongly depends on the chemical nature of the polymer (molecular weight and its distribution, molecular structure of the polymeric chains, degree of crystallinity, etc.). Moreover, viscosity also depends on the processing parameters, such as temperature and shear rate. Therefore, the study of rheological properties of polymers filled with magnetic particles is very important for choosing a proper condition for processing composites with the optimal balance between mechanical and physical properties.

The processing of PMCs utilizes the same techniques as polymer processing, which include injection molding, compression molding, and extrusion. Compression molding is the most extensively used method in the research study due to the simplicity of operation and flexibility regarding the polymer matrix selection. Injection molding is used for processing PMCs based on thermoplastics with the necessary pre-condition for thoroughly mixing raw materials. The extrusion method allows one to produce composite materials with a magnetic filler content of up to 80% vol., the value impossible with other technologies. To this end, high-oriented thermoplastics are used, e.g., ultrahigh

molecular weight polyethylene. In such a case, PMCs can be produced using the melts or solutions (gel-spinning technology) of thermoplastics.

2.1. Polymers

The characteristics of typical polymers used in the preparation of highly filled PMCs are described in Table 1, whereas Table 2 contains their advantages and limitations [24]. The symbols and abbreviations used in Table 1 are as follows: ρ – density; T– temperature; T_g– glass-transition temperature; ΔT –operating temperature range; σ – tensile strength; ε_b– elongation at break; $\tan\delta$ –dissipation factor; TP–thermoplastic, TS–thermoset, LE–liquid elastomer, HO–high-oriented.

2.2. Magnetic fillers

The most widespread magnetic fillers in PMCs used for radio absorbers are soft magnetic ferrites, carbonyl iron (CI) powders, and, more rarely, ferromagnetic alloys (alsifer, permalloy, etc.), which are characterized by high saturation magnetization, high initial magnetic permeability, wide range of electrical properties, etc. Among all types of magnetic materials, only CI is produced in powder form, other fillers are obtained by high-energy milling. Thus, the magnetic properties of powders are a function of their chemical composition and melting practice also.

The main advantage of CI is that, by varying its type (chemical composition, particle shape and size, and microstructure), one can obtain a broad region of magnetic permeability dispersion in the RF and microwave bands [25-31]. The second advantage is the availability of CI, which is produced all over the world. On the other hand, CI is not chemically stable due to the high content of α-iron (97–99 wt. %); this especially applies to processed types of CI produced by chemical or mechanical treatment of primary CI with a view to improving their magnetic properties. Primary and processed CI powders differ radically in the particle microstructure, which determines the electromagnetic properties of CI-filled composites, including their storage and thermal stability [25, 29, 31, 32].

Soft ferrites have significant advantages over metallic ferromagnets and CI in high resistivity, high chemical stability, and the capability of withstanding

Table 1.Physical and mechanical properties of polymers.

Type	Polymer	ρ (g cm^{-3})	T_g (ºC)	ΔT (ºC)	σ (MPa)	ε_b (%)	Hardness (shore A)	Dielectric constant	tanδ (1 kHz)
TP	Polyisoprene	0.91	-70	-54–90	4.5	650	75–90	2.37–2.45	0.0001–0.0003
	Chloroprene	1.25	-45	-40–100	25–38	500	70	6.5–8.1	0.03–0.086
	Butadiene-acrylonitrile	0.9–1.01	-60	-50–150	1.4–3.0	650	75–80	2.51	0.0009
	Poly(chlorotrifluoroethylene)	2.1–2.14	–	-240–150	30–40	80–250	75–80	2.2–2.8	0.02–0.03
	Polysiloxane	1.1–1.6	-70–95	-55–225	350	900	30–50	2.65–3.10	0.01–0.02
	Polyurethane	1.1–1.6	-70–140	-55–140	500	750	80–90	2.8–3.25	0.01–0.02
TS	Epoxy resin	1.1–1.4	-55	-35–140	22.7–72.3	3–4	60–76	2.8–5.6	0.008–0.09
LE	dimethylsiloxane	1.05	-127	-60–370	6.2	100	60–70	2.2	0.001
	Polyurethane diisocyanate	1.0	-43–117	-70–140	500	3	80	2.8–3.25	0.01–0.02
HO	PE (ultra high molecular weight)	1.3–1.5	melting T: 137	Upper T: 55–95	20–40	500	50–70	2.3	0.0002–0.0005
	Ftorlon (copolymer of tetraflourethylene and vinyliden chloride)	1.8–2.0	Amorphous regions: 120 crystal regions: 327	-60–120	39–55	400–500	29–39	2	0.0002

Table 2.The advantages and limitations of polymers.

Polymer	Advantages	Limitations
Polyisoprene	Outstanding resilience; high tensile strength; superior resistance to tear and abrasion; good low-temperature flexibility	Fair resistance to heat, ozone, and sunlight; little resistance to oil, benzene, and hydrocarbon solvents
Chloroprene	Very good resistance to weather, ozone, and natural aging; good resistance to abrasion and flex cracking; moderate resistance to oil and benzene	Fair resistance to aromatic and oxygenated solvents; limited low-temperature flexibility
Butadiene-acrylonitrile	Excellent resistance to oil and benzene; superior to petroleum- based hydraulic fluids; good high-temperature performance; good resistance to sunlight and oxidation	Poor resistance to oxygenated solvents
Poly(chlorotrifluoroethylene)	Excellent resistance to oil, benzene, hydraulic fluids, and hydrocarbon solvents; very good heat resistance; very good resistance to weather, oxygen, ozone, and sunlight	Poor resistance to tear and cut growth
Polysiloxane	Resistance to oxidation, ozone, and weathering corona; high tensile strength; high tear strength; low cure shrinkage; properties constant with temperature; high dielectric strength; excellent resistance to heat aging	Poor adhesion to metals and other substrates
Polyurethane	Excellent resistance to oil, solvents, oxidation, and ozone; excellent wear, tear, and chemical resistance; fair electrical; excellent adhesion; reverts in humidity	Significant dependence of physical mechanical properties upon temperature gradient
Epoxy resin	Excellent adhesion; low shrinkage; high strength; shape stability; resistance to solvents; strong bases and hot water	Sacrifice of properties for high flexibility
Dimethylsiloxane	Outstanding heat resistance; excellent flexibility at low temperature; excellent resistance to weather, ozone, sunlight, and oxidation; the loss tangent is very low (tan $\delta < 0.001$)	Fair resistance to oil benzene and solvents; poor resistance to abrasion, tear, and cut growth
Polyurethane diisocyanate	Outstanding resistance to tear and abrasion; high tensile strength and elongation; good weather resistance; good resistance to oil and benzene	Poor resistance to acids and alkalis; inferior resistance to hot water
PE (ultra high molecular weight)	High mechanical strength that allows one to apply, for example, the method of orientation drawing and roll-milling to the processing of highly filled composites	Poor contact wear resistance
Ftorlon	High mechanical strength, chemical and radiation resistance, resistance to atmospheric effects; very low water absorption (lower than 0.1% for 24 h), therefore, its dielectric properties weakly depend on the atmospheric humidity; high content of amorphous phase and the flexibility of the molecular chain make it possible to reach high values of the filling factor (up to 60 vol.%) in the composites	Poor wearing property, thus need of reinforcing agent

intense electromagnetic fields. There are two classes of ferrites that can be used for absorbing materials, namely spinel ferrites and hexagonal ferrites.

2.2.1. Ferrites with spinel structure

Ferrites with spinel-type structure have the general formula $MeFe_2O_4$ where *Me* is any divalent metal [33]. The name is derived from the mineral called spinel $MgAl_2O_4$. Oxygen ions with a diameter of 1.32 angstroms form a cubical structure with the most compact arrangement. The unit cell contains 32 ions of O^{2-}, 16 ions of Fe^{3+}, and 8 ions of divalent metal. In total 24 metallic ions with diameter of 0.4-1 angstrom are distributed over eight tetrahedral interstitial sites (surrounded by four ions of O^{2-}) and sixteen octahedral interstitial sites (surrounded by six ions of O^{2-}), as partly shown in Fig. 1.

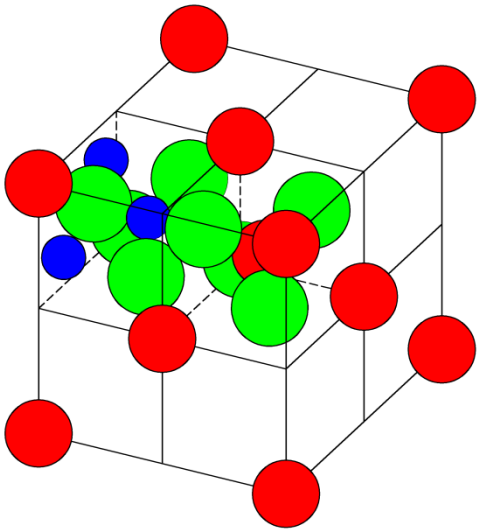

Fig. 1. Unit cell of the spinel structure. The green spheres are oxygen, the red spheres are ions on tetrahedral sites and the small blue spheres are ions on octahedral sites. Ions are drawn in only 2 of the 8 octants. There are 32 oxygen atoms, 16 atoms on octahedral sites and 8 atoms of tetrahedral sites. Modified from [33].

They are known to be soft ferrites with high magnetic permeability at DC and maximum loss frequency (resonance frequency) below about 100 MHz, depending on particular composition. Their permeability substantially decreases beyond about 100 MHz mainly due to the magnetization dynamics of domain walls. The μ value and the resonance frequency (f_r) are related according to Snoek's law, limiting the bandwidth for spinel's applications as microwave absorbers [34].

$$f_r(\mu_r - 1) = \frac{2}{3}\gamma M_s \quad (1)$$

where $\mu_r = \frac{\mu_a}{\mu_0}$ is the relative permeability (μ_a is the absolute permeability and μ_0 is the permeability of vacuum), f_r is the resonance frequency determined by the location of the magnetic loss peak, γ = 2.8 MHz/Oe is the gyromagnetic ratio, and M_s is the saturation magnetization.

Snoek's law predicts that no ferrite can have permeability higher than the Snoek's limit, as long as cubic magnetocrystalline anisotropy is present (Table 3.).

Table 3. The main structural and magnetic characteristics of spinel (-type) ferrites.

Chemical composition	Initial permeability	Magnetic dispersion region (Hz)	Resistance (Ohm cm)	References
MnZn	750-15000	10^6-10^9	10-10^2	[35-37]
NiZn	700-2000	$5\cdot10^7$-10^8	10^6	[35, 37, 38]
Ni–Zn–Cu	1400	10^6-10^7	10^3-10^6	[39]
Mg–Zn	100-800	10^6-10^8	10^6-10^8	[35, 39]
Mg–Zn–Cu	150-600	10^6-10^9	10^3-10^6	[40]
Li–Ti	10-40	10^6-10^9	10^3-10^9	[41]
Li-Zn	100-800	10^7-10^9	10^3-10^5	[42]

Figure 2 shows the frequency dependence of μ of sintered polycrystalline MnZn, which is typical of ferrites with high μ_i and cubic spinel crystal structure. In a low frequency range (f< 10^4 Hz), both μ' and μ'' remain constant. In the intermediate frequency region (10^4–10^6 Hz), the μ shows a small change. The main change occurs in the high-frequency range, where the μ' of MnZn decreases rapidly from the μ'~ 1700 at 1.2 MHz to μ'~ 1 at 1 GHz. At the same

time, the μ'' slowly increases with frequency and has a maximum of about 700–800 at about 2 MHz. The observed magnetic spectra are characterized by a single dispersion characteristic, which results from the contributions of the domain-wall motion and magnetization rotation [43]. The natural ferromagnetic resonance (NFR) nearly does not occur for MnZn ferrite at frequencies exceeding approximately 100 MHz, just as for others spinel-type ferrites, due to the low value of internal field of crystallographic anisotropy, which varies from a few to dozens of oersted.

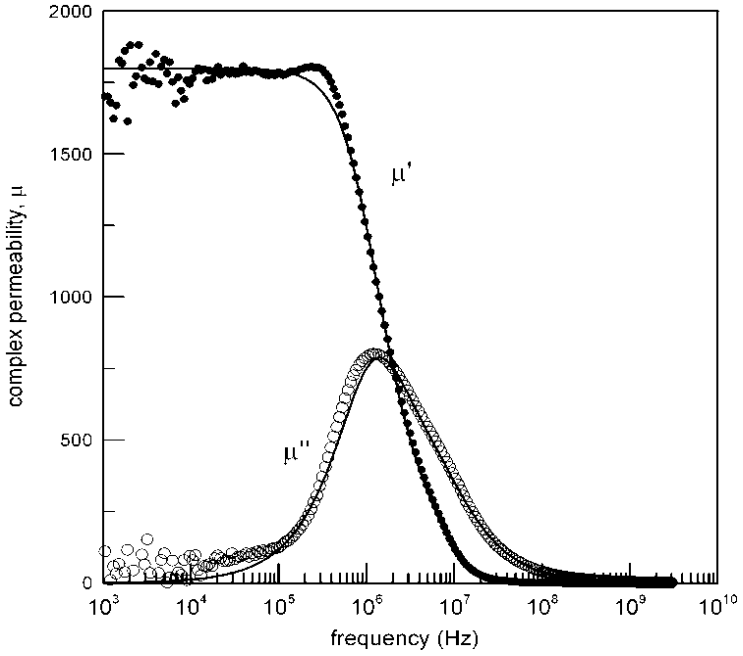

Fig. 2. Magnetic spectrum of sintered polycrystalline MnZn ferrite approximated by the Landau-Lifshitz equation [44].

2.2.2. Ferrites with hexagonal structure

Hexaferrites are ferrites with hexagonal crystal structure. Ferrites with hexagonal structure have the general formula $Me^{I}O–Me^{II}O–Fe_2O_3$. Here Me^{I} represents a divalent ion with a large ionic radius (Ba^{2+}, Pb^{2+}, Sr^{2+}, Ca^{2+}) and Me^{II} corresponds to divalent ions of the iron group transitional elements (Mg^{2+}, Mn^{2+}, Fe^{2+}, Co^{2+}, Ni^{2+}, Cu^{2+}, Zn^{2+}) with small ionic radii. Hexaferrites are classified as M-, W-, Y- and Z-types, according to the structures and concentrations of the layers containing the large metal ions.

It has been reported that some hexagonal ferrites exhibit good magnetic performance in the GHz region, since they have greater magnetic anisotropy

field and higher f_r than those of the spinels, and that their μ values are beyond the Snoek's limitation. In such a case, the f_r is given by

$$f_r(\mu_r - 1) = \frac{1}{2}\gamma M_s \sqrt{H_\theta / H_\varphi} \qquad (2)$$

where H_θ is out-of plane and H_φ is in-plane magnetic anisotropy (see fig. 3). If H_φ is higher than H_θ, then this limit is higher than the Snoek's limit given by (1).

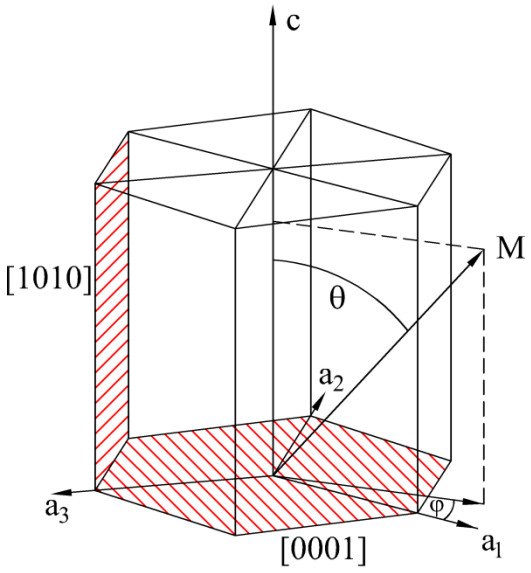

Fig. 3. Crystalline cell of hexagonal ferrite together with an indication of preferential in-plane 0001 direction for a hexaferrites with easy-plane magnetic anisotropy.

Table 4 lists various magnetic parameters for certain hexagonal ferrites for which the f_r is higher than the Snoek's limit.

Figure 4 shows the magnetic spectra of polycrystalline Co_2Z magnetoplumbite and of $NiFe_2O_4$ spinel-type ferrite [45]. The comparison of these spectra shows that, although these ferrites have close permeabilities at low frequencies, the region of permeability dispersion of Co_2Z is much higher than that of $NiFe_2O_4$. For example, the resonance frequency of $NiFe_2O_4$ is f_r~200 MHz, whereas that of Co_2Z is f_r~1.5 GHz. This fact is attributed to the difference in the crystal structure of the ferrites and the associated value of crystallographic magnetic anisotropy (H_A). $NiFe_2O_4$ has a spinel structure, which is characterized by uniaxial magnetic anisotropy and low values of H_A,

Table 4. The main structural and magnetic characteristics of hexaferrites.

Chemical formula	Description; Anisotropy	Initial permeability	Magnetic field anisotropy, kOe	Magnetic dispersion region, GHz	Resistance Ohm cm	Ref.
$Ba_3Co_2Fe_{24}O_{41}$	Co_2Z planar	12.6	6	1-6	10^5-10^9	[46]
$Ba_3Co_2Ti_{0.8}Fe_{22..9}O_{41}$	Co_2Z planar	12	11	4-10	10^8	[18]
$Ba_3Co_{2-x}Fe_{24+x-y}Cr_yO_{41}$	Ba-(Z) planar	16-20	4-7	0.4-1	10^8	[47]
$(Ba_{1-x}Sr_x)_3Co_2Fe_{24}O_{41}$ x=0, 0.2, 0.4, 0.5, 0.8	(Ba-Sr,Co)-Z planar	15	6-10	1-10	1.45×10^3 -6×10^3	[42]
$BaZn_{2-x}Co_xFe_{16}O_{27}$ x=0, 0.5, 0.7, 1.0, 1.5, 2.0	CoZnW planar	8	8	5-7	10^8	[3, 48]
$BaZn_{1..3}Co_{0.7}Fe_{16}O_{27}$	BaW uniaxial	12	4.5	5-9	10^8	[3, 48]
$BaFe_{12-2x}A_xCo_x\ O_{19}$ A - (Ti^{+4}, Ru^{+4}) Ti–Co (x=1.3); Ru–Co (x=0.3; 0.5)	BaM planar	6	7	3-6	10^8	[49]
$Ni_2BaSc_xFe_{16-x}O27$ x=0.5-0.8	Ni_2Wuniaxial	5	6-11	14-26	10^8	[50]

whereas Co_2Z magnetoplumbite has a hexagonal structure with the characteristic easy plane magnetic anisotropy and high values of H_A. Therefore, the dispersion region of complex permeability can be efficiently controlled by an appropriate choice of the ferrite composition.

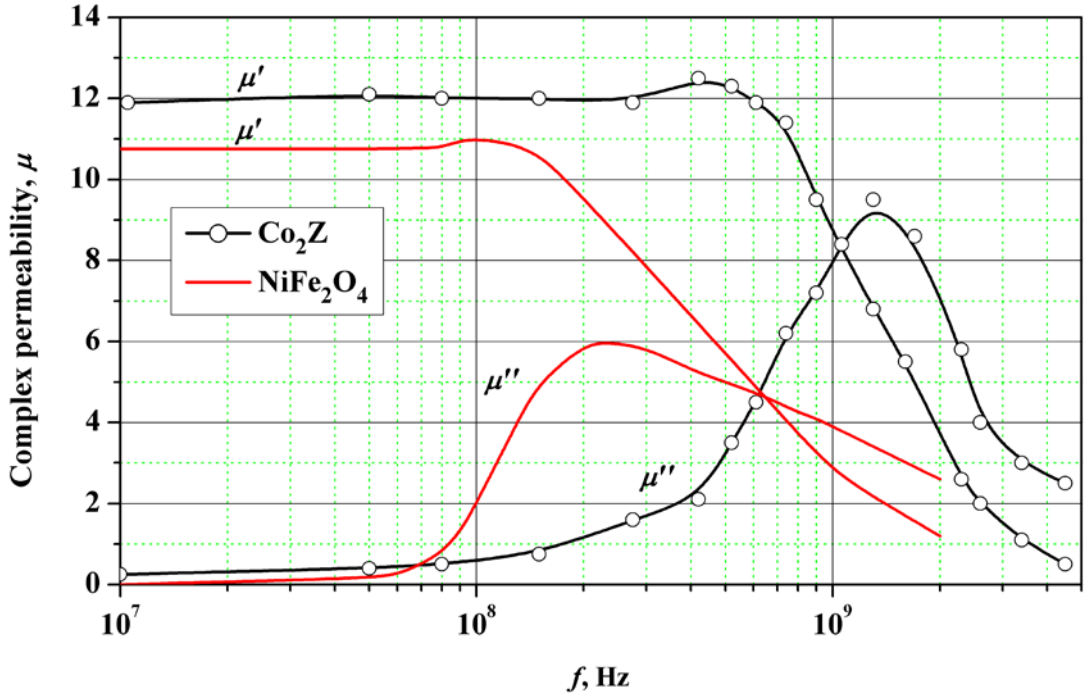

Fig. 4. Magnetic spectra of sintered polycrystalline Co_2Z and Ni_2O_4 ferrites. Redrawn from [45].

3. POLYMER MAGNETIC COMPOSITES: CORRELATION BETWEEN MICROSTRUCTURE AND MAGNETIC PROPERTIES

3.1. Effect of demagnetizing field

Polymer composites filled with ferrites are also characterized by single-dispersion magnetic spectrum. However, there are a number of significant differences between the spectra of bare ferrites and of its composites. This also applies to composites made of polymer–dielectrics [12, 51] and of polymer–semiconductors, such as PANI [16, 17, 20, 52]. Specifically, for high-permeability, low-anisotropy MnZn ferrite and its composites, these differences are: 1) bare ferrite has a magnetic spectrum of mixed relaxation–resonance type, whereas composites have a spectrum of relaxation type; 2) the complex-permeability dispersion region of ferrite extends from 10^5 Hz to 10^7 Hz, while

that of its composites with polyurethane ranges from 10^8 Hz to 3 GHz, and with PANI, from 10^7 Hz to 10 GHz; 3) ferrite has a much greater value of the low-frequency μ compared with that of composites and a lower value of the high-frequency μ. The observed changes in the magnetic spectra of polymer composites are usually attributed to the demagnetization field due to the structural inhomogeneity of a magnetic composite.

Non-uniform distribution of magnetization over the bulk of material is responsible for the interphase polarization and the formation of effective magnetic charges/dipoles. As a result, the effective magnetic field ($\vec{H}_i$) acting on a magnetic particle decreases by the value of the demagnetizing field ($\vec{H}_d$), which is proportional to the demagnetization factor:

$$\vec{H}_i = \vec{H}_e + \vec{H}_d = \vec{H}_e - \widehat{N}_M \vec{M} \quad (3)$$

where $\vec{H}_e$ is the strength of the magnetic component of the applied electromagnetic field, $\vec{H}_i$ is the strength of the magnetic component of the internal field that acts on the magnetic composite, and $\widehat{N}_M$ is the tensor of demagnetization factors, a second-rank material tensor that determines the relationship between the magnetization vector $\vec{M}$ and the demagnetization field vector $\vec{H}_d$.

$\widehat{N}_M$ takes into account the inner and outer demagnetizing effects. The inner demagnetization factor N_i is determined by: 1) the nature of the magnetic material, namely, the crystallographic anisotropy and the anisotropy due to magnetoelastic stresses (which is related to the coupling between elastic and magnetic phenomena in magnetically ordered crystallites in polycrystals), as well as the presence of pores and nonmagnetic inclusions; 2) the concentration, shape and distribution of the magnetic filler particles. The external demagnetization factor is determined by the geometrical shape of a sample (external, geometric demagnetization factor N_ex). Thus the total demagnetization factor is the sum of inner and external (geometric) demagnetization factors: $\widehat{N}_M = N_\text{i} + N_\text{ex}$. In the general form, the effective demagnetization factor of magnetic particles can be represented as [35]:

$$\widehat{N}_M = \frac{L(\mu_i - 1) - (\mu_{eff} - 1)}{(\mu_i - 1) - (\mu_{eff} - 1)} \quad (4)$$

where L is the loading factor, μ_i is the permeability of ferromagnetic particles (inclusions), and μ_eff is the effective permeability of the composite.

While the microstructural inhomogeneity of magnetic particles is ultimately responsible for the broadening of the ferromagnetic resonance linewidth in a bulk ferromagnet, the structural inhomogeneity of magnetic composites is responsible for the significant decrease in both components of μ compared with those in bulk magnetic materials and for the shift of the resonance frequencies to higher values due to the violation of the "magnetic coupling" of particles [16, 51, 53, 54]. The gaps/interphase boundaries (polymer layers) break the magnetic flux and give rise to local demagnetizing fields on the particle scale in the case of a low-concentration (distributed magnetic charges on the particle surfaces) and to the external demagnetizing field on the sample scale when the concentration of the magnetic particles is above the percolation threshold C_P. In that case the interaction between any two particles gives rise to a closed magnetic system, although the larger part of magnetic particles in the composite are isolated by a polymer layer even for the maximal loading [12, 29].

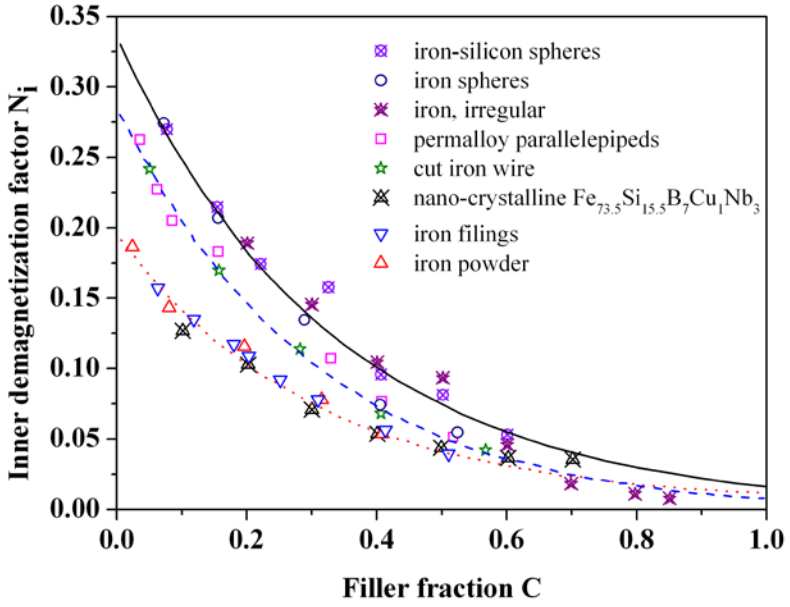

Fig. 5. Inner demagnetizing factors versus volume concentration of magnetic filler in different magnetic polymer composites (magnetic filler differ in composition, particle shape and size of particles). Redrawn from [55].

While studying the dynamic magnetization processes of the composite materials, the influence of N_{ex} can be avoided with the use of toroidal samples. However, the effect of N_i on the frequency dependence of μ has to be considered, especially in order to regulate the frequency of ferromagnetic resonance of the PMC. It has been experimentally established that in magnetic composites obtained by mixing magnetic particles with a polymer, the inner

demagnetization factor decreases with the increase in the filler concentration (Fig. 5) [55]. When the concentration of filler is above C_P, the effect of N_i on a ferromagnetic resonance frequency is negligible (Fig. 6.).

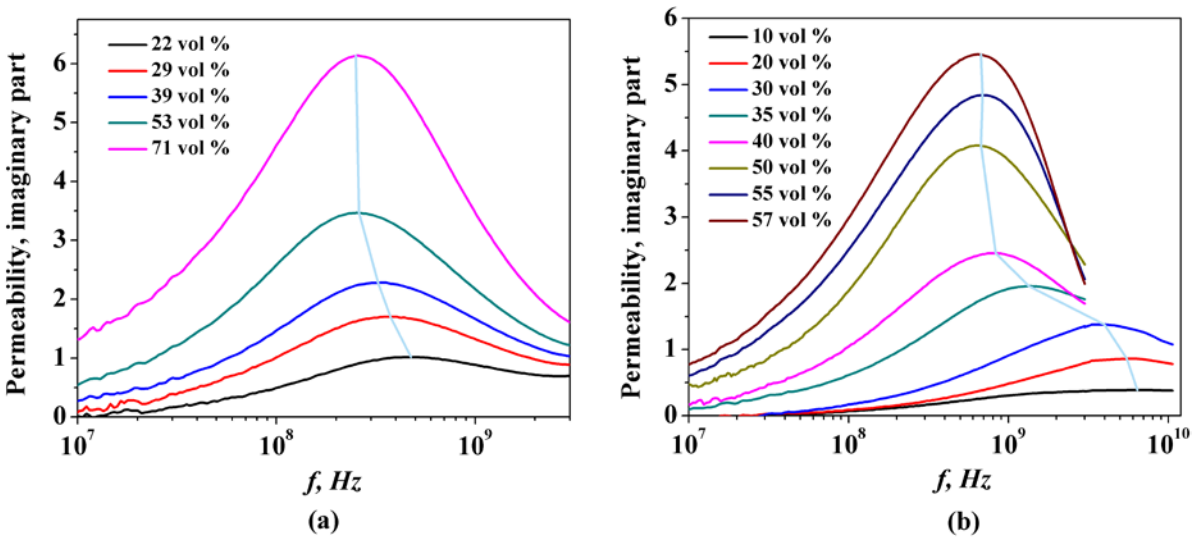

Fig. 6. Experimental variation of the imaginary part of the permeability of polymer composites of MnZn ferrite at the different volume concentration of ferrite: (a) composites prepared by mixture of MnZn ferrite powder with conducting form of PANI; (b) with polyurethane [56].

For the majority of magnetic composites C_P is about 30 - 40 vol. % [51, 55, 57, 58]. Such a concentration dependence of the N_i is explained as follows. At low concentrations ($C \leq 30$ vol. %), the magnetic interaction between particles is weak, and the value of μ_{eff} is determined by the polarizability P of individual particles {$P = \chi/1+N_d\chi$, where N_d (d = x, y, z) is demagnetizing form factor of a particle and χ is magnetic susceptibility}. With the increase in concentration of magnetic particles, a magnetic pole fading is observed, which eventually leads to such a state that above the percolation threshold magnetic flux becomes continuous as in an ensemble of magnetically interacting particles.

Nevertheless, it can be seen from Fig.5 that N_i is not zero for $C = 1$. This is due to the fact that the value of N_i depends not only on P and hence on the shape and concentration of particles, but is also determined by the micromagnetic structure of the particle: the shape of the crystallites and their distribution and the presence of mechanical stresses [55]. This is in agreement with the results of our studies [52, 56]. Elastic stresses arising in MnZn ferrite particle under the influence of polyaniline coating lead to the increase of the effective value of the

magnetic anisotropy and can be considered as an additional source of internal demagnetization field in *in-situ* MnZn-PANI composites.

3.2. Effect of loading factor, particle size and its shape and microstructure

The permeability spectra of PMCs with different concentrations of MnZn ferrite in polyurethane (PU) are shown in Fig. 7. As the filler concentration decreases, the permeability also decreases, and the resonance frequency (the maximum of magnetic losses) significantly shifts to higher frequencies.

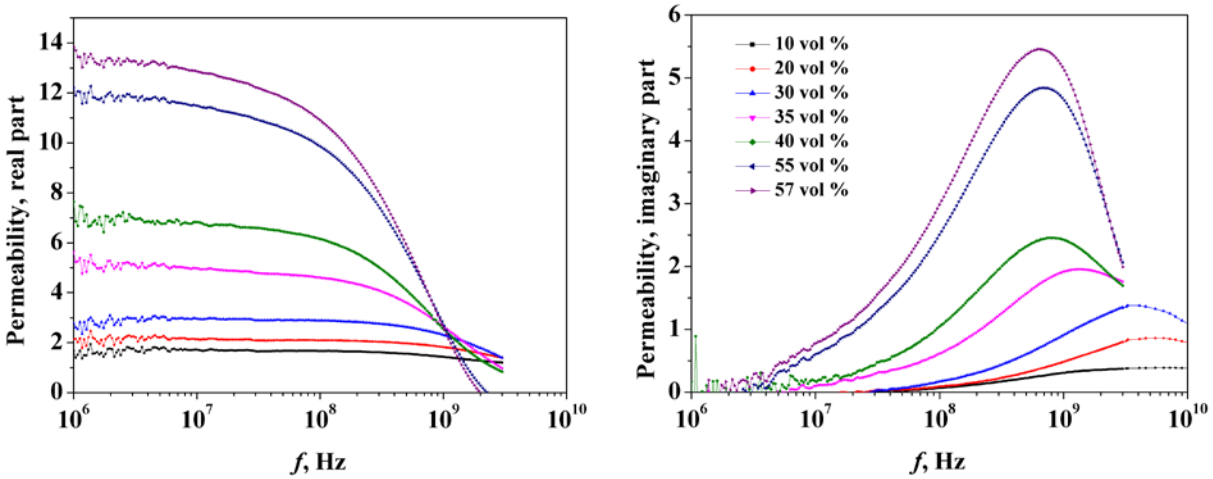

Fig. 7. Effect of MnZn loading on magnetic spectra of PMCs. Redrawn from [12].

The effect of the particle size on the magnetic spectrum of a PMC is sometimes similar to the effect of the loading of particles; this is illustrated by the magnetic spectra of MnZn-based composites with the same loading (40 vol. %) but different particle sizes (Fig. 8). One can see that a decrease in the average size of particles leads to a decrease in the permeability and shifts the resonance frequency to higher frequencies. This is caused by the internal demagnetization factor of particles, which is the higher, the smaller the magnetic particles.

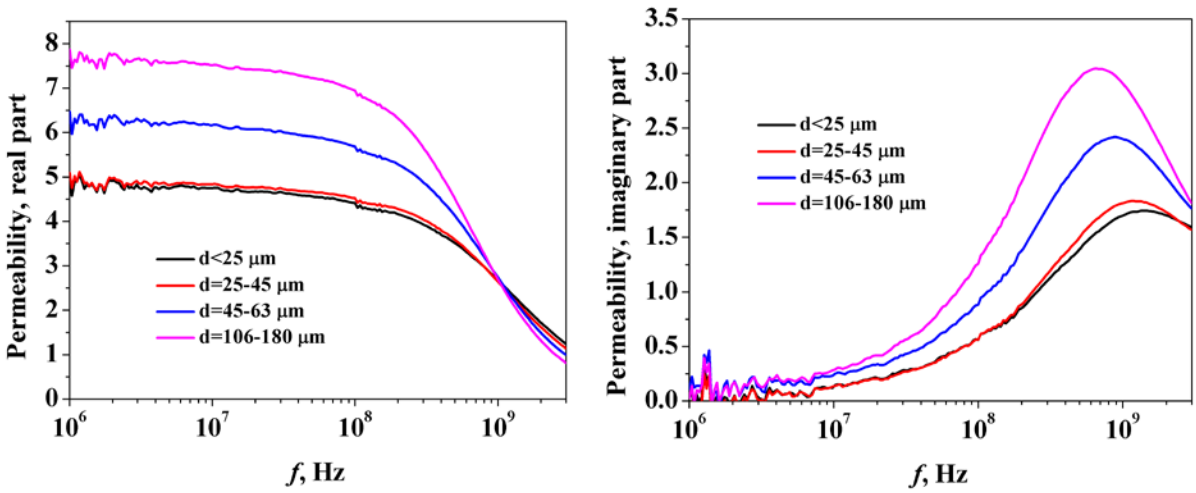

Fig. 8. Magnetic spectra for PU filled with MnZn ferrite (40 vol. %) for various particle sizes.

In contrast to the magnetic propertieas of composites filled with ferrite particles, the magnetic spectra of composites filled with CI more strongly depend on the microstructure of CI particles than on their size. In [29] a significant difference in the high frequency permeability of composites filled with primary and processed CI is shown, although the chemical composition and the particle size distribution of these powders show small difference. The observed differences are attributed to the microstructure of particles; namely, these differences depend on whether or not the particles are characterized by "onionlike" multilayered morphology. The onionlike structure is typical of primary CI, while processed CI is characterized by polycrystalline structure.

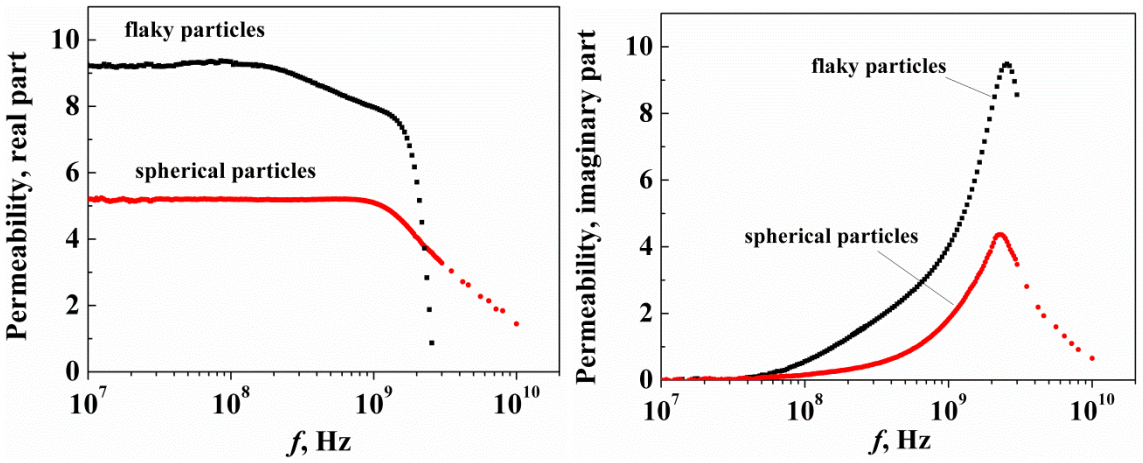

Fig. 9. Effect of particles shape on the magnetic spectra of PMCs filled with CI at the same content of CI (50 vol.%) and different particles shape. Redrawn from [29].

The shape of particles can also produce an appreciable effect on the frequency dispersion of permeability of the composites;this is illustrated by the magnetic spectra of composites filled with spherical and flaky CI particles (Fig. 9). Compared to the composites based on spherical CI particles, the composites with flakes have much higher values of μ' in the frequency range 10^7-10^9 Hz, as well as higher values of magnetic losses in the resonance region. The influence of theparticle shape on the permeability is associated with the shape demagnetization factor of particles N_d (for spherical particles, $N_x=N_y=N_z= 4\pi/3$; for flakes (normal in z-direction), $N_x=N_y= 0$ and $N_z= 4\pi$).

4. ESTIMATION OF THE EFFECTIVE PERMEABILITY

4.1. Mixing rules

The effective permeability of polymer magnetic composites μ_{eff} is a function of the intrinsic permeability of magnetic particles**,** the permeability of the matrix**,** the proportion between magnetic and dielectric phases, and the shape and spatial distribution of the magnetic particles. Thus, to calculate μ_{eff}, one needs detailed information on the microstructure of the composite. In practice, the optimization of the composition of PMCs involves approximate methods, called “mixing rules” in the literature, to simulate the dependence of μ_{eff} on the permeabilities of the components and their concentrations. A number of mixing rules have been proposed and reviewed in the literature [59-62]. The most common rules are the Maxwell–Garnett approximation (MG) and the Bruggeman effective medium theory (EMT).

Maxwell–Garnett mean-field model

The Maxwell–Garnett mean-field model [63] considers a PMC as a homogeneous medium in which isolated particles of inclusions are embedded in a host matrix. This assumption results in the following equation:

$$\frac{\chi_{eff} - 1}{1 + n_0(\chi_{eff} - 1)} = p\frac{\chi_i - 1}{1 + n_0(\chi_i - 1)} \qquad (5)$$

Where χ_{eff} and χ_i are the effective macroscopic susceptibilities of the composite and of inclusions, respectively, normalized by the permeability of the host matrix ($\chi_{eff} = \mu_{eff} / \mu_h - 1$, $\chi_i = \mu_i / \mu_h - 1$), p is a volume fraction and n_0 is a shape

factor of the inclusions. The MG model proved satisfactory in the case of dilute composites, when the interparticle interactions are negligible.

Bruggeman effective medium theory

The EMT [64] assumes the absolute equality between the phases in the mixture and is expressed as:

$$p\frac{\chi_i - \chi_{eff}}{\chi_{eff} + 1 + n_0(\chi_i - \chi_{eff})} - (1-p)\frac{\chi_{eff}}{\chi_{eff} + 1 - n_0\chi_{eff}} = 0 \qquad (6)$$

Although eqs. (5) and (6) imply the inclusions with spherical shape with n_0=1/3, they can also be applied to non-spherical inclusions with an effective shape factor differing from 1/3 [65-67].

Bruggeman asymmetric rule

The Bruggeman asymmetric rule (BAR) [64] in terms of μ is expressed as:

$$\frac{\mu_i - \mu_{eff}}{\mu_i - \mu_h} = (1-p)\left(\frac{\mu_{eff}}{\mu_h}\right)^{\frac{1}{3}} \qquad (7)$$

As can be seen from (7), BAR does not take into account the shapes of inclusions, and they can be assumed to be arbitrarily-shaped crumbs with aspect ratio close to 1.

Bruggeman symmetric rule

For randomly oriented ellipsoidal inclusions, one can use the Bruggeman symmetric rule (BSR), also known as the Polder-van-Santen (PVS) rule [68]. In contrast to BAR, BSR takes into account the shape factors of inclusions:

$$\mu_{eff} = \mu_h + \frac{p}{3}(\mu_i - \mu_h)\sum_{j=1,2,3}\frac{\mu_{eff}}{\mu_{eff} + n_j(\mu_i - \mu_{eff})} \qquad (8)$$

where n_j are the demagnetization factors of the inclusion ellipsoids in the three orthogonal directions.

Coherent potential formula

Another well-known formula, the so-called Coherent potential formula for spherical inclusions, has the following form:

$$\mu_{eff} = \mu_h + p(\mu_i - \mu_h)\frac{3\mu_{eff}}{3\mu_{eff} + (1-p)(\mu_i - \mu_h)} \qquad (9)$$

The formula for ellipsoidal inclusions looks like:

$$\mu_{eff} = \mu_h + \frac{p}{3}(\mu_i - \mu_h) \sum_{j=1,2,3} \frac{\mu_{eff}(1+n_j) - n_j\mu_h}{\mu_{eff} + n_j(\mu_i - \mu_h)} \quad (10)$$

It is worth mentioning that for dilute mixtures (p<<1) BAR, BSR and Coherent potential formulas predict the same results.

Landau–Lifshitz–Looyenga

Other mixing rules that are widely used for the interpretation of experimental results are the Landau–Lifshitz–Looyenga (LLL) mixing rule and the Musal (MU) and the Lichtenekker mixture equations.

The LLL equation is given by [44, 69]

$$\mu_{eff} = \left[\mu_h + p\left(\mu_i^{\frac{1}{3}} - \mu_h^{\frac{1}{3}}\right)\right]^3 \quad (11)$$

The LLL equation is rigorous when the difference between μ_i and μ_h is small.

Musal mixture equation

According to Musal's approach [66], the Maxwell-Garnet expressions can be extended to the entire range of compositions $0 \leq p \leq 1$. Here, the medium is described as a combination of two different phases. The isolated phase consists of particles *a* embedded in *b* (matrix), while in the agglomerated phase, the component *b* behaves as an inclusion in the extended medium *a*. The volume ratio of these two different phases changes as the volume fraction of the magnetic filler increases. The permeability of each phase can be calculated by the appropriate MG effective medium expression.

The original Musal mixture equation reads as follows:

$$\mu_{eff} = \mu_h \left[1 + 3\left(\frac{\mu_i + 2\mu_h}{p(\mu_i - \mu_h)} - 1\right)^{-1}\right] \quad (12)$$

Lichtenecker's empirical equation

Lichtenecker's empirical equation is often used in practice due to its simplicity [70]:

$$log\mu_{eff} = p \cdot log\mu_i + (1-p)log\mu_h \tag{13}$$

The Bergman-Milton theory

The Bergman-Milton (BM) theory [71, 72] offers an alternative approach to considering the properties of composites. The theory provides an unambiguous description of a composite, and the effective normalized susceptibility can be found as:

$$\chi_{eff} = \int_0^1 \frac{\chi_i B(n) dn}{1 + n\chi_i} \tag{14}$$

where *B(n)* is the spectral function which takes into account the spread in the shape factors of inclusions. The last can be due to interactions within the mixture or inhomogeneous fields excited at non-ellipsoidal inclusions, as well as due to the variation of the form factors of the inclusions.

The sum rules relate the spectral function to the volume fraction of inclusions and can be presented as:

$$\int_0^1 B(n)dn = p \quad and \quad \int_0^1 nB(n)dn = \frac{p(1-p)}{D} \tag{15}$$

where D is the dimensionality of the composite and D=3 for a bulk isotropic composite with inclusions of arbitrary shape.

All the known mixing rules can be derived from the BM theory with a particular form of the spectral function. For instance, the spectral function for MG is a delta-function:

$$B(n) = p \cdot \delta\{n - (1-p)\hat{n}\} \tag{16}$$

where $\hat{n} = 1/3$ is a mean shape factor of the inclusions.

The spectral function for BSR has the following form:

$$B(n) = \begin{cases} \dfrac{D\sqrt{(n-n_1)(n-n_2)}}{4\pi}, & for\ n_1 < n < n_2 \\ 0, & otherwise \end{cases} \tag{17}$$

n_1 and n_2 represent the range of possible form factors of inclusions.

Examples of spectral functions for several different mixing rules are presented in figure 10.

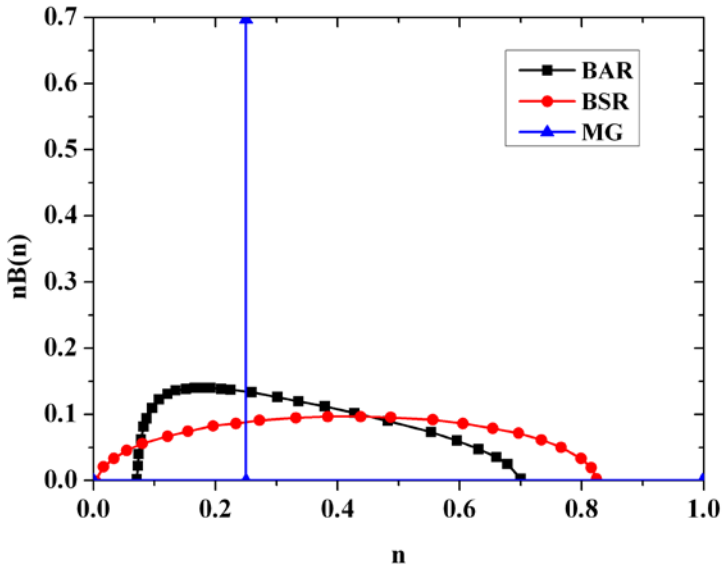

Fig. 10. Spectral functions for the BAR, BSR and MG mixing rule. Redrawn from [61]. The mean form factor is taken $\hat{n} = 1/3$ *and the volume concentration of inclusions is p=0.25.*

Presently it is recognized that the validity of mixing rules depends, first of all, on the difference between the permeabilities of the inclusions and of the host matrix. Thus, in the case of composites for which μ_i is close to μ_h, the MG and BSR mixing rules agree well with the measured effective permeability data. When the value of μ_i is high, which is the case of greatest practical interest, the better approximation results are usually obtained by Bruggeman expression and the Musal mixture equation (Fig. 11).

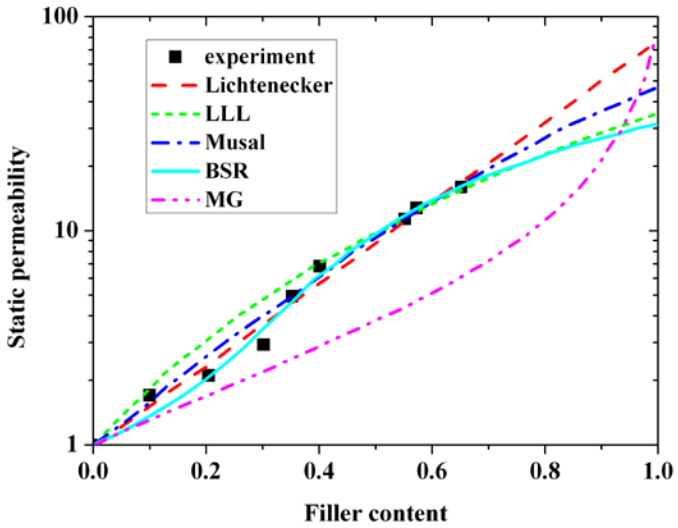

Fig. 11. The concentration dependence of real part of complex permeability of MnZn-based polyurethane at 10 MHz. The experimental data is fitted by different mixing rules.

Obviously, any mixing rule has its applicability limitations due to the requirement to fulfill some necessary conditions. Among them are 1) homogeneity of the composite material in the wavelength scale and 2) random arrangement of filler particles in the material. If these two conditions are not met, the application of the mixing rules is not effective since the discrepancies between the experimental data and those predicted by the model are noticeable. This can be demonstrated by an example of the composite in which the resistive filler particles with the shape of flat squares form regular two-dimensional arrays in dielectric matrix. The composite structure is given in Fig. 12, where the particle dimensions are: a=5 mm, d=7 mm and δ=2 mm.

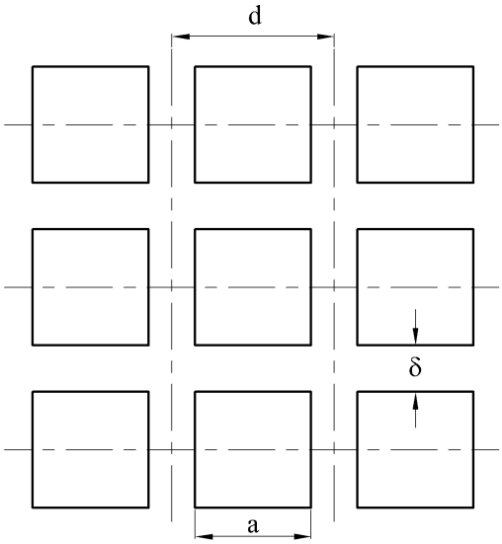

Fig. 12. The geometry of two-dimensional arrays from resistive squares.

Since the effective dielectric permittivity ε_{eff} is governed by the same mixing rules as the μ, the PVS rule (8) was applied to model the frequency dependence of ε_{eff} of the composite, with the same shape factors and μ substituted by the corresponding ε. For the calculation the resistive square was considered as a disc, whose aspect ratio is $u=l/h$, where l is diameter ($l = 2a\sqrt{1/\pi}$) and h is the height of the disc (h=0.12 mm). Inclusions with disk-like shape can be approximated as oblate spheroids with the axial form factor [44]

$$n_3 \approx 1 - \frac{1}{\sqrt{1+u^2}} \tag{18}$$

The other two depolarization factors are assumed to be equal, $n_1=n_2=0.5(1-n_3)$.

Fig. 13 shows the measured and calculated frequency dependences of ε_{eff} in a frequency range of 5–15 GHz.

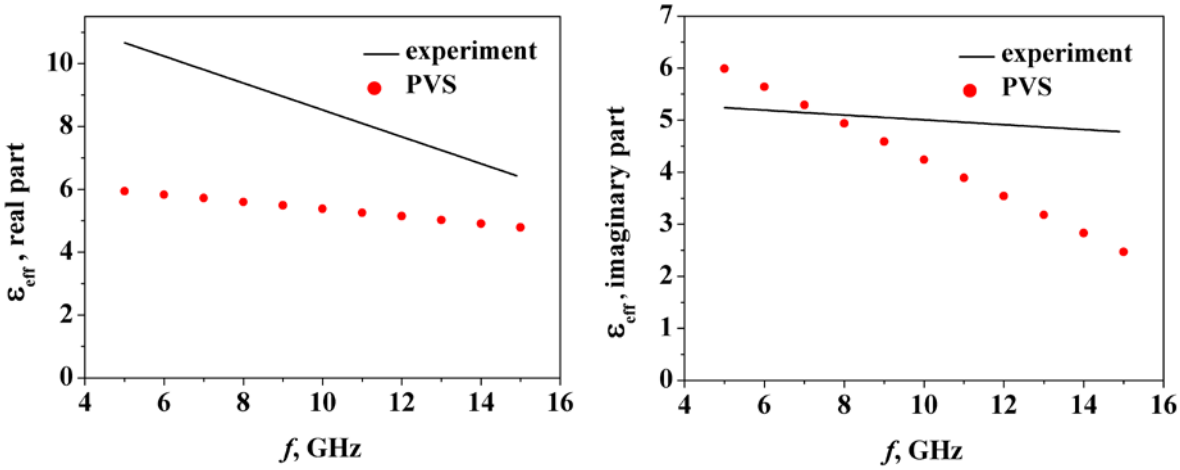

Fig. 13. Measured and calculated frequency dependences of effective dielectric permittivity.

As expected, the agreement between the measured and calculated data is very poor in this instance, which confirms that the application of mixing rules in the case of regularly arranged filler inclusions is not relevant.

5. POLYMER MAGNETIC COMPOSITES WITH HIGH VALUE OF PERMEABILITY IN THE RADIO-FREQUENCY AND MICROWAVE BANDS

In section 3 it has been shown that the μ_{eff} of PMCs is not a simple function of the magnetic permeabilities of individual components of the composite and their concentrations but it also depends on the size, shape, and the distribution of filler particles in the composite.

At the moment, several methods have been proposed to improve the high-frequency permeability dispersion of PMCs. The increase in filler permeability provides an increase in μ of composite by only several units [73]. Increasing the size of the filler particles leads to an increase in the maximum of magnetic losses, while the real part of permeability μ' changes little [12]. A significant increase in μ can be achieved by using filler particles with flaky form, because they have a low value of the shape demagnetization factor [27]. For example, in [74] it has been shown that μ of silicone based composites filled with flaky NiZn ferrite particles doped with Co is almost 300 % higher compared to composites filled with ferrite of the same composition but with an irregular shape of particles. The use of flaky carbonyl iron particles also leads to a

significant increase in μ of composites based on silicone matrix [29]. In addition, the flaky particles can be relatively easy oriented, which allows obtaining textured PMC with high values of μ.

The necessity to maintain the physical and mechanical properties of a PMC restricts the volume content of the magnetic phase; moreover, in the case of high filling ($C \geq 0.5$), the eddy current effect manifests itself in the magnetic spectrum. This especially applies to composites filled with metal magnetic particles. Therefore, one should seek new ways to further increase μ_{eff} in PMCs to make them favorable candidates for developing of RAMs.

In the case of ferrite-filled composites, one of the ways to increase μ can be the use of multicomponent particles with «core–shell» structure [24].The main advantage of such magnetic materials is that they can efficiently interact both with the electric and magnetic components of electromagnetic fields, which allows one to control the magnetic properties through electric ones and vice versa.

At present, two methods are used for the synthesis of multicomponent particles with «core–shell» structure. The *first method* consists in the metallization of magnetic particles by electrolysis plating process [75, 76]. The main problem of the metallization method is to obtain a uniform metal coating of thickness no greater than the skin-depth which, for the most conducting metals, amounts to a few micrometres in the ultra-high frequency band. The manufacturing technology of multicomponent particles with core-shell structure by the *second method* is based on the deposition of electrically conducting polymers, such as PANI and PPy, on the surface of ferrite particles by the method of oxidative polymerization of a monomer in the presence of magnetic particles [16, 17, 52]. A polymer coating of required thickness and morphology can be obtained by controlled synthesis methods [22]; the conductivity, however, is not higher than ten S cm^{-1}; therefore, these polymers have a rather weak effect on the μ of composites with multicomponent particles [24]. The effective conductivity of the polymer coatings can be increased by incorporating nanoparticles of noble metals into PANI (PPy) [77]. More detailed information on the preparation of multicomponent particles with core-shell structure and the further regulation of their electromagnetic properties is provided in the framing papers I-III.

6. MODELING OF RADIO ABSORBERS BASED ON MULTICOMPONENT PARTICLES

Nowadays, radio absorbing materials are widely used both in civil and military fields due to their ability of absorbing unwanted electromagnetic signals and eliminating electromagnetic wave pollution. RAMs can be manufactured by imbedding various magnetic and dielectric materials in powder form in a polymer matrix [78-83]. The absorption of electromagnetic waves in these materials is governed by various loss mechanisms related to the magnetization and electric polarization processes. From the point of view of electrodynamics, a more efficient absorption of electromagnetic radiation can be achieved by using materials with high permeability, high magnetic loss, a favorable form of frequency dependence of permeability, and a proper ratio between the permeability and permittivity [1, 2, 60]. The radio absorber (RA), which reduces the reflection of incident electromagnetic wave, represents a layer (layers) of a RAM placed on a metal surface.

The efficiency of RA is normally estimated by reflection and transmission coefficients, the operating frequency range and the thickness. The trend is thus the development of RAs of minimum thickness, with the minimal reflection and transmission coefficients, and with the widest possible operating frequency range.

The reflection coefficient R is a parameter that characterizes the absorbing ability of RAs in decibels (dB). The level of the reflection coefficient equal to –10 dB insures 90% absorption of incident energy by RA (presuming the absence of transmitted energy). The operating frequency range, which is another important parameter characterizing RA, is the difference between the edge frequencies (f_{max} and f_{min}) of the interval where R is below –10 dB.

A single-layer RA is one of the most widely considered cases for estimating the absorbing properties of a material. The calculation procedure of such an absorber is presented below by an example of polymer composites based on *in-situ* prepared multicomponent particles with «core–shell» structure embedded in a PU matrix. The particles contain the same amount of the magnetic phase (MnZn ferrite) but differ in conductivity and the morphological properties of the «shell» (PANI). Given that an electromagnetic wave is incident on the surface of RA along the normal, the reflection coefficient from the surface of such an absorber can be calculated by the well-known formula [84]

$$R = 20log\left|\frac{Z - Z_0}{Z + Z_0}\right|, dB \tag{19}$$

where

$$Z = j\sqrt{\frac{\mu}{\varepsilon}}\tan\left(\frac{2\pi f}{c}\sqrt{\mu\varepsilon}\, d\right) \tag{20}$$

is the input impedance of the layer, Z_0=1 is the wave impedance of free space, c is the velocity of light, f is frequency, μ and ε are the complex permeability and permittivity of the material, respectively, and d is the thickness of the sample.

The reflection from the RA is absent in case if Z=1. However, in real materials this can be reached only approximately. The frequency f_0 and thickness d_0 for which the above condition is satisfied with the highest degree of accuracy are called the matching frequency and the matching thickness, respectively.

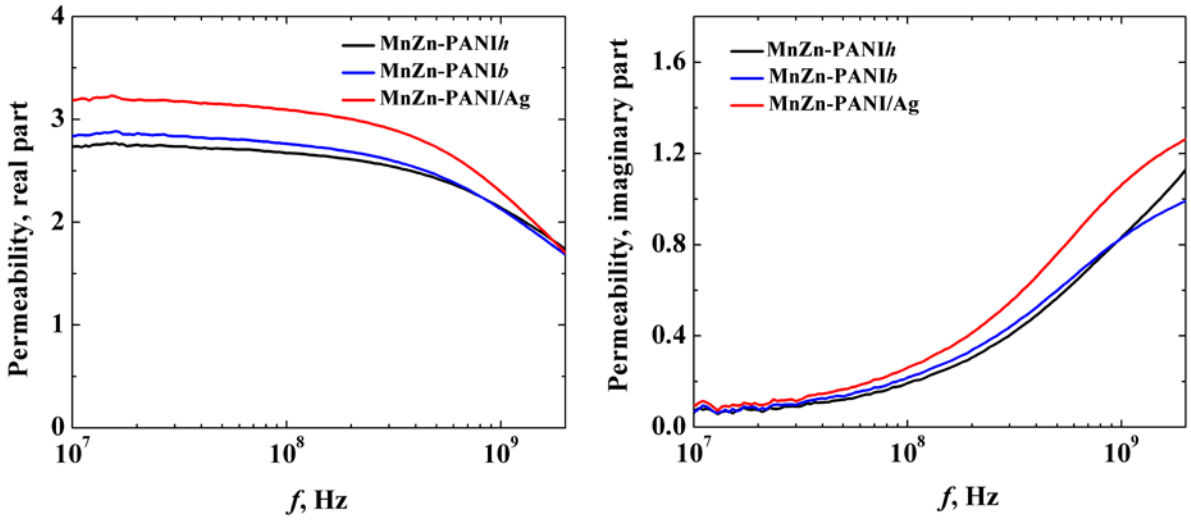

Fig. 14. Frequency dependences of the permeability of the composites based on in-situ prepared multicomponent particles with «core–shell» structure embedded in PU matrix. The loading of the particles is 40 vol% for each composite.

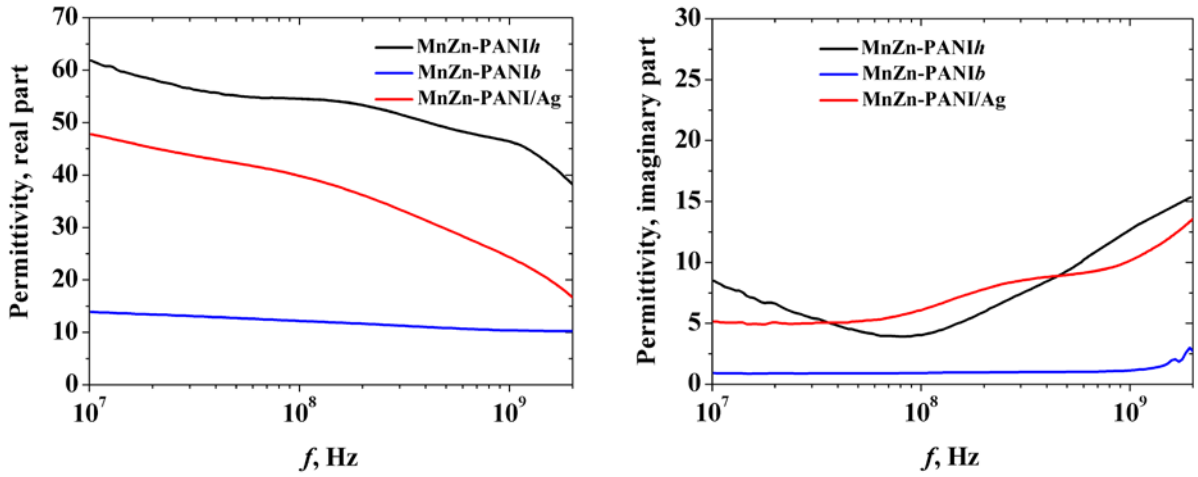

Fig. 15. Permittivity spectra of the composites based on in-situ prepared multicomponent particles with «core–shell» structure embedded in PU matrix. The loading of the particles is 40 vol% for each composite.

In practical calculations, the minimum of R is obtained only for complex values of d. Expression (20) and the condition Z=1 imply

$$d = d' + jd'' = \frac{c}{2\pi f\sqrt{\mu\varepsilon}} \arctan\left(-j\sqrt{\frac{\varepsilon}{\mu}}\right) \qquad (21)$$

By (21), we calculate the dependence of complex parameter d on frequency; after that, we take the minima satisfying the inequality $|d''/d'| \leq 0.01$ and substitute the thicknesses $d_0=d'$ into equations (19) and (20) [79].

Finally, given the experimental frequency dependences of μ and ε (Figs. 14 and 15) and the numerically obtained value of d_0, we calculate the frequency characteristics of R that have deep minima R_0 at the matching frequencies f_0 (Fig. 16).

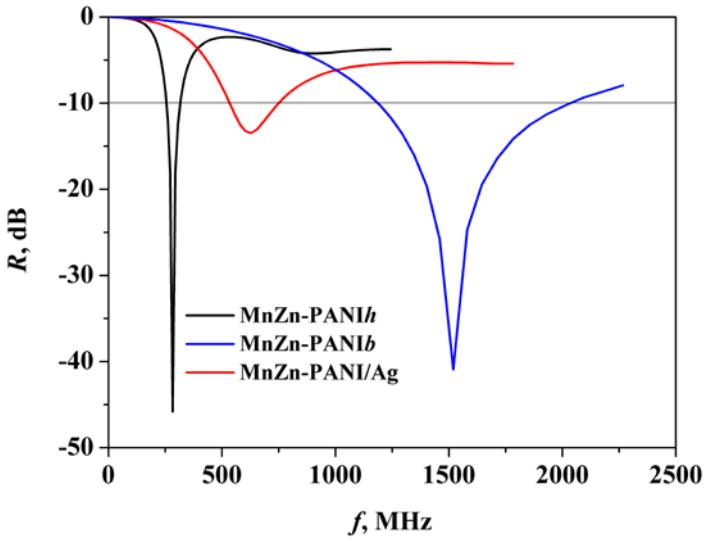

Fig. 16. Frequency dependences of the reflection coefficients of RA based on composites containing in-situ prepared multicomponent particles (40 vol%) with «core–shell» structure embedded in PU matrix.

Figure 16 and Table 5 show that radio absorbers based on multicomponent particles have different values of matching thickness and matching frequency, although the concentration of magnetic phase is the same in each absorber. Thus, by varying the particles «shell» properties, it is possible to control the matching frequencies and the thickness of the RA in a wide radio frequency range.

Table 5. Electrodynamic characteristics of RAs based on composites containing *in-situ* prepared multicomponent particles (40 vol%) with «core–shell» structure embedded in PU matrix.

Composite material	f_{min} (MHz)	f_0 (MHz)	f_{max} (MHz)	R_0 (dB)	d_0 (mm)	f_{max}/f_{min}
MnZn–PANI*h*	255	285	318	–46	23	1.24
MnZn–PANI*b*	1180	1520	2050	–41	10.54	1.74
MnZn–PANI/Ag	530	627	756	–13	13.4	1.43

7. OBJECTIVE OF THE WORK AND FINDINGS SYNOPSIS

The primary emphasis in this work was given to the development of polymer magnetic composites with controlled electromagnetic properties (complex magnetic permeability and dielectric permittivity) with a view of their application in RAs. To this end, hybrid composites based on multicomponent particles with «core–shell» structure were synthesized with MnZn ferrite being a core and polyaniline with different conductivity being a shell. These materials are attractive due to the possibility to alter their electrical and magnetic properties via controlled synthesis methods. Thus, the present work is also aimed at investigating the factors responsible for the significant changes in the electrical and magnetic properties of MnZn–PANI based composites by changing the properties of PANI overlayer, as well as at explaining the physical mechanisms behind these phenomena.

The most significant results of the current work are highlighted below as a summary of four papers.

Paper I deals with the analysis of the factors responsible for the high-frequency shift of the complex magnetic permeability dispersion region and for the increase in the thermomagnetic stability of polymer composites of high-permeability MnZn ferrite. To this end, thorough investigation of magnetic spectra of ferrite and its composites with polyurethane and polyaniline was carried out as a function of a longitudinal DC magnetizing field and temperature in a wide frequency range from 100 kHz to 3 GHz. Furthermore, to evaluate the effect of various magnetization processes on μ and to separate them, the magnetic spectra of ferrite and its polymer composites were fitted by a model allowing one to determine the specific contributions of the resonance processes associated with the domain wall motion and the rotation of magnetization vector. The numerical calculations revealed that, at high frequencies, the μ of the bare MnZn ferrite is determined solely by magnetization rotation, occurring in the region of natural ferromagnetic resonance when the ferrite is in the “single domain” state (Fig. 17).

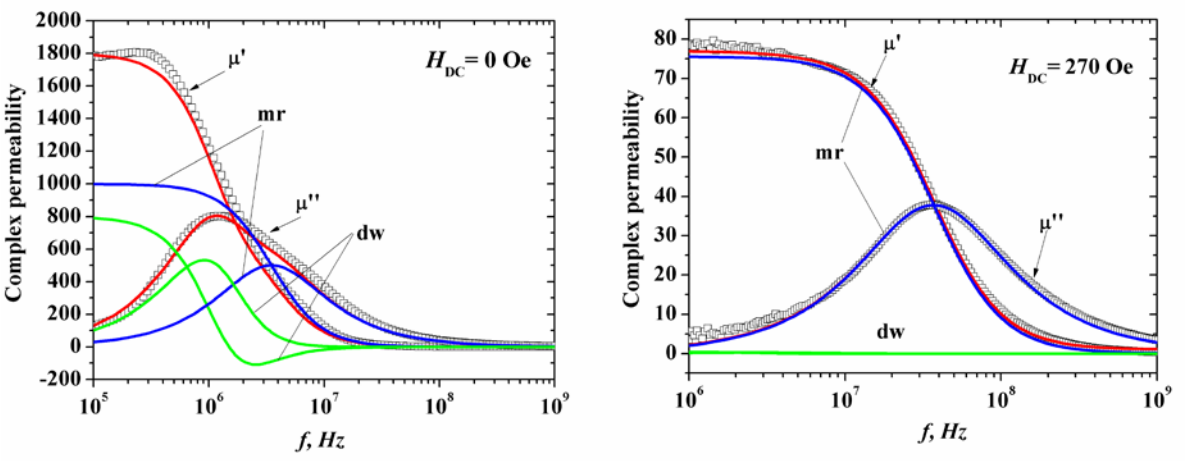

Fig. 17. Magnetic spectra of MnZn ferrite without (left) and under the influence of DC magnetizing field (right). The colored solid lines show total fitted permeability (red) obtained by combining the domain-wall motion (dw) and magnetization rotation (mr) components [52].

Although the high-frequency permeability of the polymer composites of MnZn ferrite is also determined mainly by the magnetization rotation, up to high values of magnetizing fields, there is a contribution of domain wall motion; this indicates that the “single domain” state in the ferrite is not reached (Fig. 18).

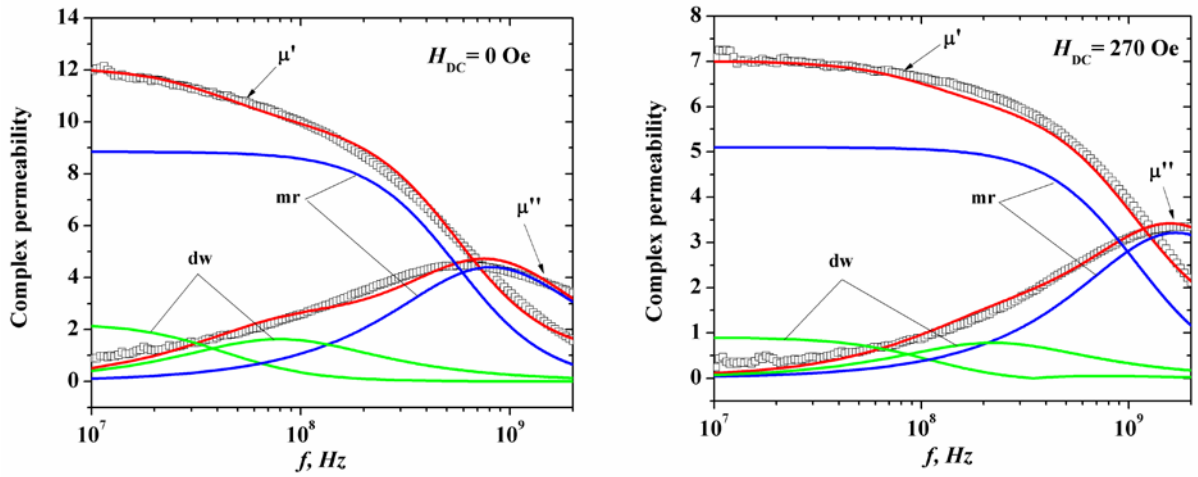

Fig. 18. Magnetic spectra of MnZn–PANI composite without (left) and under the influence of DC magnetizing field (right). The experimental values of μ′ and μ′′ are indicated by open squares. The colored solid lines show total fitted permeability (red) obtained by combining the domain-wall motion (dw) and magnetization rotation (mr) components [52].

Dynamic magnetization feature of MnZn–PU composite materials, as well as the increase in their thermomagnetic stability is determined by the effect of the demagnetizing field. However, in the case of MnZn–PANI composite it is mostly attributed to the induced magnetic anisotropy. The induced magnetic anisotropy has a magnetostrictive nature and is attributed to internal stresses that arise in ferrite particles due to the polyaniline coating. The pinning of domain walls by polyaniline during *in-situ* polymerization leads to the deceleration of domain wall motion in magnetic fields, resulting in an increase in the coercivity and a shift of the complex permeability dispersion region to the ultra-high frequency band. Simultaneously, the pinning of domain walls and the rise of induced magnetic anisotropy stabilize the domain structure of the ferrite, thus reducing its sensitivity to magnetostrictive deformations with increasing temperature, which guarantees the high thermal stability of MnZn–PANI composite (Fig 19).

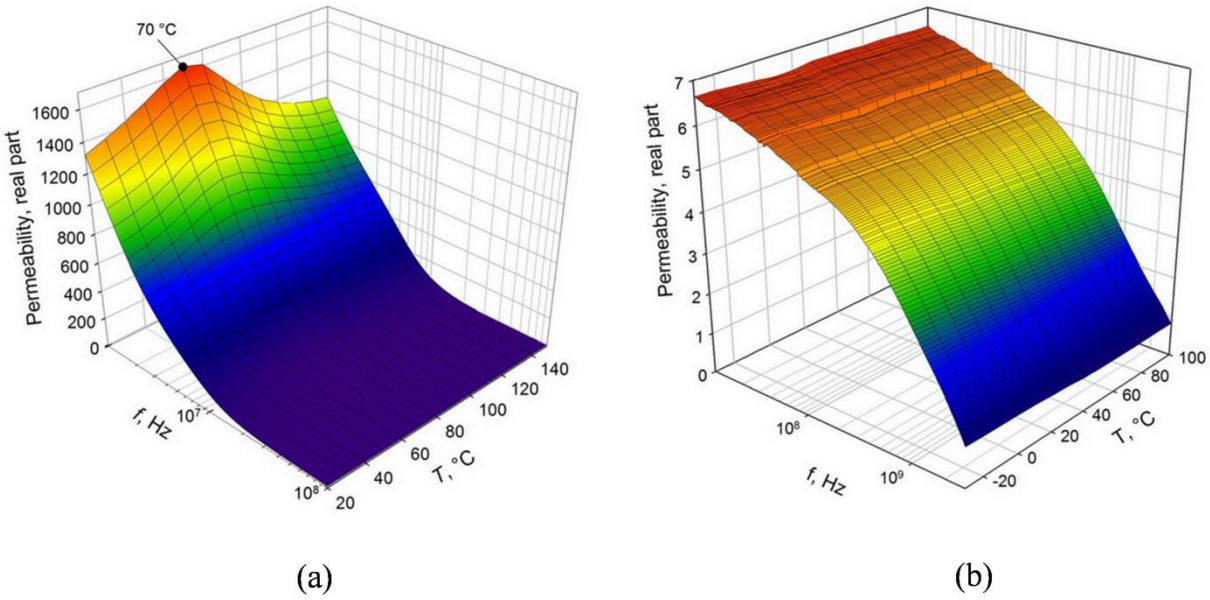

Fig. 19. Three-dimensional image of the temperature-frequency dependence of μ′ for MnZn (a) and MnZn–PANI (b) [52].

Paper II is essentially the continuation of the investigation of thin PANI film impact on the magnetic and thermomagnetic properties of MnZn–PANI composites, with more attention focused on the role of interaction between ferrite and polyaniline from the viewpoint of molecular mechanism of aniline oxidation and on the effect of the morphology and the elastic properties of polyaniline coating on the main magnetic characteristics of the hybrid

composites. To this end, samples of MnZn–PANI that differ in morphology, conductivity and elastic properties of polyaniline overlayer were prepared. The analysis of the structure of PANI films at different stages of polymerization shows that the film grows selectively, in the regions where domain walls (*dw*s) appear on the ferrite surface (Fig. 20).

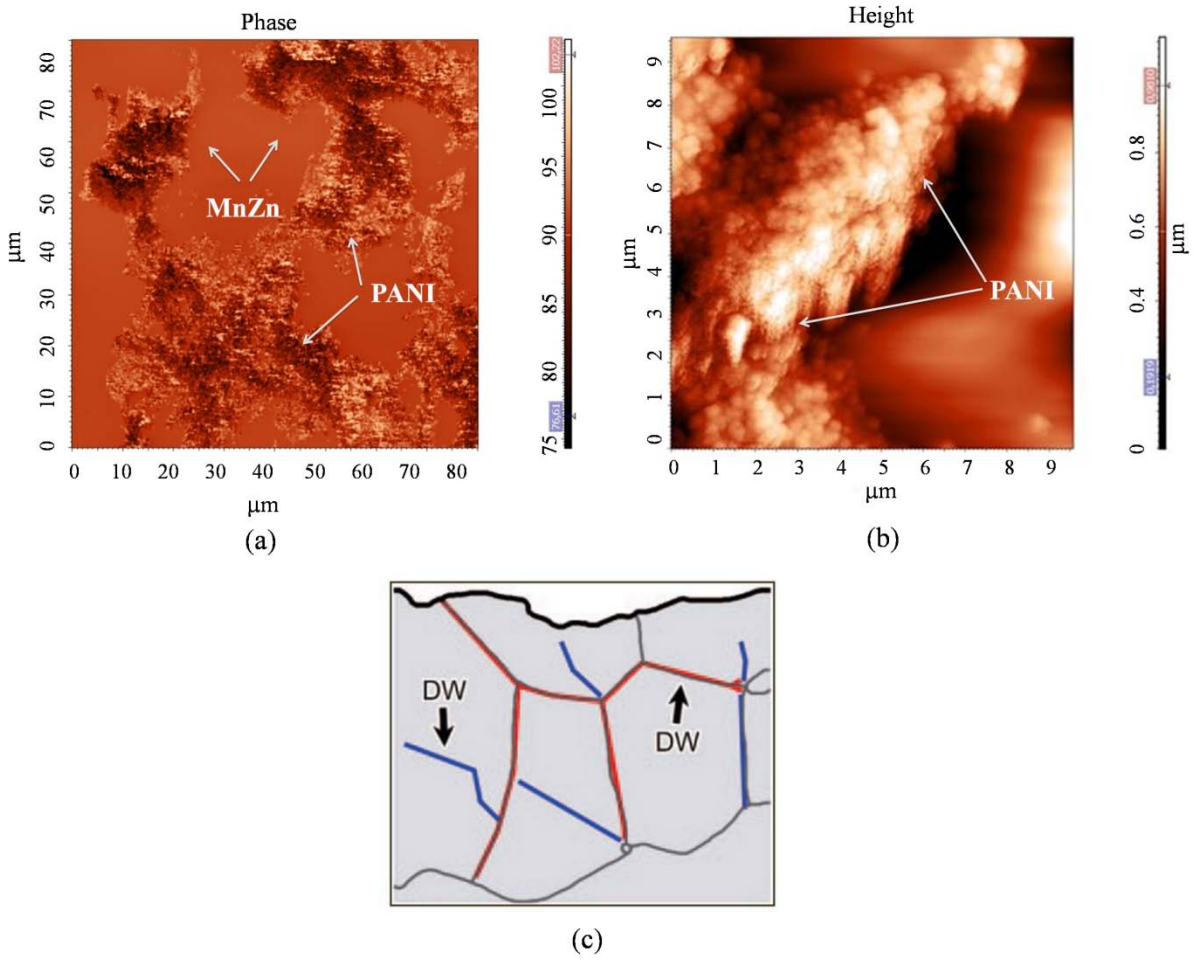

Fig. 20. Atomic force microscopy of the surface of MnZn ferrite coated with polyaniline by in-situ polymerization (a, b) and the schematic illustration of domain structure, where blue and red lines indicate the position of domain walls (c) [52, 56].

This is attributed to the selective sorption of paramagnetic phenazine nuclei (formed at the earlier stage of aniline oxidation) on the *dw*s. The strong π-electron interaction between phenazine and ferrite gives rise to the growth of polymer chains in the place of sorption of nuclei. This leads to the *dw* pinning and, as a consequence, to the damping of *dw* motion in magnetic fields. The further increase in coercivity, resonance frequency and thermomagnetic stability of polyaniline coated ferrite due to the film shrinkage after deprotonation of PANI makes it obvious that polyaniline coating induces elastic stresses in a

ferrite particle that stimulate the growth of the effective magnetic anisotropy. The stress-induced magnetic anisotropy contributes to the reorientation of the magnetization vectors in domains with respect to the new directions of easy magnetization, defined by magnetoelastic stresses, which leads to complex changes in the magnetic properties of *in-situ* prepared MnZn–PANI composites (Table 6, Fig. 21).

Table 6.Saturation magnetization, coercitivity and resonance frequency for MnZn ferrite and its composites with polyaniline [56].

Sample name	Coercivity (Oe)	Saturation Magnetization (emu g^{-1})	Resonance frequency (MHz)
bare MnZn ferrite	2.2	77	1.3
MnZn–PANI*h* (protonated PANI)	6.5	67	580
MnZn–PANI*b* (deprotonated PANI)	8.6	60	900

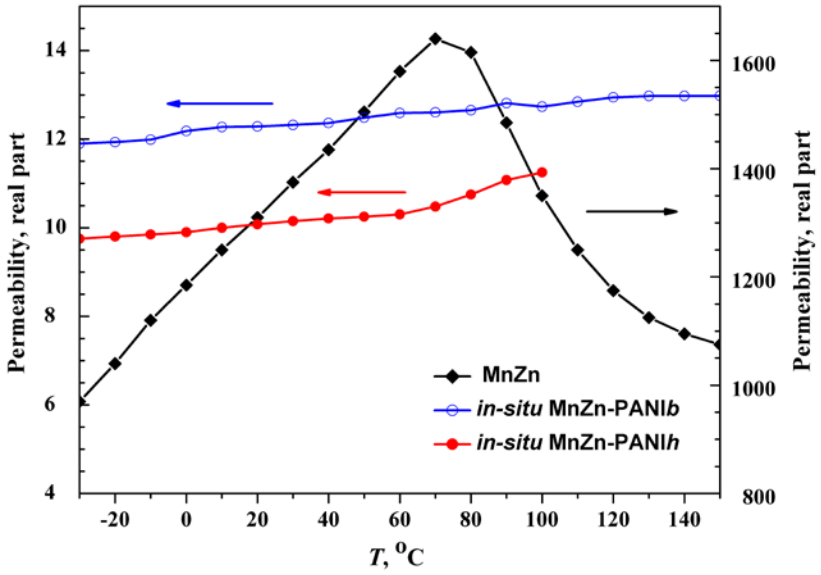

Fig. 21. Temperature dependence of the real part of complex permeability at 1 MHz for MnZn ferrite and its in-situ prepared composites [56].

The main idea in ***Paper III*** was to design a hybrid composite with core-shell structure, which provides increased values of magnetic permeability, while allowing altering the dielectric properties, which are important factors for the engineering of RAMs. The possibility of tuning electromagnetic properties was demonstrated here by an example of a ferrite-polyaniline «core-shell» composite, by incorporating noble metal into the conducting shell of PANI. Namely, it was found that a hybrid composite containing 73 vol. % of MnZn ferrite, 21 vol. % of polyaniline, and 6 vol. % of nano- and submicrometer-size silver particles is characterized by considerably higher value of complex magnetic permeability in the ultra-high frequency range compared to that of the MnZn–PANI composite (ferrite coated by PANI only) with nearly the same concentration of the magnetic phase. The hybrid composite containing silver exhibited an increase in both the real and imaginary parts of the complex permeability by more than one and a half times compared with those of ferrite-polyaniline composite (Fig. 22).

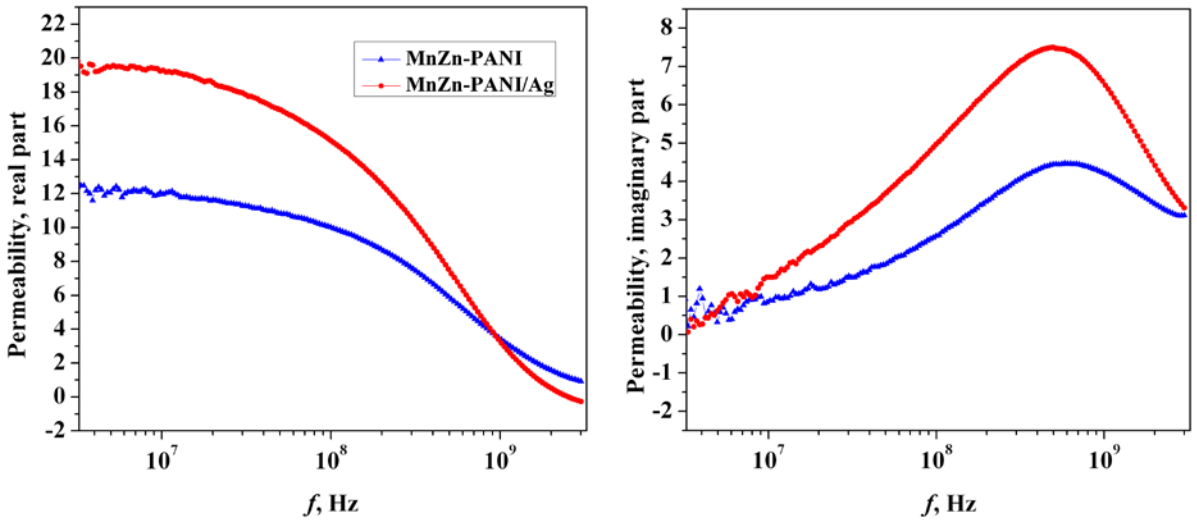

Fig. 22. Magnetic spectra of MnZn-PANI and MnZn-PANI/Ag composites [paper III].

It was proven that the above-mentioned increase in μ cannot be related to the magnetic properties of PANI/Ag shell, since the PANI/Ag shell, just as PANI alone, exhibits linear dependence of magnetization on the external magnetic field, which is typical for diamagnetic materials (Fig 23).

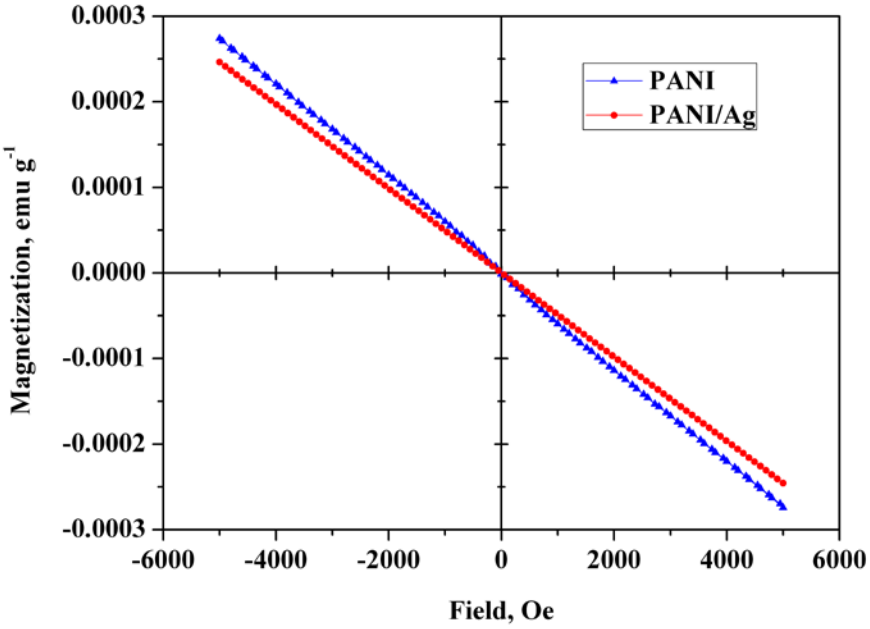

Fig. 23. Magnetization of PANI and PANI/Ag as a function of a DC magnetic field [paper III].

The phenomenon of increased μ of MnZn-PANI/Ag composite is explained in terms of the increased exchange interaction between magnetic atoms in the surface layer of the MnZn ferrite due to the electron exchange between these atoms in the PANI/Ag film.

Paper IV is devoted to the study of the magnetic properties of PANI in different oxidation and protonation states: protonated emeraldine, deprotonated emeraldine and protonated pernigraniline. The sample preparation process did not involve the introduction of magnetic ions into PANI and did not lead to changes in the morphology of the samples. As a result, samples with different electrical conductivity σ and spin concentration were obtained (Table 7).

Table 7. The electrical conductivity and spin density in different forms of polyaniline.

Polyaniline state	Electrical conductivity, (S cm^{-1})	spins density, (spin g^{-1})
Protonated emeraldine	5	10^{20}
Deprotonated emeraldine	10^{-9}	10^{16}
Protonated pernigraniline	$6.4 \cdot 10^{-4}$	not detected

The measured dependences of the magnetization *M* on the external magnetic field *H* shown that, in magnetic fields above 1 kOe, all forms of PANI have the dependence *M*=*M*(*H*),which is characteristic of diamagnetic materials (Fig. 24).

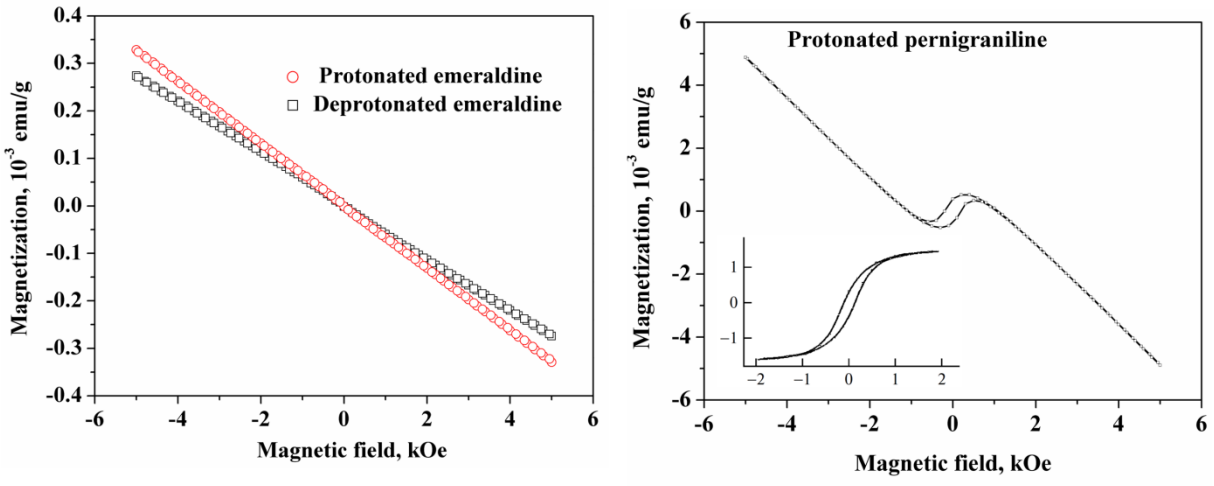

(a) (b)

Fig. 24. Magnetization curves of different forms of PANI. The inset in figure (b) shows, on an enlarged scale, the hysteresis part of the magnetization curve in weak magnetic fields (H < 2 kOe), where the field-linear component is subtracted from the experimentally obtained dependence [85].

The main differences between samples are observed in magnetic fields below 1 kOe. Protonated pernigraniline in the region of small magnetic fields shows the magnetization hysteresis and a positive sign of the susceptibility (Fig. 24 b). It is believed that such behavior of the magnetization is characteristic of a ferro- or ferromagnetic material. It is difficult to explain the nature of PANI magnetism on the basis of experimental data obtained. One of the mechanisms that is responsible for ferro- or ferrimagnetism of PANI is the spin-spin interaction in three-dimensional crystalline areas with densely packed polymer chains formed by the spherical particles of the polymer. These areas were revealed by high-resolution transmission electron microscopy in [86] (Fig. 25).

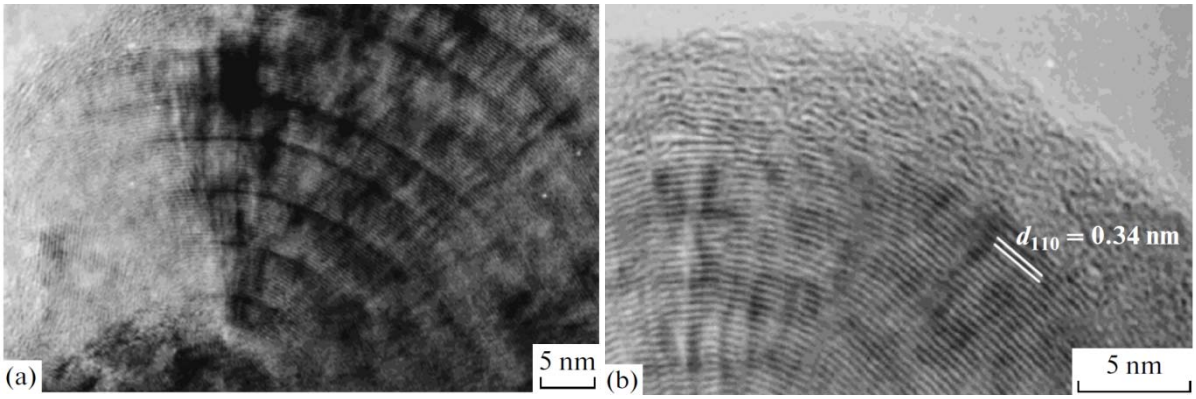

Fig. 25. Crystal structure of the central region of PANI granules (high resolution transmission electron microscopy data). Reproduced from [86].

In such structure, the distance between nitrogen atoms in the neighboring chains, and, hence, the distance between the elementary magnetic moments (spins) of unpaired electrons in nitrogen atoms is 0.6 nm. This distance can provide the exchange interaction between the magnetic moments and, thus giving rise to ferromagnetism. Thus, ferromagnetism in protonated pernigraniline can be associated with crystalline areas. The concentration of these areas in the bulk of the polymer is very low, which can explain the low value of magnetization of the composite.

This study is important for the development of new materials with an unusual combination of properties, providing new opportunities for electronics.

8. CONCLUSIONS

- PMCs based on multicomponent particles with «core–shell» structure have been prepared by *in-situ* oxidative polymerization of aniline in the presence of MnZn ferrite in the reaction media.

  The electrical and magnetic characteristics of MnZn–PANI composites, as well as the electromagnetic properties in the radio-frequency band have been studied.
- It is established that MnZn–PANI composites obtained by *in-situ* polymerization method considerably differ in terms of magnetic properties from the composites obtained by simple mixing of the ferrite with PANI and polymer dielectrics. They show higher coercivity and thermomagnetic stability compared with mixed composites, as well as a high-frequency shift of complex permeability dispersion. The observed phenomenon is explained by interaction between the ferrite surface and PANI film, which results in the damping of domain wall motion in magnetic fields and gives rise to induced magnetic anisotropy.
- The main feature of MnZn–PANI composites is that the value of high-frequency permeability and permittivity, as well as the position of the absorption peak can be tuned by the synthesis conditions and post-polymerization treatment.
- It has been shown that the materials obtained can be effectively applied in the development of RAs.
- Relevant results of this work include the experimental findings on the magnetic properties of protonated pernigraniline, which is important in terms of the design of organic magnets.

BIBLIOGRAPHY

[1] ANNADURAI, P., MALLICK, A.K., TRIPATHY, D.K. Studies on microwave shielding materials based on ferrite- and carbon black-filled EPDM rubber in the X-band frequency. *J. Appl. Polym. Sci.* 2002, vol. 83, no. 1, p. 145-150.

[2] KAZANTSEVA, N.E., RYVKINA, N.G., CHMUTIN, I.A. Promising materials for microwave absorbers. *J. Commun. Technol. Electron.* 2003, vol. 48, no. 2, p. 173-184.

[3] LI, Z.W., CHEN, L., WU, Y., ONG, C.K. Microwave attenuation properties of W-type barium ferrite $BaZn_{2-x}Co_xFe_{16}O_{27}$ composites. *J. Appl. Phys.* 2004, vol. 96, no. 1, p. 534-539.

[4] DOSOUDIL, R., USAKOVA, M., FRANEK, J., SLAMA, J., OLAH, V. RF electromagnetic wave absorbing properties of ferrite polymer composite materials. *J. Magn. Magn. Mater.* 2006, vol. 304, no. 2, p. E755-E757.

[5] FENG, Y.B., QIU, T., SHEN, C.Y., LI, X.Y. Electromagnetic and absorption properties of carbonyl iron/rubber radar absorbing materials. *IEEE Trans. Magn.* 2006, vol. 42, no. 3, p. 363-368.

[6] ABBAS, S.M., DIXIT, A.K., CHATTERJEE, R., GOEL, T.C. Complex permittivity, complex permeability and microwave absorption properties of ferrite-polymer composites. *J. Magn. Magn. Mater.* 2007, vol. 309, no. 1, p. 20-24.

[7] FENG, Y.B., QIU, T., SHEN, C.Y. Absorbing properties and structural design of microwave absorbers based on carbonyl iron and barium ferrite. *J. Magn. Magn. Mater.* 2007, vol. 318, no. 1-2, p. 8-13.

[8] FISKE, T.J., GOKTURK, H., KALYON, D.M. Enhancement of the relative magnetic permeability of polymeric composites with hybrid particulate fillers. *J. Appl. Polym. Sci.* 1997, vol. 65, no. 7, p. 1371-1377.

[9] KASAGI, T., TSUTAOKA, T., HATAKEYAMA, K. Complex permeability of permalloy-ferrite hybrid composite materials. *J. Magn. Magn. Mater.* 2004, vol. 272, no. 3, p. 2224-2226.

[10] SHEN, Y., YUE, Z.X., LI, M., NAN, C.W. Enhanced initial permeability and dielectric constant in a double-percolating $Ni_{0.3}Zn_{0.7}Fe_{1.95}O_4$-Ni-polymer composite. *Adv. Funct. Mater.* 2005, vol. 15, no. 7, p. 1100-1103.

[11] LI, B.W., SHEN, Y., YUE, Z.X., NAN, C.W. High-frequency magnetic and dielectric properties of a three-phase composite of nickel, Co_2Z ferrite, and polymer. *J. Appl. Phys.* 2006, vol. 99, no. 12, article number 123909.

[12] MOUCKA, R., LOPATIN, A.V., KAZANTSEVA, N.E., VILCAKOVA, J., SAHA, P. Enhancement of magnetic losses in hybrid polymer composites with MnZn-ferrite and conductive fillers. *J. Mater. Sci.* 2007, vol. 42, no. 22, p. 9480-9490.
[13] ANHALT, M., WEIDENFELLER, B. Magnetic properties of hybrid-soft magnetic composites. *Mater. Sci. Eng. B-Adv. Funct. Solid-State Mater.* 2009, vol. 162, no. 1, p. 64-67.
[14] KATHIRGAMANATHAN, P. Unusual electromagnetic shielding characteristics of inherently conducting polymer-coated metal-powder polymer composites. *J. Mater. Chem.* 1993, vol. 3, no. 3, p. 259-262.
[15] JAYASEKARA, W.P., BAIN, J.A., KRYDER, M.H. High frequency initial permeability of NiFe and FeAlN. *IEEE Trans. Magn.* 1998, vol. 34, no. 4, p. 1438-1440.
[16] KAZANTSEVA, N.E., VILCAKOVA, J., KRESALEK, V., SAHA, P., SAPURINA, I., STEJSKAL, J. Magnetic behaviour of composites containing polyaniline-coated manganese-zinc ferrite. *J. Magn. Magn. Mater.* 2004, vol. 269, no. 1, p. 30-37.
[17] KAZANTSEVA, N.E., BESPYATYKH, Y.I., SAPURINA, I., STEJSKAL, J., VILCAKOVA, J., SAHA, P. Magnetic materials based on manganese-zinc ferrite with surface-organized polyaniline coating. *J. Magn. Magn. Mater.* 2006, vol. 301, no. 1, p. 155-165.
[18] KAZANTSEVA, N.E., PONOMARENKO, A.T., SHEVCHENKO, V.G., KLASON, C. Magnetically textured composite materials as elements of electromagnetic wave absorbers. *Electromagnetics* 2000, vol. 20, no. 6, p. 453-466.
[19] WEIDENFELLER, B., ANHALT, M., RIEHEMANN, W. Variation of magnetic properties of composites filled with soft magnetic FeCoV particles by particle alignment in a magnetic field. *J. Magn. Magn. Mater.* 2008, vol. 320, no. 14, p. E362-E365.
[20] BESPYATYKH, Y.I., KAZANTSEVA, N.E. Electromagnetic properties of hybrid polymer composites. *J. Commun. Technol. Electron.* 2008, vol. 53, no. 2, p. 143-154.
[21] YAVUZ, O., RAM, M.K., ALDISSI, M., PODDAR, P., HARIHARAN, S. Synthesis and the physical properties of MnZn ferrite and NiMnZn ferrite-polyaniline nanocomposite particles. *J. Mater. Chem.* 2005, vol. 15, no. 7, p. 810-817.

[22] SAPURINA, I., STEJSKAL, J. The mechanism of the oxidative polymerization of aniline and the formation of supramolecular polyaniline structures. *Polym. Int.* 2008, vol. 57, no. 12, p. 1295-1325.
[23] SAPURINA, I.Y., STEJSKAL, J. The effect of pH on the oxidative polymerization of aniline and the morphology and properties of products. *Russ. Chem. Rev.* 2010, vol. 79, no. 12, p. 1123-1143.
[24] N. E. KAZANTSEVA, Magnetic particle-filled polymer microcomposites, in: Sabu Tomas et al. (Eds.), *Polymer Composites*, Weinheim: Willey-VCH, 2012, vol. 1, p. 613–669.
[25] VOLKOV, V.G., SYRKIN, V. G., TOLMASSKII, I. S., *Carbonil Iron*, Moscow, Metallurgy, 1969. 256 p.
[26] WU, L.Z., DING, J., JIANG, H.B., CHEN, L.F., ONG, C.K. Particle size influence to the microwave properties of iron based magnetic particulate composites. *J. Magn. Magn. Mater.* 2005, vol. 285, no. 1-2, p. 233-239.
[27] LIN, G.Q., LI, Z.W., CHEN, L.F., WU, Y.P., ONG, C.K. Influence of demagnetizing field on the permeability of soft magnetic composites. *J. Magn. Magn. Mater.* 2006, vol. 305, no. 2, p. 291-295.
[28] ZHANG, B.S., FENG, Y., XIONG, H., YANG, Y., LU, H.X. Microwave-absorbing properties of De-aggregated flake-shaped carbonyl-iron particle composites at 2-18 GHz. *IEEE Trans. Magn.* 2006, vol. 42, no. 7, p. 1778-1781.
[29] ABSHINOVA, M.A., LOPATIN, A.V., KAZANTSEVA, N.E., VILCAKOVA, J., SAHA, P. Correlation between the microstructure and the electromagnetic properties of carbonyl iron filled polymer composites. *Compos. Pt. A-Appl. Sci. Manuf.* 2007, vol. 38, no. 12, p. 2471-2485.
[30] KIM, I., BAE, S., KIM, J. Composition effect on high frequency properties of carbonyl-iron composites. *Mater. Lett.* 2008, vol. 62, no. 17-18, p. 3043-3046.
[31] ABSHINOVA, M.A., KURITKA, L., KAZANTSEVA, N.E., VILCAKOVA, J., SAHA, P. Thermomagnetic stability and heat-resistance properties of carbonyl iron filled siloxanes. *Mater. Chem. Phys.* 2009, vol. 114, no. 1, p. 78-89.
[32] ABSHINOVA, M.A., KAZANTSEVA, N.E., SAHA, P., SAPURINA, I., KOVAROVA, J., STEJSKAL, J. The enhancement of the oxidation resistance of carbonyl iron by polyaniline coating and consequent changes in electromagnetic properties. *Polym. Degrad. Stabil.* 2008, vol. 93, no. 10, p. 1826-1831.
[33] FULLER, A.J.B., *Ferrites at microwave frequencies*, London, Peter Peregrinus, 1987. 280 p. ISBN 0863410642

[34] SNOEK, J.L. Dispersion and absorption in magnetic ferrites at frequencies above one Mc/s. *Physica* 1948, vol. 14, no. 4, p. 207-217.
[35] LETYUK, L.M., BALBASHOV, A.M., KRUTOGIN, D.G., GONCHAR, A.V., KUDRIASHKIN, I.G., *Production engineering of materials for magneto-electronics*, Moscow, Metallurgy, 1994. 416 p. ISBN 9785229010627
[36] KIM, D.Y., CHUNG, Y.C., KANG, T.W., KIM, H.C. Dependence of microwave absorbing property on ferrite volume fraction in MnZn ferrite-rubber composites. *IEEE Trans. Magn.* 1996, vol. 32, no. 2, p. 555-558.
[37] TSUTAOKA, T. Frequency dispersion of complex permeability in Mn-Zn and Ni-Zn spinel ferrites and their composite materials. *J. Appl. Phys.* 2003, vol. 93, no. 5, p. 2789-2796.
[38] TSUTAOKA, T., UESHIMA, M., TOKUNAGA, T., NAKAMURA, T., HATAKEYAMA, K. Frequency dispersion and temperature-variation of complex permeability of Ni-Zn ferrite composite-materials. *J. Appl. Phys.* 1995, vol. 78, no. 6, p. 3983-3991.
[39] NAKAMURA, T. Snoek's limit in high-frequency permeability of polycrystalline Ni-Zn, Mg-Zn, and Ni-Zn-Cu spinel ferrites. *J. Appl. Phys.* 2000, vol. 88, no. 1, p. 348-353.
[40] HAQUE, M.M., HUQ, M., HAKIM, M.A. Densification, magnetic and dielectric behaviour of Cu-substituted Mg-Zn ferrites. *Mater. Chem. Phys.* 2008, vol. 112, no. 2, p. 580-586.
[41] SILVESTROVICH, M.I., *Microwave ferrite in low fields*, Moscow, 1970.
[42] NAKAMURA, T., MIYAMOTO, T., YAMADA, Y. Complex permeability spectra of polycrystalline Li-Zn ferrite and application to EM-wave absorber. *J. Magn. Magn. Mater.* 2003, vol. 256, no. 1-3, p. 340-347.
[43] CHIKAZUMI, S., GRAHAM, C.D., *Physics of ferromagnetism*, 2nd ed., Oxford, Clarendon Press, 1997. 655 p. ISBN 0198517769.
[44] LANDAU, L.D., LIFSHITS, E.M., SYKES, J.B., BELL, J.S., *Electrodynamics of continuous media*, Oxford, Pergamon, 1960. 417 p. ISBN 0080091059.
[45] SMIT, J., WIJN, H.P.J., *Ferrites : Physical properties of ferrimagnetic oxides in relation to their technical applications*, New York, Wiley, 1959. 369 p.
[46] ROZANOV, K.N., LI, Z.W., CHEN, L.F., KOLEDINTSEVA, M.Y. Microwave permeability of Co(2)Z composites. *J. Appl. Phys.* 2005, vol. 97, no. 1, article number 013905.
[47] TACHIBANA, T., NAKAGAWA, T., TAKADA, Y., SHIMADA, T., YAMAMOTO, T.A. Influence of ion substitution on the magnetic structure and

permeability of Z-type hexagonal Ba-ferrites: $Ba_3Co_{2-x}Fe_{24+x-y}Cr_yO_{41}$. *J. Magn. Magn. Mater.* 2004, vol. 284, no. 1-3, p. 369-375.
[48] LI, Z.W., CHEN, L.F., ONG, C.K. High-frequency magnetic properties of W-type barium-ferrite BaZn2-xCoxFe16O27 composites. *J. Appl. Phys.* 2003, vol. 94, no. 9, p. 5918-5924.
[49] CHO, H.S., KIM, S.S. M-hexaferrites with planar magnetic anisotropy and their application to high-frequency microwave absorbers. *IEEE Trans. Magn.* 1999, vol. 35, no. 5, p. 3151-3153.
[50] NEDKOV, I., CHEPARIN, W., HANAMIROV, A. Ferromagnetic resonance of polycrystalline Al-substituted M-type hexagonal ferrite. *J. Phys-Paris* 1988, vol. 49, no. C-8, p. 945-946.
[51] MATTEI, J.L., LE FLOC'H, M. Effects of the magnetic dilution on the ferrimagnetic resonance of disordered hetero structures. *J. Magn. Magn. Mater.* 2003, vol. 264, no. 1, p. 86-94.
[52] BABAYAN, V., KAZANTSEVA, N.E., MOUCKA, R., SAPURINA, I., SPIVAK, Y.M., MOSHNIKOV, V.A. Combined effect of demagnetizing field and induced magnetic anisotropy on the magnetic properties of manganese-zinc ferrite composites. *J. Magn. Magn. Mater.* 2012, vol. 324, no. 2, p. 161-172.
[53] NAKAMURA, T., TSUTAOKA, T., HATAKEYAMA, K. Frequency dispersion of permeability in ferrite composite-materials. *J. Magn. Magn. Mater.* 1994, vol. 138, no. 3, p. 319-328.
[54] SLAMA, J., DOSOUDIL, R., VICEN, R., GRUSKOVA, A., OLAH, V., HUDEC, I., USAK, E. Frequency dispersion of permeability in ferrite polymer composites. *J. Magn. Magn. Mater.* 2003, vol. 254, p. 195-197.
[55] ANHALT, M., WEIDENFELLER, B., MATTEI, J.L. Inner demagnetization factor in polymer-bonded soft magnetic composites. *J. Magn. Magn. Mater.* 2008, vol. 320, no. 20, p. E844-E848.
[56] BABAYAN, V., KAZANTSEVA, N.E., SAPURINA, I., MOUCKA, R., VILCAKOVA, J., STEJSKAL, J. Magnetoactive feature of in-situ polymerised polyaniline film developed on the surface of manganese-zinc ferrite. *Appl. Surf. Sci.* 2012, vol. 258, no. 19, p. 7707-7716.
[57] CHEVALIER, A., LE FLOC'H, M. Dynamic permeability in soft magnetic composite materials. *J. Appl. Phys.* 2001, vol. 90, no. 7, p. 3462-3465.
[58] MATTEI, J.L., LE FLOC'H, M. Percolative behaviour and demagnetizing effects in disordered heterostructures. *J. Magn. Magn. Mater.* 2003, vol. 257, no. 2-3, p. 335-345.
[59] SIHVOLA, A.H., *Electromagnetic mixing formulas and applications*, London, Institution of Electrical Engineers, 1999. 284 p. ISBN 0852967721.

[60] LAGARKOV, A.N., ROZANOV, K.N. High-frequency behavior of magnetic composites. *J. Magn. Magn. Mater.* 2009, vol. 321, no. 14, p. 2082-2092.
[61] KOLEDINTSEVA, M., ROZANOV, K.N., DREWNIAK, J., Engineering, modeling and testing of composite absorbing materials for EMC applications, in: B. Attaf (Ed.) *Advances in composite materials - ecodesign and analysis,* Rijeka: Intech, 2011, p. 303-316.
[62] ROZANOV, K.N., KOLEDINTSEVA, M.Y., DREWNIAK, J.L. A mixing rule for predicting frequency dependence of material parameters in magnetic composites. *J. Magn. Magn. Mater.* 2012, vol. 324, no. 6, p. 1063-1066.
[63] GARNETT, J.C.M. Colours in metal glasses and in metallic films. *Philos T R Soc Lond* 1904, vol. 203, p. 385-420.
[64] BRUGGEMAN, D.A.G. Calculation of various physics constants in heterogenous substances I Dielectricity constants and conductivity of mixed bodies from isotropic substances. *Ann. Phys-Berlin* 1935, vol. 24, no. 7, p. 636-664.
[65] YAMADA, T., UEDA, T., KITAYAMA, T. Piezoelectricity of a High-Content Lead Zirconate Titanate Polymer Composite. *J. Appl. Phys.* 1982, vol. 53, no. 6, p. 4328-4332.
[66] MUSAL, H.M., HAHN, H.T., BUSH, G.G. Validation of mixture equations for dielectric-magnetic composites. *J. Appl. Phys.* 1988, vol. 63, no. 8, p. 3768-3770.
[67] STARKE, T.K.H., JOHNSTON, C., HILL, S., DOBSON, P., GRANT, P.S. The effect of inhomogeneities in particle distribution on the dielectric properties of composite films. *J. Phys. D-Appl. Phys.* 2006, vol. 39, no. 7, p. 1305-1311.
[68] POLDER, D., VANSANTEN, J.H. The Effective Permeability of Mixtures of Solids. *Physica* 1946, vol. 12, no. 5, p. 257-271.
[69] LOOYENGA, H. Dielectric constants of heterogeneous mixtures. *Physica* 1965, vol. 31, no. 3, p. 401-406.
[70] LICHTENECKER, K. The common root of the logarithmic mixture law and the beginning of the entrophy function. *Phys Z* 1927, vol. 28, p. 417-418.
[71] BERGMAN, D.J., STROUD, D. Physical properties of macroscopically inhomogeneous media. *Solid State Phys.* 1992, vol. 46, no., p. 147-269.
[72] MILTON, G.W. Bounds on the Transport and optical properties of a 2-component composite-material. *J. Appl. Phys.* 1981, vol. 52, no. 8, p. 5294-5304.

[73] PITTINI-YAMADA, Y., PERIGO, E.A., DE HAZAN, Y., NAKAHARA, S. Permeability of hybrid soft magnetic composites. *Acta Mater.* 2011, vol. 59, no. 11, p. 4291-4302.
[74] LI, Z.W., YANG, Z.H., HUANG, R.F., KONG, L.B. Greatly enhanced permeability and expanded bandwidth for spinel ferrite composites with flaky fillers. *IEEE Trans. Microw. Theory Tech.* 2010, vol. 58, no. 11, p. 2794-2799.
[75] PONOMARENKO, V.I., BERZHANSKIY, V.N., ZHURAVLEV, V.N., PERSHINA, Y.D. Permittivity and permeability of a synthetic dielectric with metal-plated ferrite particles at microwave frequencies. *Soviet journal of communications technology and electronics* 1991, vol. 36, no., p. 133-136.
[76] PAN, X.F., SHEN, H.G., QIU, J.X., GU, M.Y. Preparation, complex permittivity and permeability of the electroless Ni-P deposited strontium ferrite powder. *Mater Chem Phys* 2007, vol. 101, no. 2-3, p. 505-508.
[77] BLINOVA, N.V., STEJSKAL, J., TRCHOVA, M., SAPURINA, I., CIRIC-MARJANOVIC, G. The oxidation of aniline with silver nitrate to polyaniline-silver composites. *Polymer* 2009, vol. 50, no. 1, p. 50-56.
[78] LOPATIN, A.V., KAZANTSEV, Y.N., KAZANTSEVA, N.E., APLETALIN, V.N., MAL'TSEV, V.P., SHATROV, A.D., SAHA, P. Radio absorbers based on magnetic polymer composites and frequency-selective surfaces. *J. Commun. Technol. Electron.* 2008, vol. 53, no. 9, p. 1114-1122.
[79] LOPATIN, A.V., KAZANTSEVA, N.E., KAZANTSEV, Y.N., D'YAKONOVA, O.A., VILCAKOVA, J., SAHA, P. The efficiency of application of magnetic polymer composites as radio-absorbing materials. *J. Commun. Technol. Electron.* 2008, vol. 53, no. 5, p. 487-496.
[80] KAZANTSEV, Y.N., LOPATIN, A.V., KAZANTSEVA, N.E., SHATROV, A.D., MAL'TSEV, V.P., VILCAKOVA, J., SAHA, P. Broadening of Operating Frequency Band of Magnetic-Type Radio Absorbers by FSS Incorporation. *IEEE Trans. Antennas Propag.* 2010, vol. 58, no. 4, p. 1227-1235.
[81] BABAYAN, V.A., KAZANTSEV, Y.N., LOPATIN, A.V., MAL'TSEV, V.P., KAZANTSEVA, N.E. Extension of the Operating Frequency Range of a Dielectric Radio Absorber with the Help of Frequency-Selective Surfaces. *J. Commun. Technol. Electron.* 2011, vol. 56, no. 11, p. 1357-1362.
[82] ABBAS, S.M., AIYAR, R.P.R.C., PRAKASH, O. Synthesis and microwave absorption studies of ferrite paint. *Bull. Mat. Sci.* 1998, vol. 21, no. 4, p. 279-282.
[83] CHANDRASEKHAR, P., NAISHADHAM, K. Broadband microwave absorption and shielding properties of a poly(aniline). *Synth. Met.* 1999, vol. 105, no. 2, p. 115-120.
[84] ZAKHARYEV, L.N., LEMANSKII, A.A., *Wave scattering by "black bodies"*, Moscow, Sov. Radio, 1972. 288 p.

[85] KOMPAN, M.E., SAPURINA, I.Y., BABAYAN, V., KAZANTSEVA, N.E. Electrically conductive polyaniline–a molecular magnet with the possibility of chemically controlling the magnetic properties. *Phys. Solid State* 2012, vol. 54, no. 12, p. 2412-2418.
[86] MAZEROLLES, L., FOLCH, S., COLOMBAN, P. Study of polyanilines by high-resolution electron microscopy. *Macromolecules* 1999, vol. 32, no. 25, p. 8504-8508.

CURRICULUM VITAE

Personal information	
Surname(s) / First name(s)	Babayan Vladimir
Address(es)	nam. T.G.M. 3050,76001 Zlín, Czech Republic
Telephone(s)	+420 57 603 8112 mobile +420 777 817 404
E-mail	Babayan@ft.utb.cz
Nationality	Armenian
Date of birth	6th September 1985
Work experience	
Dates	March 2010 – present
Occupation or position held	Research project stuff
Name of employer	Tomas Bata University in Zlín, University Institute , Czech Republic
Dates	March 2006 - November 2008
Occupation or position held	Designer-Engineer
Name of employer	H_2 Economy , CJSC, Yerevan, Armenia
Education and training	
Dates	2009–present
Title of qualification awarded	PhD study
Principal branch	Technology of Macromolecular Substances
Name and type of organisation providing education and training	Tomas Bata University in Zlín, Faculty of Technology, Czech Republic
Dates	2003–2008
Title of qualification awarded	M.Sc.
Principal branch	Mechanical Engineering
Name and type of organisation providing education and training	State Engineering University of Armenia

Projects

2012	IGA/FT/2012/033, Synthesis and characterization of iron oxide based nanocomposites for application in magnetic mediated hyperthermia, member of research team
Since 2011	Centre of Polymer Systems (reg. number: CZ.1.05/2.1.00/03.0111), member of research team

2011 IGA/7/FT/11/D, Electromagnetic properties regulation in magnetic composite materials, solver

2010 IGA/25/FT/10/D, Ferrofluids, member of research team

Publications

1. BABAYAN, V., KAZANTSEVA, N. E., SAPURINA, I., MOUCKA, R., VILCAKOVA, J., STEJSKAL, J. Magnetoactive feature of in-situ polymerisedpolyaniline film developed on the surface of manganese–zinc ferrite. *Appl. Surf. Sci*. 2012, vol. 258, no. 19, p. 7707–7716.

2. BABAYAN, V., KAZANTSEVA, N. E., MOUCKA, R., SAPURINA, I., SPIVAK, Y.M., MOSHNIKOV, V.A. Combined effect of demagnetizing field and induced magnetic anisotropy on the magnetic properties of manganese–zinc ferrite composites. *J. Magn. Magn.Mater*.2012, vol. 324, no. 2, p. 161-172.

3. BABAYAN, V., KAZANTSEVA, N. E., SAPURINA, I., MOUCKA, R., STEJSKAL, J., SÁHA, P. Increasing the high-frequency magnetic permeability of MnZn ferrite in polyaniline composites by incorporating silver. Submitted for publication to *J. Magn.Magn.Mater.* (manuscript number MAGMA-D-12-00986R1).

4. KOMPAN, M. E., SAPURINA, I. Yu., BABAYAN, V., KAZANTSEVA, N. E. Electrically conductive polyaniline–molecular magnet with the possibility of chemically controlling the magnetic properties. *Phys. Solid State* 2012, vol. 54, no. 12, p. 2412-2418.

5. BABAYAN, V.A., KAZANTSEV, YU. N., LOPATIN, A. V., MAL'TSEV, V. P., KAZANTSEVA, N. E. Extension of the operating frequency range of a dielectric radio absorber with the help of frequency-selective surfaces. *J. Commun. Technol. Electron.* 2011, vol. 56, no. 11, p. 1357-1362.

6. HAKOBYAN, T.A., BABAYAN, V.A. et al PEM fuel cell end plates optimization and investigation of operating characteristics. *Proceedings of Engineering Academy of Armenia* 2007, vol. 4, no. 1, p. 64-67.

7. HAKOBYAN, T., BABAYAN, V. et al Supply gases pressure drop observation in the fuel cells. *State Engineering University of Armenia, Collection of Annual Scientific Seminar Materials* 2006, vol. 1, no. 1, p. 288-291.

8. HAKOBYAN, T.A., BABAYAN, V.A. et al Design, assembly and investigation of an air breathing fuel cell. *Proceedings of Engineering Academy of Armenia* 2006, vol. 3, no. 4, p. 625-628.

Presentations at conferences

1. BABAYAN, V., KAZANTSEVA, N., VILČÁKOVÁ, J., MOUČKA, R., SÁHA, P. The effect of polyaniline coating on the magnetic properties of manganese-zinc–polyaniline core–shell composites. In: PLASTKO 2012, April 11th-12th, Zlín (Czech Republic).
2. KAZANTSEVA, N. E., BABAYAN, V., MOUČKA, R., VILČÁKOVÁ, J., SÁHA, P., SAPURINA, I. YU., STEJSKAL, J. Effect of polyaniline coating on magnetic properties of MnZn ferrite. In: Electromagnetic field and materials, 19th International Conference, November 18^{th}–20^{th} 2011, Moscow (Russian Federation), p. 509-527.
3. BABAYAN, V., KAZANTSEVA, N. E., MOUCKA, R., VILCAKOVA, J., SAHA, P., SAPURINA, I. YU. and STEJSKAL, J. Electromagnetic properties regulation in MnZn polyaniline composites. *In*: EUROMAT 2011, European Congress and Exhibition on Advanced Materials and Processes, September 12^{th}-15^{th}, Montpellier (France).
4. KAZANTSEVA, N. E., BABAYAN, V., MOUČKA, R., VILČÁKOVÁ, J., SÁHA, P., SAPURINA, I. YU., STEJSKAL, J. Magnetoactive feature of polyaniline coating on the surface of Manganes-Zinc ferrite. *In*: Conducting polymers 2011, 75^{th} Prague Meeting on Macromolecules, July 10^{th}-14^{th}, Prague (Czech Republic).
5. BABAYAN, V., KAZANTSEVA, N., VILČÁKOVÁ, J., MOUČKA, R., SÁHA, P., SAPURINA, I.YU. AND STEJSKAL, J. Polymer magnetic composites with enhanced permeability in RF band. *In*: JEMS 2010,Joint European Magnetic Symposia, August 23^{th}-28^{th}, Krakow (Poland).
6. KOZAKOVA, Z., BAZANT, P., MACHOVSKY, M., BABAYAN, V. and KURITKA, I. Fast microwave-assisted synthesis of uniform magnetic nanoparticles. In: 14th Czech and Slovak Conference on Magnetism, July 6th-9th, Košice (Slovakia).
7. BABAYAN, V., KAZANTSEVA, N., VILČÁKOVÁ, J., MOUČKA, R. and SÁHA, P. Magnetostatic and magnetodynamic properties of polymer magnetic composites. In: PLASTKO 2010, April 13th-14th, Zlín (Czech Republic).

PAPER I

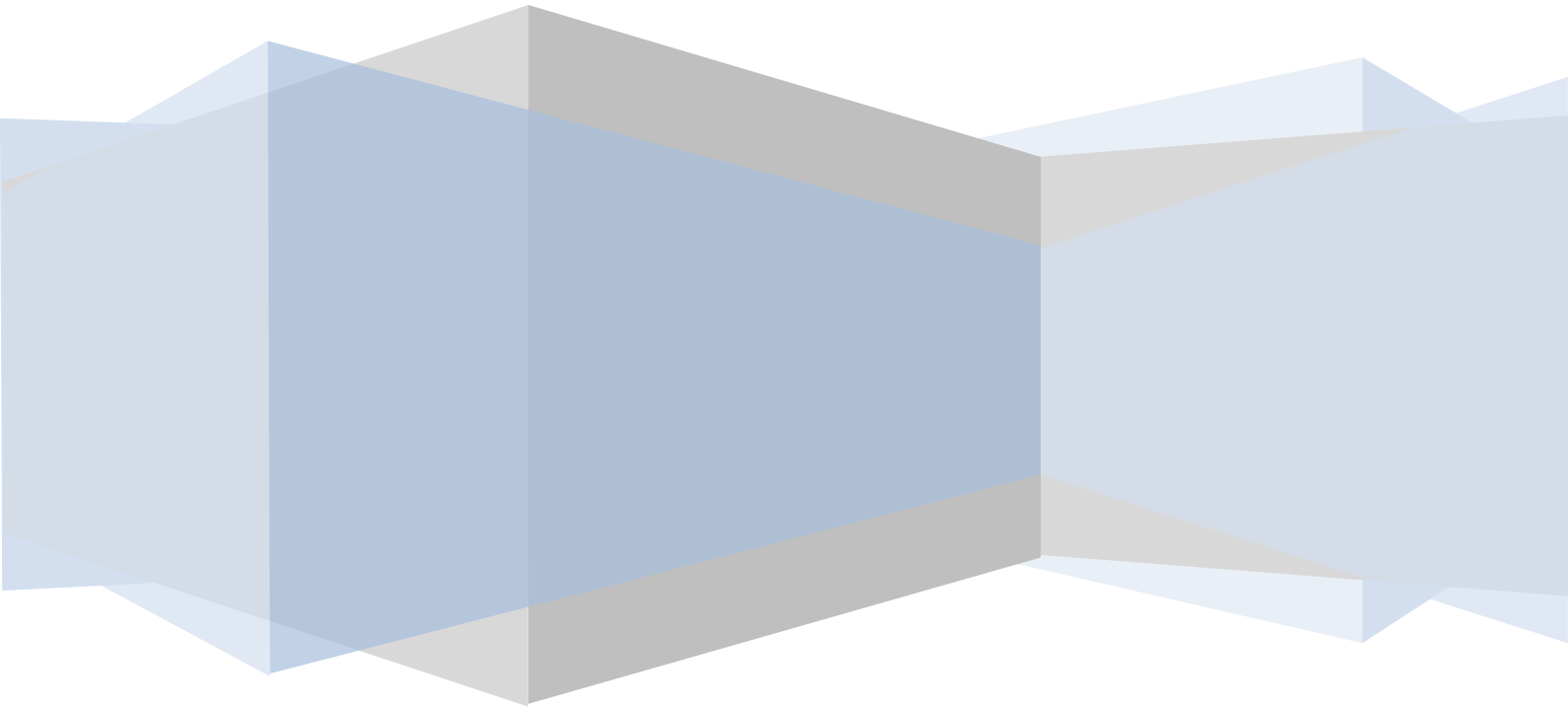

Journal of Magnetism and Magnetic Materials 324 (2012) 161–172

Contents lists available at ScienceDirect

Journal of Magnetism and Magnetic Materials

journal homepage: www.elsevier.com/locate/jmmm

Combined effect of demagnetizing field and induced magnetic anisotropy on the magnetic properties of manganese–zinc ferrite composites

V. Babayan [a], N.E. Kazantseva [a,*], R. Moučka [a], I. Sapurina [b], Yu.M. Spivak [c], V.A. Moshnikov [c]

[a] Centre of Polymer Systems, Polymer Centre, Tomas Bata University in Zlin, nám T. G. Masaryka 5555, 760 01 Zlin, Czech Republic
[b] Institute of Macromolecular Compounds, Russian Academy of Sciences, 199004 St. Petersburg, Russia
[c] St. Petersburg Electrotechnical University "LETI", 197376 St. Petersburg , Russia

ARTICLE INFO

Article history:
Received 21 June 2011
Received in revised form
29 July 2011
Available online 6 August 2011

Keywords:
MnZn ferrite
Ferromagnetic material
Dynamic magnetization process
Magnetic anisotropy
Magnetic permeability
Coated particle
Polyaniline
Conducting polymer

ABSTRACT

This work is devoted to the analysis of factors responsible for the high-frequency shift of the complex permeability (μ^*) dispersion region in polymer composites of manganese–zinc (MnZn) ferrite, as well as to the increase in their thermomagnetic stability. The magnetic spectra of the ferrite and its composites with polyurethane (MnZn–PU) and polyaniline (MnZn–PANI) are measured in the frequency range from 1 MHz to 3 GHz in a longitudinal magnetization field of up to 700 Oe and in the temperature interval from -20 °C to $+150$ °C. The approximation of the magnetic spectra by a model, which takes into account the role of domain wall motion and magnetization rotation, allows one to determine the specific contribution of resonance processes associated with domain wall motion and the natural ferromagnetic resonance to the μ^*. It is established that, at high frequencies, the μ^* of the MnZn ferrite is determined solely by magnetization rotation, which occurs in the region of natural ferromagnetic resonance when the ferrite is in the "single domain" state. In the polymer composites of the MnZn ferrite, the high-frequency permeability is also determined mainly by the magnetization rotation; however, up to high values of magnetizing fields, there is a contribution of domain wall motion, thus the "single domain" state in ferrite is not reached. The frequency and temperature dependence of μ^* in polymer composites are governed by demagnetizing field and the induced magnetic anisotropy. The contribution of the induced magnetic anisotropy is crucial for MnZn–PANI. It is attributed to the elastic stresses that arise due to the domain wall pinning by a polyaniline film adsorbed on the surface of the ferrite during *in-situ* polymerization.

1. Introduction

MnZn ferrites containing a small amount of ferrous iron cations (Fe^{2+}) are characterized by low magnetocrystalline anisotropy, and as a result, by high initial magnetic permeability (μ_i). The last factor is responsible for the traditional application of MnZn ceramic as a material for the elements of electronic devices as well as a disperse magnetic filler for polymer radioabsorbing materials [1–3]. The values of μ_i of MnZn ceramic may vary from 1000 to 10,000 and higher, depending on the chemical composition and the specific features of the synthesis. The Fe^{2+} cations are responsible for the low values of resistivity of MnZn ferrite. Depending on the concentration of Fe^{2+}, the conductivity varies from 2×10^{-2} to 5×10^{-4} S m cm^{-1}. The low resistivity is the main obstacle to the use of MnZn ceramic at high frequencies because of their high eddy-current losses and, as a consequence, the skin effect. In most cases, the critical frequencies (f_c) of high-permeability MnZn ferrites lie near 1 MHz. To reduce eddy current losses, one uses special additions to the working mixture for producing ferrite, for example, CaO and SiO_2, which ensure the electric and magnetic isolation of individual grains (crystallites). As a result, one obtains an increase in f_c to ~5 MHz and higher thermal stability (the relative temperature coefficient of magnetic permeability $\alpha_\mu\times10^{-6}$ °C varies from -0.1 to -0.2); however, this leads to a significant decrease in μ_i.

Similar changes in properties are also observed in composite ferrimagnets that represent a conglomerate of finely dispersed ferrite powder and a dielectric. The insulation of ferrite particles by dielectric leads to a considerable decrease in the skin effect, a shift of the complex permeability dispersion region to higher frequencies, a decrease (by orders of magnitude) in μ^*, and an increase in its thermal stability compared with ferrite ceramic [4–7]. The variation of the magnetic properties is associated with the structural inhomogeneity of composite magnetic materials. Non-uniform distribution of magnetization over the bulk of material is responsible for the interphase polarization and the formation of effective magnetic charges/dipoles. As a result, the effective magnetic field acting on a magnetic particle decreases by the value of the demagnetizing field,

* Correspondence to: Polymer Centre, Faculty of Technology Tomas Bata University in Zlin, T. G. Masaryk Sq. 275, 762 72 Zlin, Czech Republic. Tel.: +420 576 038 114; fax: +420 576 031 444.
E-mail address: nekazan@yahoo.com (N.E. Kazantseva).

0304-8853/$ - see front matter © 2011 Elsevier B.V. All rights reserved.
doi:10.1016/j.jmmm.2011.08.002

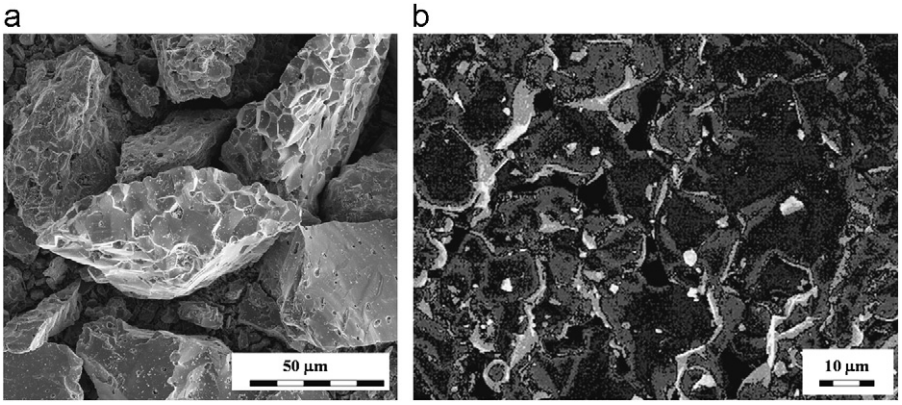

Fig. 1. SEM image of MnZn ferrite: (a) grinded ferrite (b) the surface of ferrite particle.

which is proportional to the demagnetization factor [8–10]. It is also assumed that the magnetic spectra of composites containing magnetically soft ferrites are mainly determined by the magnetization rotation of relaxation type.

A specific feature of the magnetic spectra of MnZn ferrites is their single-dispersion character, which is associated with the superposition of domain-wall motion resonances (DWRs) and the natural ferromagnetic resonance (NFR) [11]. The relative specific contributions of DWR and NFR to the complex permeability of MnZn ferrites, just as of other ferrites, are determined by the domain structure of ferrite: the size of crystallites (grains), the properties of domain walls, and quasi-elastic domain wall pinning forces. Polymer composites filled with ferrites are also characterized by single-dispersion magnetic spectra, with the difference that the complex permeability dispersion region lies in the high-frequency part of the radio-frequency band. In this case, the relation between DWR and NFR depends on both the domain structure of ferrite and the concentration of ferrite particles in the polymer. To optimize the electromagnetic properties of polymer magnetic composites, in particular, to increase the value of μ^* in the ultrahigh frequency (UHF) and microwave bands, it is important to have information on the specific contributions of DWR and NFR to μ^*. The analysis of the magnetic spectra of ferrites and their composites as a function of a DC magnetizing field (H_{DC}) allows one to sufficiently accurately evaluate the effect of various magnetization processes on μ^* [9,12–15]. Extreme configurations in the analysis of magnetic spectra as a function of H_{DC} are the longitudinal magnetization, when H_{DC} is parallel to the AC magnetic field H_{AC}, and the transverse magnetization, when these fields are perpendicular.

This work is devoted to the analysis of factors that lead to the high-frequency shift of the complex permeability dispersion region and to the increase in the thermomagnetic stability of polymer composites of high-permeability MnZn ferrite. To this end, we evaluate the effects of domain wall motion and magnetization rotation on the high-frequency permeability of magnetic materials. The procedure consists in analyzing the magnetic spectra as a function of a DC magnetizing field and temperature, followed by the approximation of the magnetic spectra with the frequency dispersion formula that takes into account domain wall motion and magnetization rotation [16].

2. Experimental

2.1. Materials and sample Preparation

Sintered MnZn ferrite with spinal structure that was used in this study is a commercially available low-frequency sintered ferrite core for weak magnetic fields (3000-NM, produced by Ferropribor, Russian Federation) with an initial magnetic permeability of $\mu_i \sim 2700–3000$, a maximum magnetic permeability of $\mu_{max} \sim 3700–5200$, a saturation magnetization of $M_s = 3.5$ kOe, low magnetocrystalline anisotropy, a Curie temperature of $T_C \sim 200$ °C, a conductivity of $\sigma_f = 2 \times 10^{-2}$ S cm^{-1}, and a density of $\rho_f = 4.8$ g cm^{-3}. The composition of this ferrite is 53.75 mol% of Fe_2O_3, 26.10 mol% of MnO, and 21.15 mol% of ZnO. Ferrite particles of random shape were obtained by mechanical grinding of sintered MnZn ferrite cores in a ball mill. The resulting ferrite powder was disseminated using a set of sieves so that the particle size distribution was controlled to be between 40 and 80 μm (the mean particle size is of 60 μm). The scanning electron microscopy (SEM) image of ferrite particles are the evidence of it.(Fig. 1).

MnZn–PU composite was prepared by mixing ferrite particles with prepolymer (AXSON UR 3420, Axson; France) and pressing between two metallic plates separated by a spacer. Samples were kept at 80 °C in vacuum for 4 h. The volume fraction of ferrite in the composite was calculated from the density by assuming the additivity of densities of the constituents, polycrystalline MnZn ferrite (4.8 g cm^{-3}) and polyurethane (PU) matrix (1.02 g cm^{-3}), and amounted to 40 vol%. Toroidal samples for permeability measurements were cut out of composite plates by a screw press.

MnZn–PANI composites were prepared by oxidative *in-situ* polymerization of aniline on the surface of ferrite particles [17,18]. The polymerization was performed by mixing an aqueous solution of aniline hydrochloride (0.2 M) with ammonium peroxydisulfate (0.25 M) at room temperature. The mass concentration of ferrite was chosen to be ten times higher than that of aniline salt. The mixture was stirred during the polymerization of aniline, which was completed within 1 h. Next day, ferrite particles coated with PANI were collected on a paper filter, rinsed with dilute hydrochloric acid and acetone, and dried. The typical PANI film thickness was about 200 nm. The coated particles contained ~10 wt% of PANI hydrochloride and had a conductivity of 0.34 S cm^{-1} after being compressed into a pellet at 200 MPa. The PANI hydrochloride prepared in the absence of ferrite had a conductivity of 4.4 S cm^{-1}.

To analyze the structure and the growth dynamics of a conductive PANI film on the surface of MnZn ferrite by an atomic force microscope (AFM), the PANI film was deposited on a single crystal MnZn ferrite (with elemental composition similar to that of 3000-NM MnZn ferrite) during the standard polymerization procedure described above. The growth dynamics of the polymer layer was analyzed by the "interrupted polymerization" technique [19]. Samples (plates) of MnZn ferrite were withdrawn from the polymerization medium at different stages of synthesis and washed out of the traces of the monomer and oxidant.

2.2. Characterization

2.2.1. Structural characterization

2.2.1.1. Microscopy. The structural characterization of ferrite particles and ferrite particles coated with polyaniline hydrochloride was carried out by Scanning Electron Microscopy (JEOL JXA 733; Superprobe microscope).

To study the structure and the growth dynamics of a conductive PANI film on the surface of MnZn ferrite by an AFM, we used the following equipment: an Ntegra Terma probe nanolaboratory (NT-MDT) and a JSPM-5400 scanning probe microscope (JEOL). The investigations were carried out with the use of NSG01 silicon probes (NT-MDT) with an elasticity constant of about 2.5–10 N/m and a rounding-off radius of $\geq$10 nm. The AFM data on the surface were compared with the phase contrast data of the same region of the surface. The data were recorded by the AFM operating in the semicontact mode with amplitude feedback. The phase contrast of the surface in this mode is formed by the vibrations of the probe whose phase shift is determined by the morphology of the surface, the distribution of mechanical, magnetic, electrophysical, adhesive properties of the surface, and the inhomogeneity of the chemical composition [20]. To separate different contributions to the phase contrast and obtain additional information on the properties of the surface, we applied different techniques, including the combined analysis of data on the surface using different analytical responses [21].

2.2.2. Magnetic properties

The magnetization measurements were performed by a Vibrating Sample Magnetometer (Lake Shore 7404) in a magnetic field of up to 5 kOe. The measurements of samples in the form of toroids and powders were carried out at room temperature in air atmosphere.

The complex permeability spectra of MnZn ferrite and its composites were studied in the frequency range from 40 Hz to 3 GHz by the impedance method using Impedance/Material Analyzers (Agilent 4294 A in the frequency interval from 40 Hz to 110 MHz, and Agilent E4991A in the interval from 1 MHz to 3 GHz). The measurements were carried out on toroidal samples with an inner diameter of 3.1 mm and an outer diameter of 8 mm. The thickness of the samples was controlled to be less than 2 mm to avoid the skin effect.

The complex permeability measurements in an external DC magnetic field of up to 700 Oe were performed using commercially available permanent magnets based on M-type barium hexaferrite, which were arranged so that the DC-magnetic field was applied parallel to the AC magnetic field. The schematic diagram of the measurement setup is shown in Fig. 2. The DC magnetic field strength was controlled by changing the distance between the permanent magnets, and was measured in the vicinity of a sample by a microprocessor-controlled teslameter (ELIMAG MP-1). The homogeneity of the magnetic field was provided by a large area of permanent magnet poles (200 cm^2), which is much greater than the sample size (the outer diameter and the thickness of toroidal samples are 8 mm and about 2 mm, respectively).

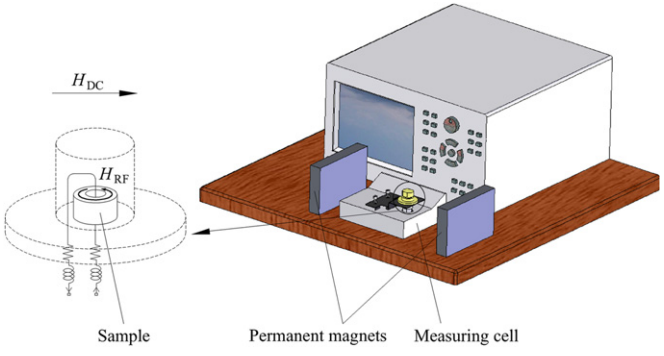

Fig. 2. The experimental setup for the measurement of the frequency dependence of complex magnetic permeability (impedance method) in a longitudinal magnetization field. The directions of external DC magnetizing field (H_{DC}) and high-frequency AC magnetic field (H_{RF}) are shown in the schematic view of a measuring cell with a toroidal sample.

The temperature dependence of permeability in the frequency range from 1 MHz to 3 GHz was investigated at a series of temperature points ranging from –20 °C to 150 °C with a step of 10 °C with the use of a temperature chamber (Espec SU 271, Japan). The measurements of the complex permeability of the composites were limited to a temperature of 100 °C because of the thermal destruction of polymers at higher temperatures.

3. Results

3.1. Magnetostatic properties

Fig. 3 shows the magnetization curves of MnZn ferrite and MnZn–PU and MnZn–PANI composites measured on toroidal samples and powders. The saturation magnetization (M_s) of the samples is reached in fields on the order of 3500–4000 Oe. The main magnetostatic parameters of the samples are presented in Table 1. One can see that both the saturation magnetization M_s and the coercivity H_c of different samples exhibit appreciable difference. As expected, the saturation magnetization of the composites is smaller than those of the ferrites. On the other hand, the composites have higher H_c than the ferrite. It is noteworthy that the coercivity of the MnZn–PANI composite is higher than that of a composite obtained by simply mixing MnZn ferrite with polyaniline powder (MnZn–PANI-*mix*).

3.2. Frequency-field dependence of complex permeability

The magnetic spectrum of MnZn ferrite in the absence of H_{DC} shows a mixed-type dispersion—an increase in μ' at frequencies of about 300 kHz and a sharp decrease from $\mu'=1800$ to $\mu'=1$ at $\sim$200 MHz (Fig. 4a). The magnetic loss peak is rather wide, with a maximum of $\mu''_{max}\sim850$ at resonance frequency $f_r\sim1.3$ MHz. The samples exhibit an asymmetry of the resonance curve with a steeper slope on the low-frequency side. The application of H_{DC} parallel to the radio-frequency field (H_{RF}) deforms the magnetic spectrum, especially the loss curve (Fig. 5). As the magnetizing field strength increases, the magnetic dispersion region is shifted to higher frequencies, the μ' decreases, and the width of the resonance curve increases and reaches its maximum at $H_{DC}=200$ Oe (Fig. 3c). For $H_{DC}=225$ Oe, the asymmetry of the resonance curve has the opposite shape: with a steeper slope on the high-frequency side (Fig. 4d). For $H_{DC}=270$ Oe, the magnetic spectrum takes the form of a Debye relaxation spectrum with $\omega=1/\tau$, where $\omega=2\pi f$ is the relaxation frequency and τ is the relaxation time (Fig. 4e). A further increase in the DC magnetic field strength leads to a considerable decrease in μ''_{max} and to a shift of the f_r closer to 1 GHz (Fig. 5).

Compared with the magnetic spectra of MnZn ferrite, the complex permeability dispersion region in MnZn–PU and MnZn–PANI is significantly shifted to the high-frequency part of the radio-frequency band, and the spectrum has a relaxation character (Figs. 6 and 7). As the field strength H_{DC} increases, f_r is shifted to the gigahertz band. The difference between the spectra of the composites is that, in MnZn–PU, the μ''_{max} remains virtually constant ($\mu''_{max}\sim2.4$) as H_{DC} increases, and even slightly increases for $H_{DC}\geq200$ Oe, whereas, in MnZn–PANI, μ''_{max} decreases from $\sim$4.5 to $\sim$3.5 as H_{DC} increases to 300 Oe.

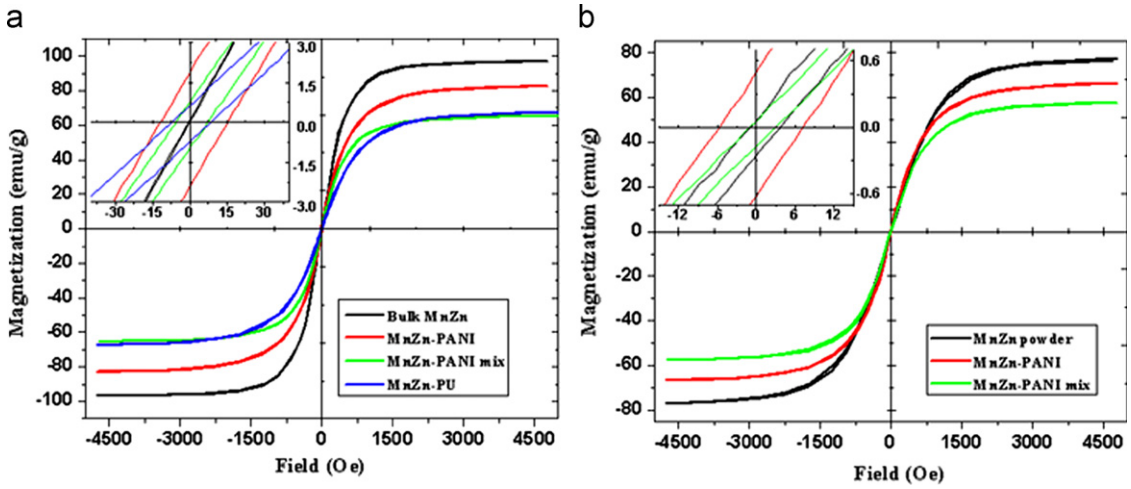

Fig. 3. The magnetization curves of MnZn ferrite and its polymer composites: MnZn–PU, MnZn–PANI, MnZn–PANI-*mix*, measured on a toroidal (a) and powder (b) samples.

Table 1
Saturation magnetization and coercitivity of manganese-zinc ferrite and its polymer composites measured on toroidal and powder samples.

Sample name	Coercivity (Oe)		Saturation magnetization (emu/g)	
	Toroid	Powder	Toroid	Powder
Bulk MnZn	0.24	2.2	96.9	77.2
MnZn–PANI	13.5	6.5	82.8	66.5
MnZn–PU	7.9	–	68.6	–
MnZn–PANI mix (10 wt% PANI)	6.4	2.2	66.7	58.6

We approximated the magnetic spectra by the frequency dispersion formula, according to which the magnetization due to domain wall motion exhibits resonance behavior, while the rotation of the magnetization vector exhibits relaxation behavior [16]

$$\mu = 1+\chi_s+\chi_{dw} = 1+\frac{\chi_{s0}}{1+j(f/f_s)}+\frac{\chi_{d0}f_d^2}{f_d^2-f^2+j\beta f}$$

where μ is the magnetic permeability, χ_s and χ_{dw} correspond to the magnetic susceptibilities due to spin rotation and domain wall motion, respectively, f_d and f_s are the resonance frequencies of the domain wall and spin components, respectively, χ_{d0} and χ_{s0} are the static magnetic susceptibilities of each component, β is the damping factor, and f is the electromagnetic field frequency. The dispersion parameters (f_d, f_s, χ_{d0}, χ_{s0}, and β) are determined from the approximation of the experimental magnetic spectra by a nonlinear least-square fitting method.

The results of approximation have shown that magnetization processes in MnZn ferrite in the low-frequency part of the radio-frequency band are equally attributed to the domain wall motion and magnetization rotation, whereas, in the high-frequency part, they are attributed solely to magnetization rotation. The dominant role in the magnetization dynamics of MnZn–PU and MnZn–PANI is played by the magnetization rotation; however, the contribution of domain wall motion to μ^* manifests itself up to very high values of H_{DC}.

3.3. Temperature–frequency dependence of the complex permeability

The temperature–frequency dependence of the complex permeability of MnZn ferrite and its composites is demonstrated in Figs. 8–10. In the case of MnZn ceramic, as temperature increases, the magnetic dispersion region is shifted to lower frequencies, and the temperature dependence of μ' and μ'' has a maximum at 70 °C followed by a decrease and further increase in μ' and μ'' up to 150 °C: $\mu'_{1\ MHz}$ (70 °C)=1600 and μ''_{max} (70 °C)=1200, while $\mu'_{1\ MHz}$ (150 °C)=1075 and μ''_{max} (150 °C)=840 (Fig. 8). MnZn ferrite composites exhibit thermal stability in the temperature interval from −20 °C to +100 °C (Figs. 9 and 10). In MnZn–PU, the μ^* remains nearly constant as temperature increases, and f_r is shifted to lower frequencies, whereas, in MnZn–PANI, neither μ^* nor f_r show any variation as temperature increases.

4. Discussion

The magnetization dynamics of polycrystalline ferrites in the radio-frequency band is determined by domain wall motion, rotation of the magnetization vector in domains and domain walls, as well as by the NFR [22]. The low-frequency part of the magnetic spectrum may exhibit either resonance or relaxation character, which depends on the domain structure, the properties of the domain walls, and the quasielastic domain wall pinning forces.

Usually, the NFR is observed in the high-frequency part of the radio-frequency band and the microwave band. The character of magnetic dispersion in the region of the NFR is determined by the magnetic anisotropy, namely, by the specific contribution of magnetocrystalline anisotropy, magnetic-dipole anisotropy, the anisotropy of elastic stresses (magnetoelastic anisotropy or magnetostrictive anisotropy), shape anisotropy, surface magnetic anisotropy, etc. Here the domain structure manifests itself in the distribution of NFR frequencies from $\omega_{min}=2\gamma H_{eff}$ to $\omega_{max}=2\gamma H_{eff}+4\pi M_s$, where γ is the gyromagnetic ratio and H_{eff} is the effective magnetic anisotropy. Such a distribution of resonance frequencies is associated with the internal dynamic magnetic field, which results from the precession of magnetic moments in domain walls. The values of this field depend on the orientation of the magnetization vector with respect to the external magnetic field. Thus, the characteristic frequencies of the magnetic spectrum are structure-sensitive parameters.

4.1. Magnetic spectrum of polycrystalline MnZn ferrite: contributions of domain wall motion and magnetization rotation

A micrograph of the surface of a 3000-NM polycrystalline MnZn ferrite (Fig. 1b) shows that this is a coarse-grain ferrite with

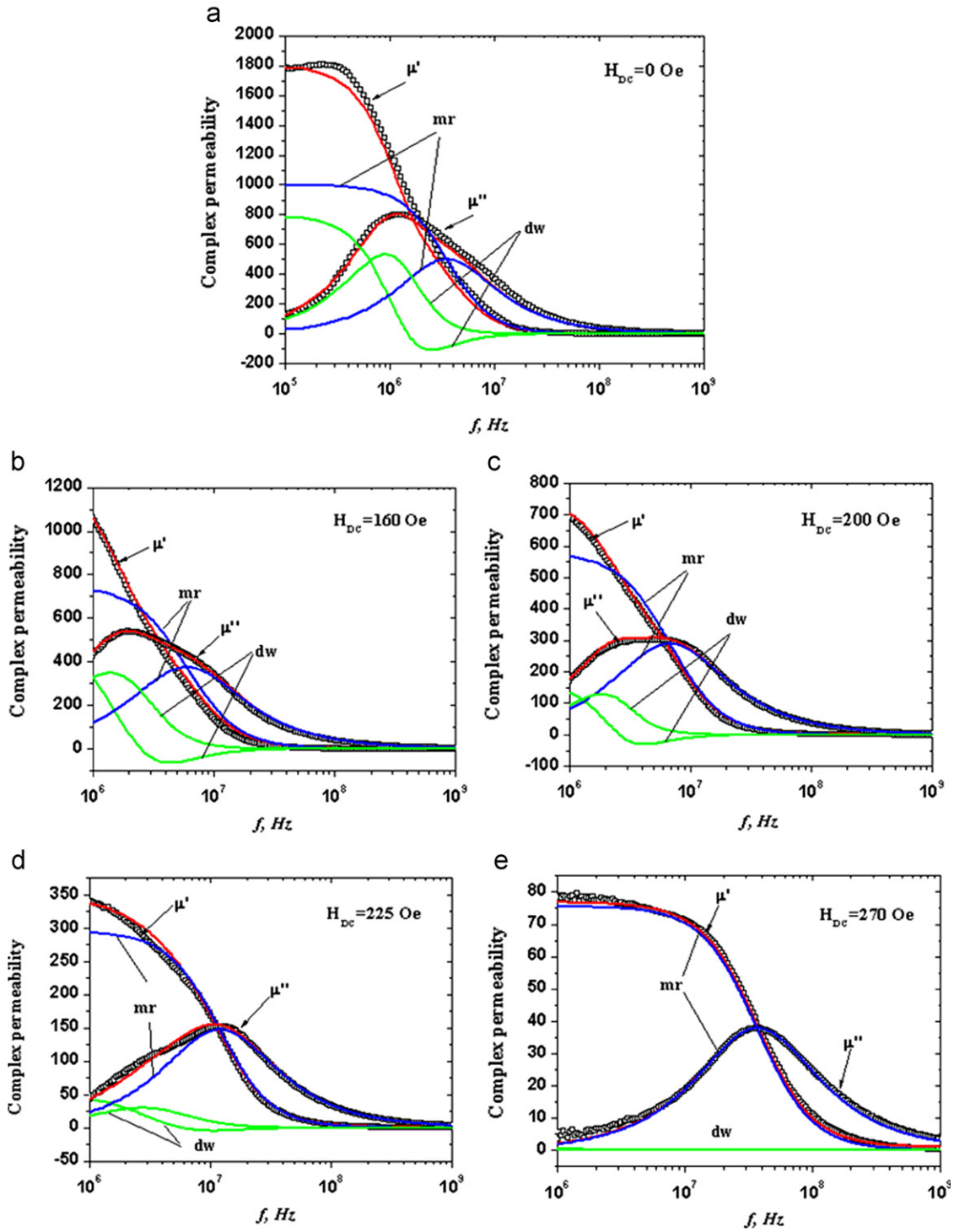

Fig. 4. Magnetic spectra of MnZn ferrite in various DC magnetizing fields (H_{DC}). The experimental values of μ' and μ'' are indicated by open squares. The colored solid lines show total calculated permeability (red) obtained by combining the domain wall motion (dw) and magnetization rotation (mr) components. (For interpretation of the references to color in this figure legend, the reader is referred to the web version of this article.)

a wide range of grain sizes (5–20 μm) with intergranular porosity. Adjacent grains are misoriented with respect to each other, which is indicative of the structural disorder due to defects in the ferrite. It is well known that defects, especially dislocations, have a strong effect on the structure and the magnetic properties of a ferrite. An increase in the number of defects results in an increase in the coercivity and the width of the magnetic loss peak $\mu''(f)$, a smearing of the ferromagnetic–paramagnetic phase transition, and an increase in the Curie temperature [22–24]. Thus, the mixed relaxation-resonance type of magnetic dispersion, a broad magnetic loss peak, and the asymmetry of the loss peak in the magnetic spectra of a 3000-NM MnZn ferrite are determined by the ferrite microstructure: the size dispersion of grains and the presence of defects (Fig. 4a). The asymmetry of the loss curve with a steeper slope on the low-frequency side provides evidence for the overlapping of the resonance region associated with domain wall motion and the region of NFR associated with rotation of the magnetization vector around the local direction

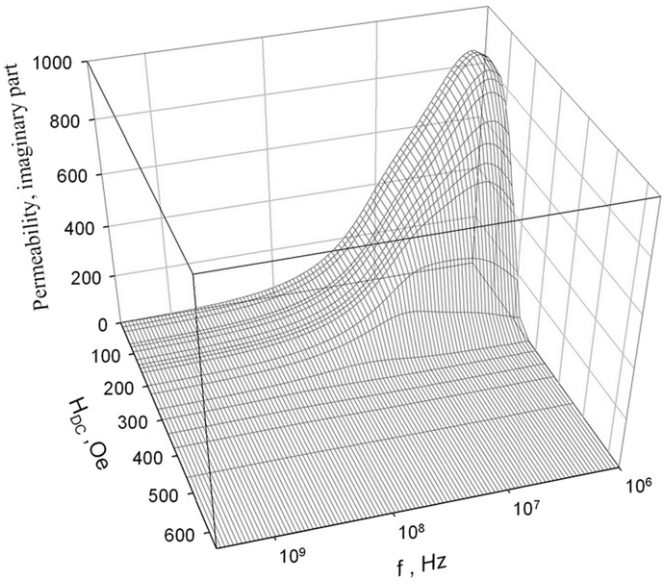

Fig. 5. Three-dimensional image of frequency-field dependence of the imaginary part of complex magnetic permeability of MnZn ferrite.

of easy magnetization. The separation of these processes is clearly illustrated by the frequency and field dependence $\mu^*(f, H_{DC})$ (Fig. 4b–e), especially by the curves of $\mu''(f, H_{DC})$ (Fig. 5).

The application of H_{DC} leads to the suppression of the domain structure and the reduction of the demagnetizing fields related to magnetization jumps on the boundaries of the grains and defects. Therefore, as the field increases, magnetic losses decrease due to the reduced contribution of domain wall motion and the shift of the complex permeability dispersion region to higher frequencies. For example, at sufficiently low fields ($H_{DC} \leq 160$ Oe), the maximum of magnetic losses decreases as the field strength increases (from $\mu''_{max} \sim 850$ for $H_{DC}=0$ to $\mu''_{max} \sim 540$ for $H_{DC}=160$ Oe); in this case, the resonance frequency is almost unchanged ($f_r \sim 1.3$ MHz for $H_{DC}=0$ and $f_r \sim 2$ MHz for $H_{DC}=160$ Oe). In this region of fields and frequencies, the processes of domain wall motion and magnetization rotation make virtually the same contribution to μ^*. As H_{DC} increases further, the contribution of domain wall motion decreases, whereas the contribution of magnetization rotation increases. At $H_{DC}=225$ Oe, the asymmetry of the resonance curve changes its sign: the resonance curve has a steeper slope on the high-frequency side, which indicates that the processes of magnetization rotation prevail over the processes of domain wall motion. In the fields of $H_{DC} \geq 270$ Oe, the domain

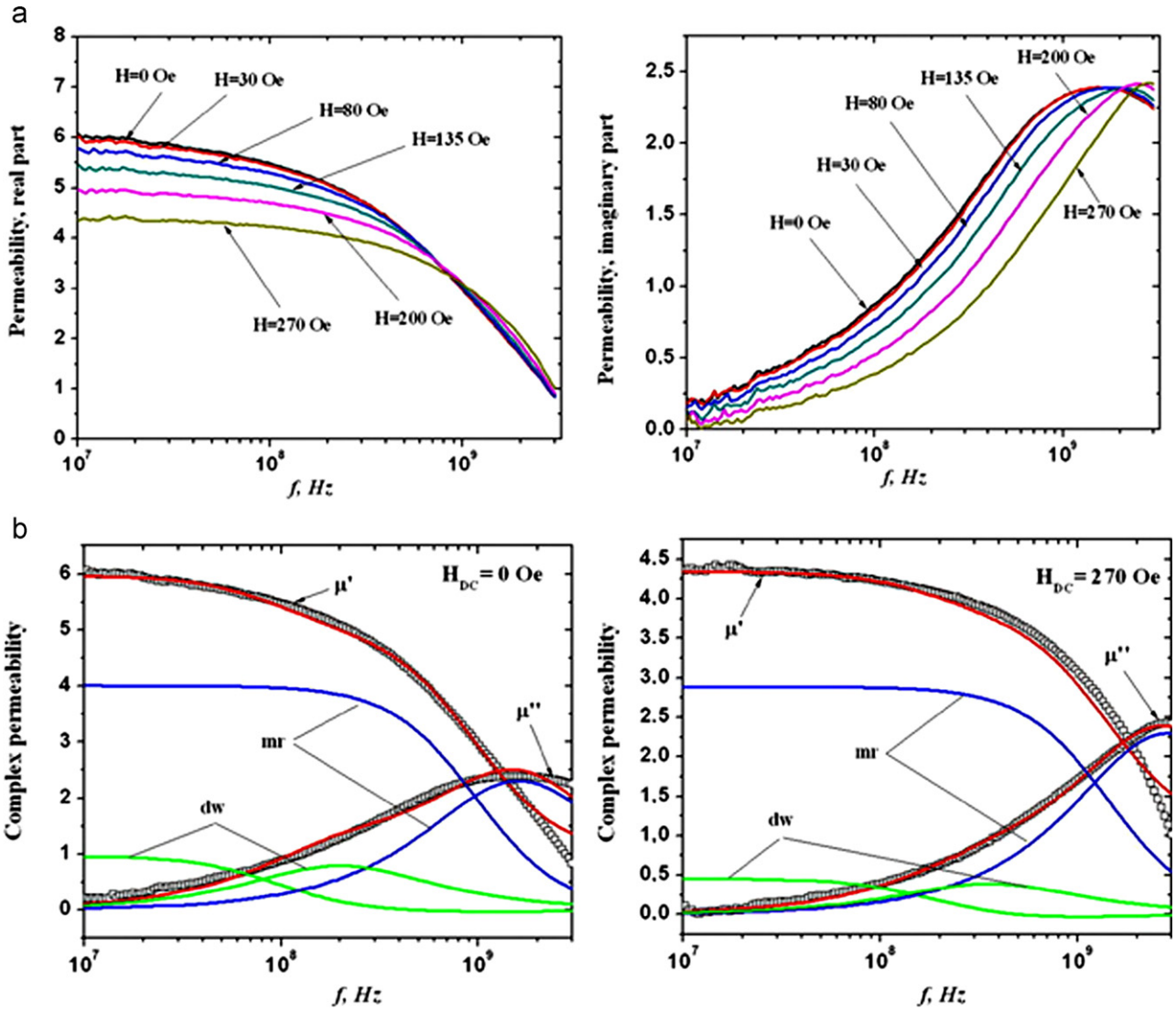

Fig. 6. Magnetic spectra of MnZn–PU composite in various DC magnetizing fields (H_{DC}): (a) the experimental results; (b) calculated results: the experimental values of μ' and μ'' are indicated by open squares; the colored solid lines show total calculated permeability (red) obtained by combining the domain wall motion (dw) and magnetization rotation (mr) components. (For interpretation of the references to color in this figure legend, the reader is referred to the web version of this article.)

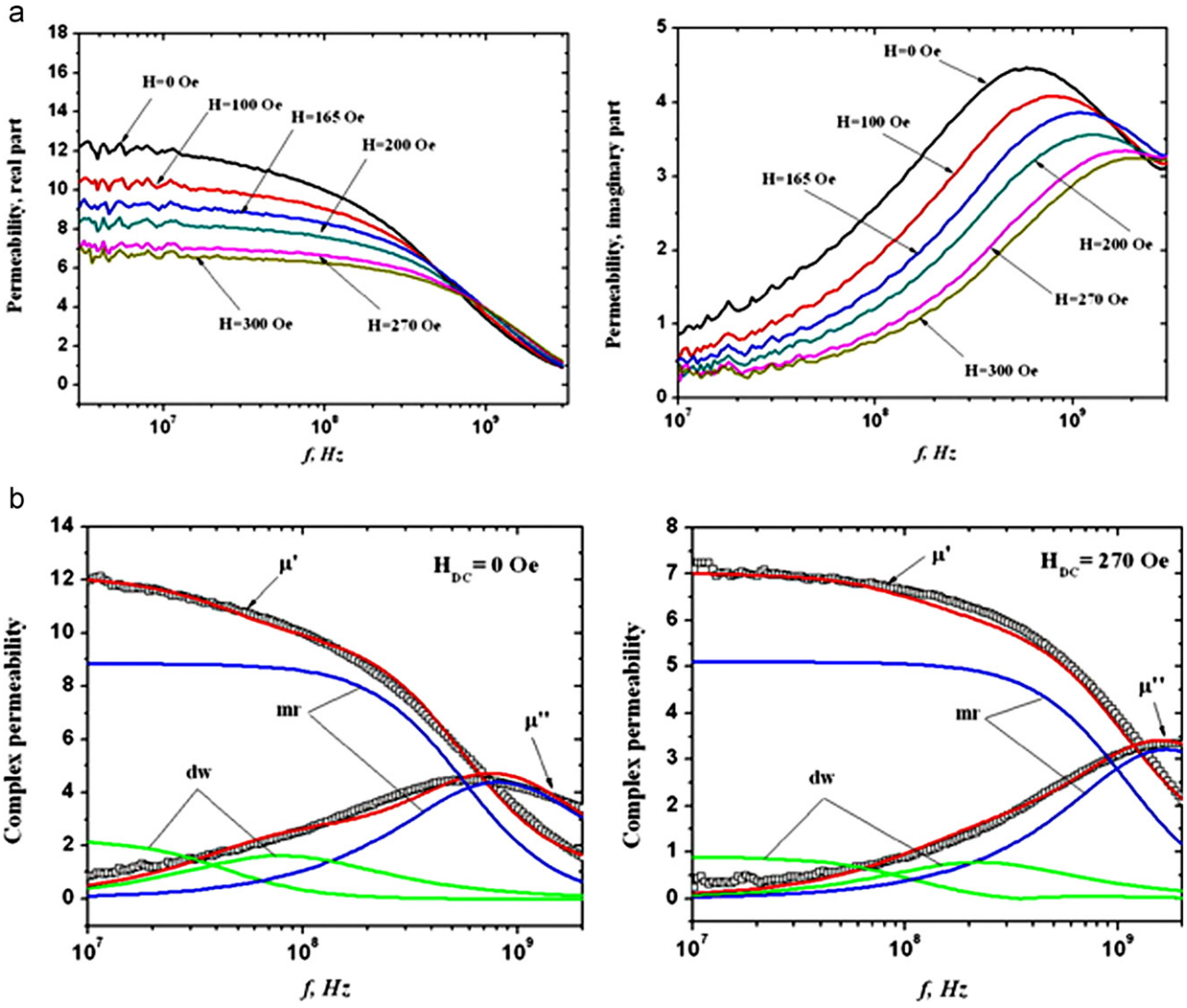

Fig. 7. Magnetic spectra of MnZn–PANI composite in various DC magnetizing fields (H_{DC}): (a) the experimental results; (b) calculated results: the experimental values of μ' and μ'' are indicated by open squares; the colored solid lines show total calculated permeability (red) obtained by combining the domain wall motion (dw) and magnetization rotation (mr) components. (For interpretation of the references to color in this figure legend, the reader is referred to the web version of this article.)

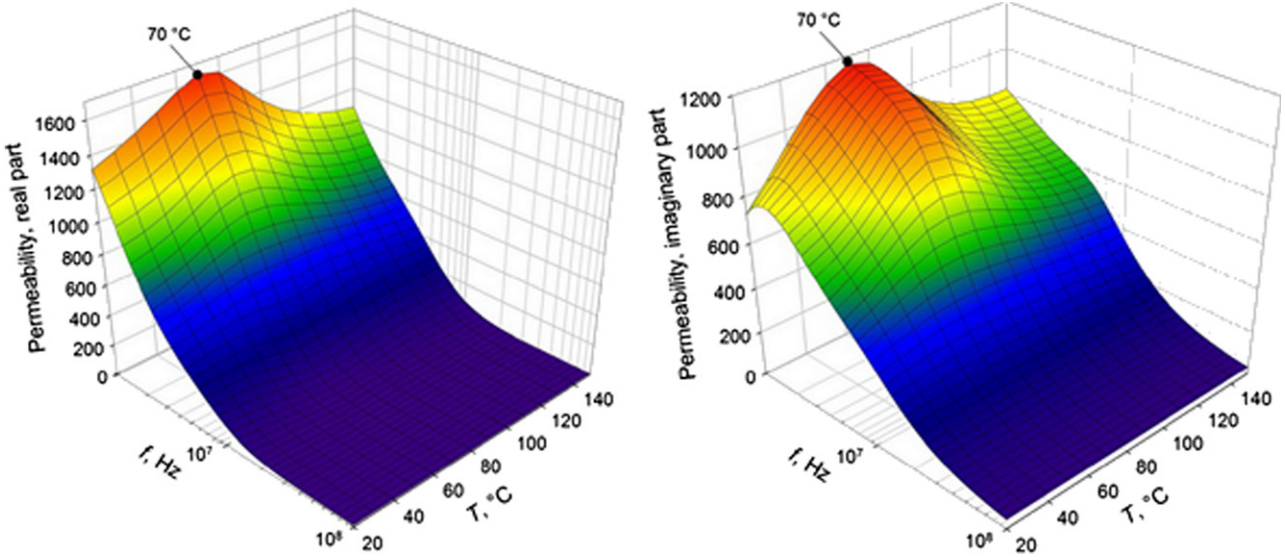

Fig. 8. Three-dimensional image of the temperature–frequency dependence of complex magnetic permeability of MnZn ferrite.

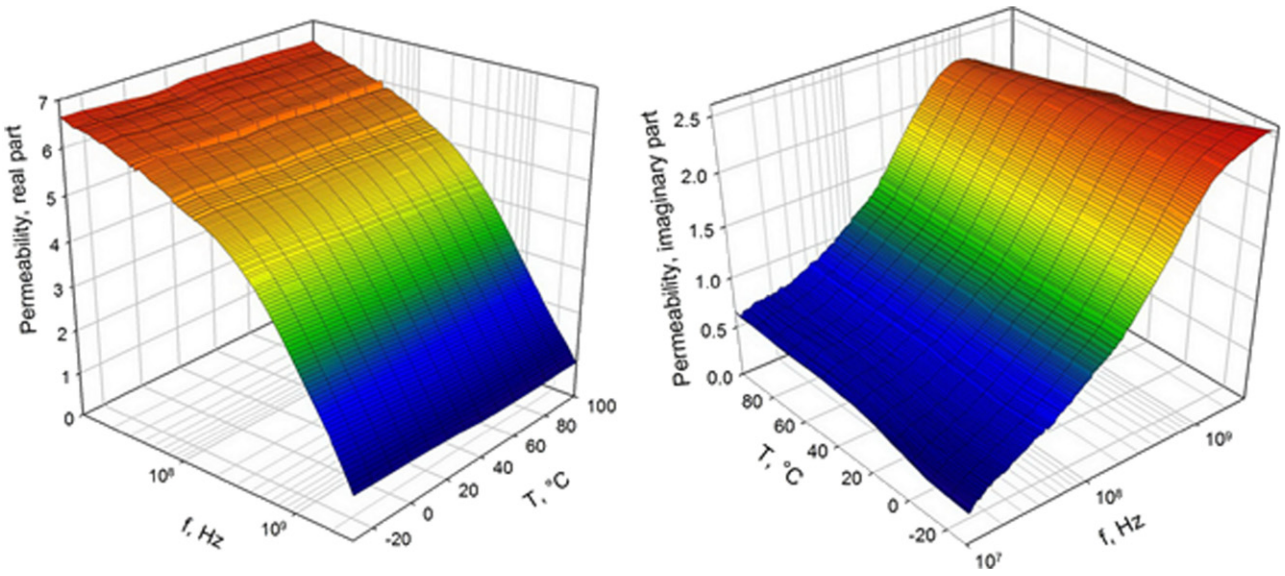

Fig. 9. Three-dimensional image of the temperature–frequency dependence of complex magnetic permeability of MnZn–PU.

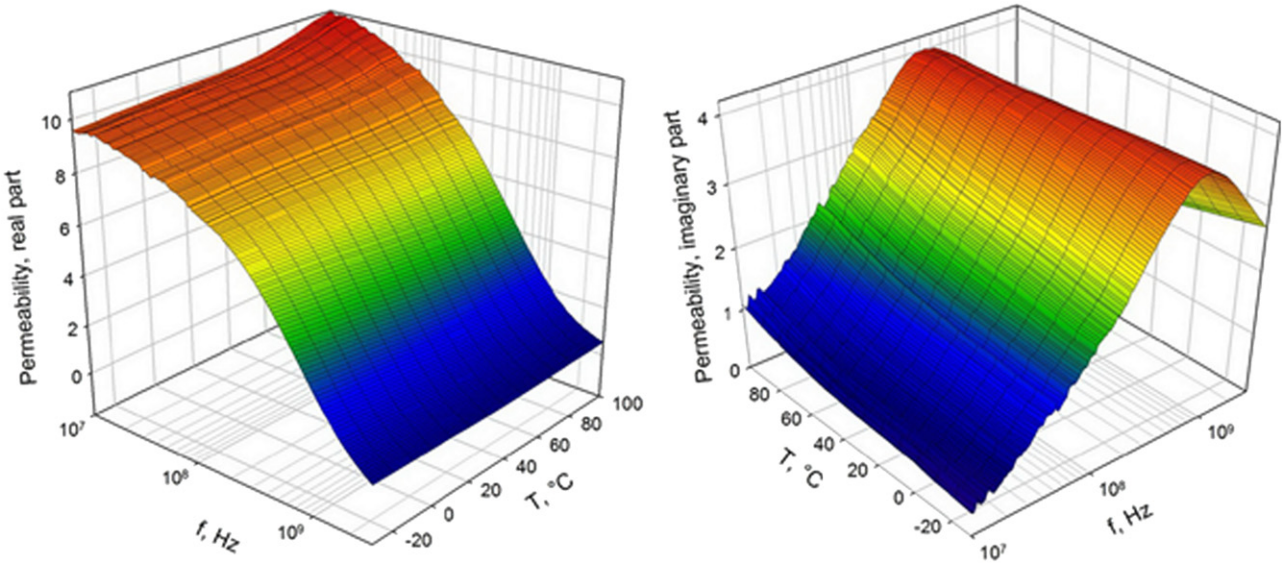

Fig. 10. Three-dimensional image of the temperature-frequency dependence of complex magnetic permeability of MnZn–PANI.

structure is suppressed, and the magnetization is determined only by magnetization rotation. This is the beginning of the NFR region. Therefore, an external field of $H_{DC}=270$ Oe corresponds to the transition of ferrite to the "single domain" state.

4.2. Analysis of factors responsible for the high-frequency shift of the complex permeability dispersion region in MnZn ferrite composites

The shift of the complex permeability dispersion towards higher frequencies in ferromagnetic composites is attributed to the non-uniform distribution of magnetization over the material volume. This is explained, first of all, by demagnetizing fields that arise as a result of interphase polarization. Another possible reason for the high-frequency shift is the magnetic anisotropy induced in magnetic particles by elastic stresses that arise in a composite during its fabrication. The interaction between polymer and the surface of a ferrite particle is mainly associated with adhesion, i.e., with the action of intermolecular forces. Depending on the polymer nature and the manufacturing technology of a composite, this interaction may give rise to tensile and compressive stresses.

The MnZn ferrite, a ferrite with cubic structure, exhibits a domain structure with prismatic domains of closure [25,26]. In this case, the magnetic anisotropy energy and the energy of magnetic dipolar interaction virtually vanish; as a result, the domain size is determined by internal stresses [23]. This is likely to be responsible for the fact that even relatively small mechanical stresses may result in the reconstruction of the domain structure of the ferrite. To date, the role of internal stresses, just as the role of the surface domain structure in the high-frequency oscillations of magnetization in a material with domain structure, has been virtually unstudied.

Compared with ferrite ceramic, MnZn–PANI and MnZn–PU composites are characterized by higher coercivity (Fig. 3), high-frequency complex permeability dispersion region (from 300 MHz to 3 GHz), and a symmetric magnetic loss curve with broad maximum (Figs. 6 and 7). A significant shift of the complex permeability dispersion region to higher frequencies is accompanied by a considerable decrease in the permeability compared

with that of ferrite ceramic. In spite of the similarity between the magnetic spectra of composites, an almost identical shift of the magnetic dispersion region occurs at substantially different contents of the polymer phase: at about 10 mass% of PANI in MnZn–PANI and at about 80 mass% of PU in MnZn–PU. This fact is associated with the fundamental difference in the properties of the polymer components of the polymer magnetic composites and in their fabrication methods. While polyurethane is a good dielectric with electric conductivity below 10^{-13} S cm^{-1};polyaniline is an organic semiconductor whose electric conductivity ranges, depending on the doping level, from 10^{1} to 10^{-8} S cm^{-1}. MnZn–PU is produced by blending ferrite powder with PU prepolymer, followed by solidification, whereas MnZn–PANI is obtained by *in-situ* polymerization technique, which combines the polymer synthesis and the formation of a composite material into a single stage. Ferrite powder is immersed into an acidified solution of aniline, and polymerization is initiated after adding an oxidant. During oxidative polymerization, polymer chains grow on the surface of the ferrite, coating the particles with a nanometer-size film [27,28].

The formation of a PANI film on the surface of ferrite was investigated by an AFM with the use of a single crystal MnZn ferrite. The growth of the film under conditions similar to those of MnZn–PANI composite production was studied at different stages of synthesis. It was established that, at the initial stage of polymerization, a discontinuous PANI film with unusual honeycomb structure is formed on the ferrite surface, and the film turns into a continuous polymer layer only at the final stage of synthesis (Fig. 11). The analysis of the initial honeycomb structure shows that PANI grows as a "wall" (Fig. 11c) forming cells with a size of about 10 μm. As is shown by the phase contrast method, the central parts of the cells are not occupied by polymer (Fig. 11a). The PANI "walls" on the surface of ferrite are oriented in different directions; however, one can distinguish dominant growth directions and fixed angles between them. In Fig. 11a, these are lines intersecting at angles of 90° and 120°. The honeycomb structure of the growing film is not typical of PANI films grown on other types of substrates. The shape and the size of cells of this structure resemble grains in the MnZn ferrite structure (Fig. 1b). One can assume that such a structure indicates that a PANI film is formed predominantly along the boundaries of grains, where most of the domain walls are concentrated (Fig. 12), as is shown in [26] by an example of high-permeability MnZn ferrite. It is well known that a domain wall represents a defect in the system of ordered magnetic moments. It is quite possible that this leads to a specific sorption of active polymerization centers (which are paramagnetic by their nature [19]), and to the formation of polymer chains precisely where the domain walls appear at the ferrite surface, where the magnetic field is inhomogeneous.

The pinning of the domain walls appearing at the surface of a ferrite particle by PANI hampers a free motion of domain walls in magnetic fields, thus contributing to the increase in coercivity,

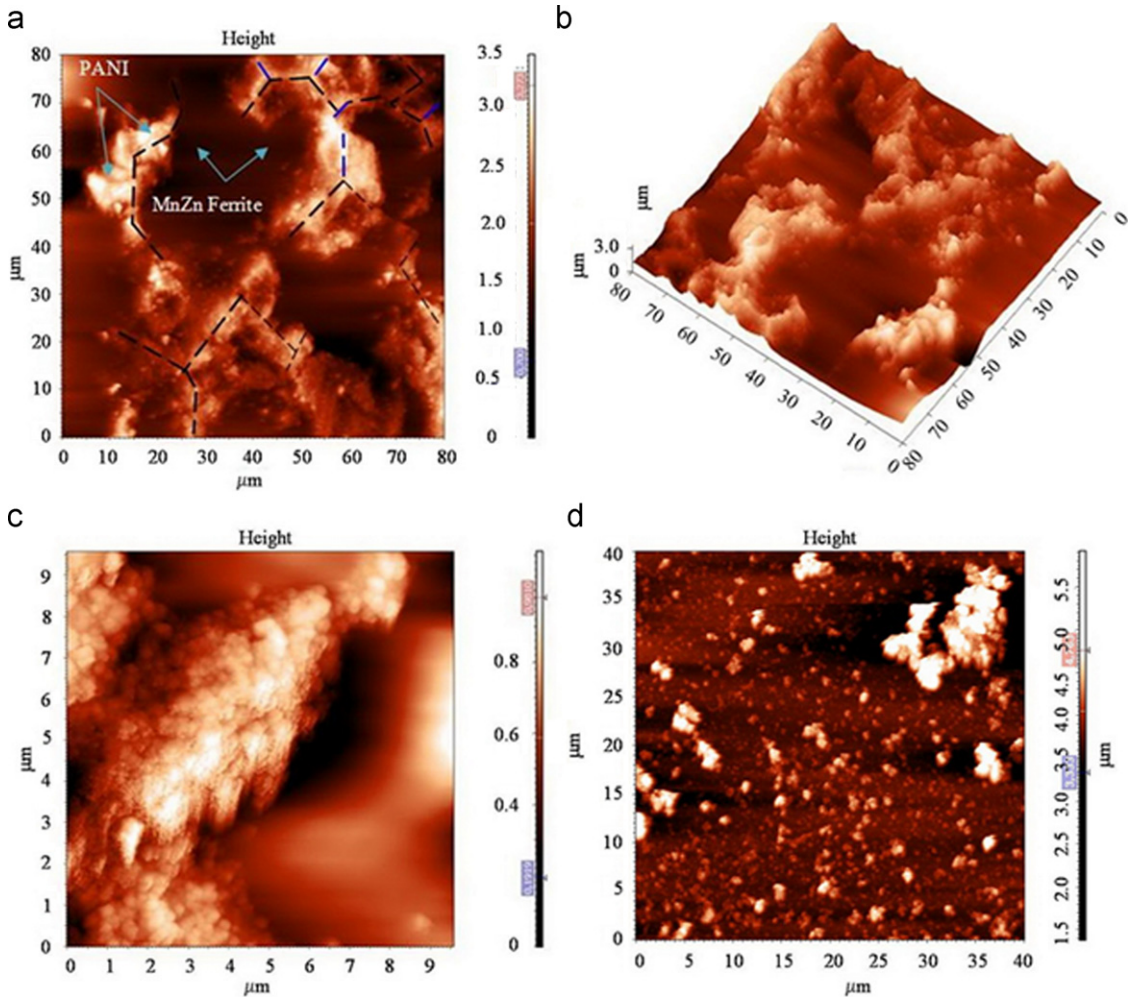

Fig. 11. Atomic force microscopy of the surface of MnZn ferrite coated with polyaniline by *in-situ* polymerization: (a)–(c) initial stage of polymerization (discontinuous polyaniline film with a "honeycomb" structure), (d) final stage of polymerization (continuous polyaniline film).

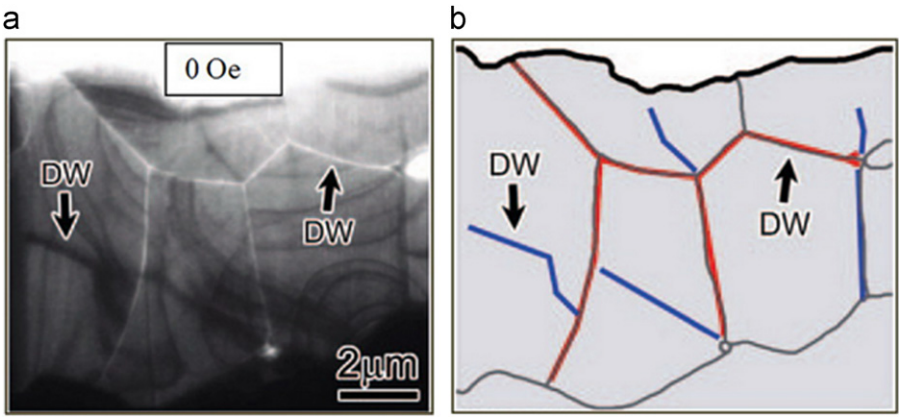

Fig. 12. (a) Domain structure of MnZn ferrite in demagnetized state revealed by Lorentz microscopy. The white lines show the grain boundaries. The domain walls are indicated by an arrow. (b) Schematic illustration of domain structure, where blue and red lines indicate the position of domain walls. Reprinted from T. Kasahara, D. Shindo, H. Yoshikawa, T. Sato, K. Kondo. In situ observations of domain structures and magnetic flux distributions in Mn–Zn and Ni–Zn ferrites by Lorentz microscopy and electron holography, J Electron Microsc. 56 (2007) 7, Copyright 2007, with permission from Oxford University Press. (For interpretation of the references to color in this figure legend, the reader is referred to the web version of this article.)

the decrease in the low-frequency value of μ^*, and the shift of the complex permeability dispersion region to the high-frequency part of the radio-frequency band. The magnetic field strength needed to shift a domain wall can be identified with the coercive force, which is the characteristic of a sample as a whole; this field is much higher for MnZn–PANI than for MnZn–PU and MnZn–PANI-*mix* (Table 1).

The coercive force in ferrites with the spinel structure is related to the magnetic anisotropy by the relations $H_c = p_c\,(K_1/M_s)$, where M_s is the saturation magnetization, K_1 is the first constant of anisotropy, and p_c is coefficient that depends on the symmetry of the crystalline structure and the magnetization mechanism (domain wall motion or magnetization rotation). As the H_c increases almost three times for the coated ferrite, rather small decrease in the value of M_s cannot on its own cause this increase. Therefore, we assume that the enchantment in H_c is caused by increase of p_c and/or K_1, so the increase in H_c can be associated with the increased magnetic anisotropy. The magnetocrystalline anisotropy of MnZn ferrite (of a given chemical composition) is nearly zero and so the magnetic anisotropy in MnZn–PANI can be attributed to the anisotropy of internal stresses (magnetostrictive anisotropy). We suppose that PANI coating produces stresses in a ferrite particle that are sufficient to create a magnetostrictive deformation, which is maintained due to the strong adhesion of polyaniline to the ferrite surface. Thus, in MnZn–PANI we have "induced" magnetic anisotropy of the magnetostrictive nature.

Let us consider from this point of view the variation pattern of the magnetic spectra of MnZn–PANI and MnZn–PU in DC magnetizing fields. In the case of MnZn–PU, f_r is shifted from 1.5 GHz to 3 GHz as the field strength H_{DC} increases to 270 Oe; however, the value of μ''_{max} remains almost constant ($\mu''_{max} \sim 2.4$) due to the primacy of magnetization rotation, which is the main dynamic process in the region of NFR. In MnZn–PANI, the shift of f_r from 580 MHz to 2 GHz as H_{DC} increases to 300 Oe is accompanied by a decrease in μ''_{max} from 4.5 to 3.2, which is associated with a decrease in the contribution of domain wall motion. It is important that this contribution remains in the interval of critical fields, $H_{DC} \geq 270$ Oe, where the neat ferrite should be in the "single-domain" state. Thus, MnZn ferrite particles coated by PANI are kept in the "multidomain" state as a consequence of magnetic anisotropy induced by the polyaniline coating. It is known [29] that the induced magnetic anisotropy may lead to the stabilization of the magnetization vector in domains and domain walls. If the induced anisotropy is much stronger than the magnetocrystalline anisotropy, then stabilized domain walls are thick and almost fixed.

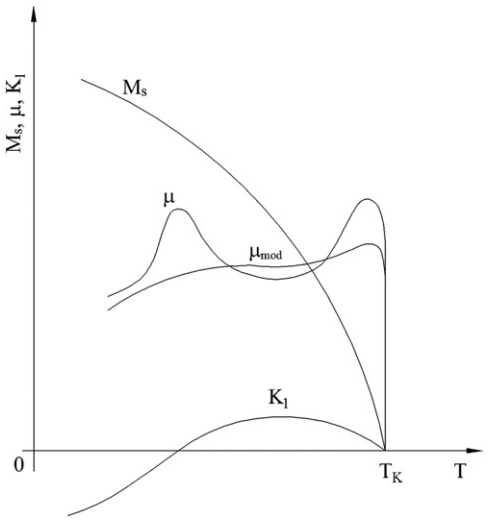

Fig. 13. A schematic diagram of temperature dependence of magnetic permeability (μ), saturation magnetization (M_s), and the first anisotropy constant (K_1) in MnZn ferrite.

4.3. Thermal stability of MnZn ferrite polymer magnetic composites

Generally, the magnetic permeability of ferrites with the spinel structure is a complex function of temperature, which is associated with the behavior of M_s and the energy of magnetocrystalline anisotropy as a function of temperature [25]. For spinel ferrites the reduction of the magnetocrystalline anisotropy as temperature increases, leads to a decrease in the losses associated with domain wall motion and an increase in the contribution of magnetization rotation processes to magnetic permeability. The value of magnetic permeability due to the magnetization rotation processes is directly proportional to square of M_s and inversely proportional to the energy of magnetocrystalline anisotropy. As a result, the magnetic permeability in spinel ferrites increases, as a rule, up to the Curie temperature. It is well-known that the temperature dependence of magnetic permeability in MnZn ferrites with a concentration of Fe_2O_3 of more than 50 mol% is characterized by two maxima, the first of which is observed at the temperature corresponding to the zero value of the first magnetic anisotropy constant, $K_1 = 0$, while the second, occurs near the Curie temperature (Fig. 13, curve μ) [30–32]. The temperature dependence of magnetic permeability can be stabilized (Fig. 13, curve μ_{mod}) by reducing the sensitivity of the

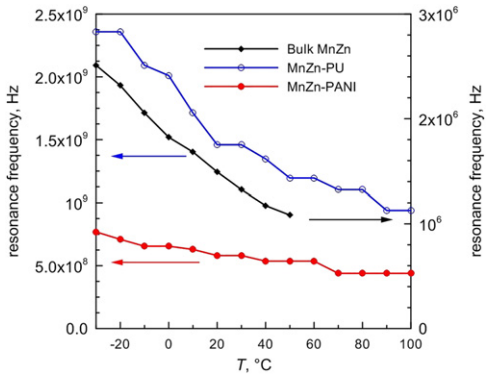

Fig. 14. Temperature dependence of the resonance frequency for MnZn ferrite and its composite materials.

ferrite to magnetostrictive deformations due to the elimination of the magnetic texture and strengthening the surface tension of the grain boundaries; the latter is reached by introduction of special modifying dopants and decreasing the grain size (less than 3 μm) [33].

The temperature dependence of the complex magnetic permeability of 3000-NM MnZn ferrite confirms the nonlinear behavior and the presence of two peaks, which is characteristic of MnZn ferrites with a more than 50 mol% concentration of Fe_2O_3 (Fig. 8). The first maximum on the curves of $\mu'(T)$ and $\mu''(T)$ is observed at 70 °C. The second maximum lies above 150 °C. The positions of the peaks correspond to the transition to the isotropic state at two temperatures: at the temperature of compensation of K_1 (most likely, this is 70 °C) and at the Curie temperature (~200 °C). As temperature increases, the resonance frequency appreciably shifts toward lower frequencies (Fig. 14). Composite materials exhibit stabilization of the temperature dependence of μ^*: small variations in μ' and μ'' and shift of f_r towards low-frequencies with increasing temperature are observed in MnZn–PU, whereas, in the case of MnZn–PANI, both μ' and μ'' remain constant, and the position of f_r slightly shift towards low-frequencies (Figs. 9, 10, and 14). The thermomagnetic stability of composites is always associated with the effect of demagnetizing field, however in the case of MnZn–PANI it is also attributed to the induced magnetic anisotropy. The latter is in such case manifested by a decrease in the temperature sensitivity of ferrite to magnetostrictive deformations due to the stabilization of its domain structure.

5. Conclusions

We have analyzed factors responsible for the high-frequency shift of complex permeability dispersion region in polymer composites of MnZn ferrite and the increase in their thermomagnetic stability. The approximation of the frequency-field dependence of the complex magnetic permeability by the frequency dispersion formula has shown that, in the high-frequency part of the radio-frequency band, the magnetization of MnZn ferrite is mainly due to the magnetization rotation. However, while the magnetization rotation processes in a ferrite become dominant when the ferrite reaches the "single-domain" state, high-frequency oscillations of magnetization in ferrite composites are observed in a material with ferrite in "multidomain" state. This feature of dynamic magnetization of composite materials, as well as the increase in their thermomagnetic stability, is explained by the effect of demagnetizing field; in the case of MnZn–PANI, these properties are also attributed to the induced magnetic anisotropy. The induced magnetic anisotropy has a magnetostrictive nature and is attributed to internal stresses that arise in ferrite particles due to the polyaniline coating. The pinning of domain walls by polyaniline during *in-situ* polymerization leads to the deceleration of domain wall motion in magnetic fields, resulting in an increase in the coercivity and a shift of the complex permeability dispersion region to the high-frequency part of the radio-frequency band. Simultaneously, the pinning of domain walls and the rise of induced magnetic anisotropy stabilize the domain structure of the ferrite, thus reducing its sensitivity to magnetostrictive deformations with increasing temperature, which guarantees the high thermal stability of MnZn–PANI.

Acknowledgments

This paper was written with the support of Operational Program Research and Development for Innovations co-funded by the European regional development fund (ERDF) and national budget of Czech Republic, within the framework of project Centre of Polymer Systems (reg. number: CZ.1.05/2.1.00/03.0111) and Russian Federation Program (reg. number: 2011-1.6-516-015-031).

References

[1] L.M. Letyuk, A.M. Balbashov, D.G. Krutogin, A.V. Gonchar, I.G. Kudriashkin, Technology of Magnetoelectronic Materials, Metallurgia, Moscow, 1994.
[2] G. Ott, J. Wrba, R. Lucke, Recent developments of Mn–Zn ferrites for high permeability applications, J. Magn. Magn. Mater. 254 (2003) 535–537.
[3] A. Verma, M.I. Alam, R. Chatterjee, T.C. Goel, R.G. Mendiratta, Development of a new soft ferrite core for power applications, J. Magn. Magn Mater. 300 (2006) 500–505.
[4] T. Tsutaoka, M. Ueshima, T. Tokunaga, T. Nakamura, K. Hatakeyama, Frequency dispersion and temperature-variation of complex permeability of Ni–Zn ferrite composite-materials, J. Appl. Phys. 78 (1995) 3983–3991.
[5] J.H. Paterson, R. Devine, A.D.R. Phelps, Complex permeability of soft magnetic ferrite polyester resin composites at frequencies above 1 MHz, J. Magn. Magn. Mater. 197 (1999) 394–396.
[6] J.L. Mattei, M. Le Floc'h, Effects of the magnetic dilution on the ferrimagnetic resonance of disordered hetero structures, J. Magn. Magn. Mater. 264 (2003) 86–94.
[7] R. Moucka, A.V. Lopatin, N.E. Kazantseva, J. Vilcakova, P. Saha, Enhancement of magnetic losses in hybrid polymer composites with MnZn-ferrite and conductive fillers, J. Mater. Sci. 42 (2007) 9480–9490.
[8] J.A. Stratton, Electromagnetic Theory, McGraw-Hill, New York, 1941.
[9] T. Tsutaoka, Frequency dispersion of complex permeability in Mn–Zn and Ni–Zn spinel ferrites and their composite materials, J. Appl. Phys. 93 (2003) 2789–2796.
[10] G.Q. Lin, Z.W. Li, L.F. Chen, Y.P. Wu, C.K. Ong, Influence of demagnetizing field on the permeability of soft magnetic composites, J. Magn. Magn. Mater. 305 (2006) 291–295.
[11] T.Y. Byun, K.S. Hong, C.S. Yoon, C.K. Kim, Impedance spectroscopic study on the magnetization of polycrystalline MnZn ferrite with very low magnetic anisotropy, J Magn. Magn. Mater. 253 (2002) 72–76.
[12] G. Rankis, Dynamics of Magnetization in Polycrystalline Ferrites, Zinatne, Riga, 1981.
[13] T. Tsutaoka, T. Nakamura, K. Hatakeyama, Magnetic field effect on the complex permeability spectra in a Ni–Zn ferrite, J. Appl. Phys. 82 (1997) 3068–3071.
[14] T. Tsutaoka, T. Kasagi, K. Hatakeyama, Magnetic field effect on the complex permeability for a Mn–Zn ferrite and its composite materials, J. Eur. Ceram. Soc. 19 (1999) 1531–1535.
[15] G.F. Dionne, Magnetic relaxation and anisotropy effects on high-frequency permeability, IEEE Trans. Magn. 39 (2003) 3121–3126.
[16] T. Nakamura, T. Tsutaoka, K. Hatakeyama, Frequency dispersion of permeability in ferrite composite-materials, J. Magn. Magn. Mater. 138 (1994) 319–328.
[17] J. Stejskal, R.G. Gilbert, Polyaniline. preparation of a conducting polymer (IUPAC technical report), Pure Appl. Chem. 74 (2002) 857–867.
[18] I. Sapurina, J. Stejskal, The mechanism of the oxidative polymerization of aniline and the formation of supramolecular polyaniline structures, Polym. Int. 57 (2008) 1295–1325.
[19] I.Y. Sapurina, J. Stejskal, The effect of pH on the oxidative polymerization of aniline and the morphology and properties of products, Russ. Chem. Rev. 79 (2010) 1123–1143.
[20] R. Garcia, R. Perez, Dynamic atomic force microscopy methods, Surf. Sci. Rep. 47 (2002) 197–301.
[21] Y.M. Spivak, V.A. Moshnikov, I. Sapurina, N.E. Kazantseva, Atomic force microscopy of polyaniline with globular structure, in: International Scientific and Applied Conference Opto-nano Electronics and Renewable Energy Sources, Technical University of Varna, Bulgaria, 2010.

[22] S. Chikazumi, C.D. Graham, Physics of Ferromagnetism, 2nd ed., Clarendon Press, Oxford University Press, Oxford, New York, 1997.
[23] S.V. Vonsovsky, Magnetism, Nauka, Moscow, 1971.
[24] A.G. Gurevich, G.A. Melkov, Magnetization Oscillations and Waves, CRC Press, Boca Raton, 1996.
[25] J. Smit, H.P.J. Wijn, Ferrites; Physical Properties of Ferrimagnetic Oxides in Relation to their Technical Applications, Wiley, New York, 1959.
[26] T. Kasahara, D. Shindo, H. Yoshikawa, T. Sato, K. Kondo, In situ observations of domain structures and magnetic flux distributions in Mn–Zn and Ni–Zn ferrites by Lorentz microscopy and electron holography, J. Electron. Microsc. 56 (2007) 7–16.
[27] N.E. Kazantseva, J. Vilcakova, V. Kresalek, P. Saha, I. Sapurina, J. Stejskal, Magnetic behaviour of composites containing polyaniline-coated manganese–zinc ferrite, J. Magn. Magn. Mater. 269 (2004) 30–37.
[28] N.E. Kazantseva, Y.I. Bespyatykh, I. Sapurina, J. Stejskal, J. Vilcakova, P. Saha, Magnetic materials based on manganese–zinc ferrite with surface-organized polyaniline coating, J. Magn. Magn. Mater. 301 (2006) 155–165.
[29] S. Krupicka, Physics of Ferrites and related Magnetic Oxides, Academia, Prague, 1969.
[30] J. Loaec, Thermal hysteresis of the initial permeability in soft ferrites at transition-temperatures, J. Phys. D Appl. Phys. 26 (1993) 963–966.
[31] F. Fiorillo, C. Beatrice, M. Coisson, L. Zhemchuzhna, Loss and permeability dependence on temperature in soft ferrites, IEEE Trans. Magn. 45 (2009) 4242–4245.
[32] D. Stoppels, Frequency-dependence of the complex permeability of mono-crystalline MnZn ferrous ferrites, J. Appl. Phys. 52 (1981) 2433–2435.
[33] S.B. Menshova, Development of Technological Processes for the Formation of the Structure and Properties of Thermally Stable MnZn Ferrite Materials with High Magnetic Permeability, Penza State University, Penza, Russia, 2007.

PAPER II

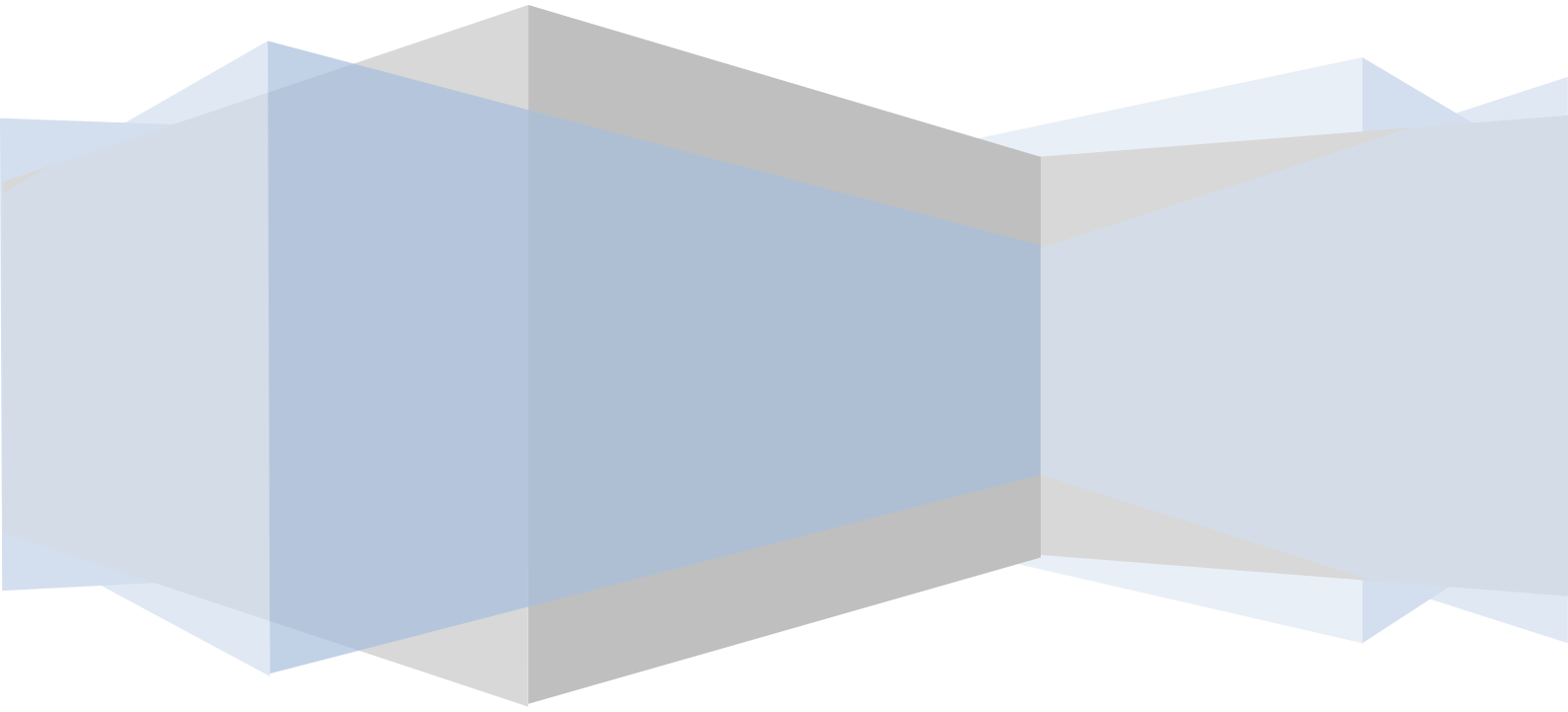

Applied Surface Science 258 (2012) 7707–7716

Contents lists available at SciVerse ScienceDirect

Applied Surface Science

journal homepage: www.elsevier.com/locate/apsusc

Magnetoactive feature of in-situ polymerised polyaniline film developed on the surface of manganese–zinc ferrite

V. Babayan [a], N.E. Kazantseva [a,b,*], I. Sapurina [c], R. Moučka [a,b], J. Vilčáková [a,b], J. Stejskal [d]

[a] Centre of Polymer Systems, University Institute, Tomas Bata University in Zlin, Nad Ovcirnou 3685, 760 01 Zlin, Czech Republic
[b] Polymer Centre, Faculty of Technology, Tomas Bata University in Zlin, T. G. Masaryk Sq. 5555, 760 01 Zlin, Czech Republic
[c] Institute of Macromolecular Compounds, Russian Academy of Sciences, St. Petersburg 199004, Russia
[d] Institute of Macromolecular Chemistry, Academy of Sciences of the Czech Republic, 162 06 Prague 6, Czech Republic

ARTICLE INFO

Article history:
Received 1 December 2011
Received in revised form 28 March 2012
Accepted 20 April 2012
Available online 26 April 2012

Keywords:
Ferrite
Polyaniline
Core–shell particles
Coercivity
Complex magnetic permeability
Induced magnetic anisotropy
Inner demagnetisation factor

ABSTRACT

A polyaniline film exhibits magnetoactive properties when deposited on the surface of multidomain particles of manganese–zinc ferrite during in-situ polymerisation of aniline. This is reflected in the increased coercivity and thermomagnetic stability of an in-situ prepared composite compared with bare ferrite and its *mixed* composite with polyaniline. In addition, the deposition of a polyaniline film results in a shift of the complex-permeability dispersion region towards ultrahigh frequency band. These changes in the magnetic properties of polyaniline-coated ferrite are attributed to the increased value of the inner demagnetisation factor, which results from stress-induced magnetic anisotropy due to the pinning of domain walls appearing on the surface of ferrite. This study is focused on the mechanism of pinning of domain walls and its influence on the magnetic properties of in-situ prepared composites in terms of the molecular mechanism of oxidative polymerisation of aniline. Ferrite stimulates the propagation of polyaniline chains, which start to grow on the domain walls on the ferrite surface. It leads to the pinning of domain walls and restricts their mobility in a magnetic field. The further increase in the coercivity and the resonance frequency of polyaniline-coated ferrite due to film shrinkage after deprotonation of polyaniline makes it obvious that polyaniline coating induces elastic stresses in a ferrite particle that stimulate the growth of the effective magnetic anisotropy. Stress-induced magnetic anisotropy contributes to the reorientation of the magnetisation vectors in domains with respect to the new directions of easy magnetisation, given by magnetoelastic stresses, which leads to complex changes in the magnetic properties of in-situ prepared composites.

1. Introduction

Polyaniline (PANI) represents a class of conducting polymers possessing a unique set of properties together with environmental stability and low cost. The electric conductivity and the paramagnetic and redox properties of PANI can be reversibly changed by oxidising and/or protonating the polymer [1]. PANI is used in energy storage devices [2], in heterogeneous catalysis [3], for inhibiting metal corrosion [4,5], as an active component of chemical sensors [6–8], for shielding of electromagnetic radiation [9–11], etc.

PANI belongs to the category of non-processable materials: it does not melt and is insoluble in most solvents. To obtain mixed composites, PANI is used either in the form of colloidal dispersion or as a powder. Such composites have no organised structure and are not homogeneous. Nanostructured composites of PANI with various materials are obtained by the in-situ polymerisation method. During in-situ oxidation of aniline, a substrate placed into the polymerisation medium is coated by a firmly adsorbed layer of PANI of submicrometre thickness [12,13]. The introduction of finely dispersed powders as a template results in composites with the "core–shell" structure. As a rule, an in-situ grown PANI film is obtained in the protonated emeraldine form with conductivity of 10^0–10^1 S cm^{-1}. The properties of the film in the composite, however, can be reversibly changed. For example, when it is deprotonated in alkalis to corresponding emeraldine base, the conductivity of the film is reduced by 8–10 orders of magnitude [1].

Nowadays, of great practical interest are hybrid composites of PANI with ferro- (Co, Fe, Ni [11]) and ferrimagnetic materials (Fe_3O_4, $BaFe_2O_{19}$, MnZn, NiZn, NiMnZn, LiNi, and other mixed ferrites [14–20]). Such hybrids exhibit superparamagnetic or ferromagnetic behaviour, which is mainly determined by: (1) the nature of the magnetic component; (2) microstructure, size, shape, and the concentration of magnetic particles; and (3) interparticle interaction [21]. For particles with size from tens of nanometers to a

* Corresponding author at: Polymer Centre, Faculty of Technology, Tomas Bata University in Zlin, T. G. Masaryk Sq. 275, 762 72 Zlin, Czech Republic.
Tel.: +420 576 038 114; fax: +420 576 031 444.
E-mail address: nekazan@yahoo.com (N.E. Kazantseva).

0169-4332/$ – see front matter © 2012 Elsevier B.V. All rights reserved.
http://dx.doi.org/10.1016/j.apsusc.2012.04.126

few microns, the saturation magnetisation of hybrid materials can amount to tens of emu g^{-1}, for coercivity of up to thousands of Oe [10,22,23]. The electric conductivity of hybrid composites is determined, as a rule, by the conductivity of PANI and may reach several S cm^{-1}, whereas the conductivity of most ferrites amounts to 10^{-7}–10^{-8} S cm^{-1} (exceptions being Fe_3O_4 and manganese–zinc (MnZn) ferrite, with conductivities of 140 S cm^{-1} and 0.02 S cm^{-1}, respectively). These materials have great demand in the fields related to information storage, nonlinear optics, magnetic refrigeration [24,25], and in medicine, such as in magnetic mediated hyperthermia, separation and purification of biomolecules, drug delivery and magnetically controlled transport of anti-cancer drugs [26]. As a rule, both inorganic and polymer components of a hybrid composite possess oxidation–reduction properties, which is used for manufacturing electrode materials in supercapacitors [27] or in detection materials of sensors [24]. The polymer component of a hybrid composite is easily modified either by noble-metal particles or by organic functional groups and amino acids; this also expands the range of biomedical applications and facilitates obtaining new sensor materials and catalysts. Furthermore, hybrid composites are used in the design of radio-frequency absorbers for their ability to alter the frequency dependence of complex permittivity and complex magnetic permeability and thereby to meet requirements such as matching conditions and high absorption [19,28–30].

Hybrid composites of PANI with magnetic materials are obtained by various methods. They can be obtained either by mixing [20,31] or by the in-situ polymerisation method [14,15,19,22,28]. One should note that the magnetic properties of hybrid composites with similar composition may exhibit very strong difference in magnetic and dielectric properties depending on the method of preparation. This fact accounts for the divergence of the results obtained by various authors and is often interpreted as some "instability of the material properties", which ultimately hampers the practical application of these materials.

The present study is a continuation of our previous work [14–16,29,30] on the study of the electromagnetic properties of hybrid composites based on multidomain particles of MnZn ferrite in PANI. In [32] the high-frequency shift of the complex permeability (μ) dispersion region, as well as the enhanced coercivity and thermomagnetic stability in MnZn ferrite–PANI composite prepared by in-situ polymerisation method has been explained in terms of the combined effect of demagnetising field and induced magnetic anisotropy. It was suggested that the induced magnetic anisotropy arises due to the domain-wall (*dw*) pinning by a PANI film absorbed on the surface of ferrite during in-situ polymerisation, and hence is correlated with the oxidative polymerisation of aniline. The main purpose of this paper is to study the mechanism of pinning of *dw*s and its influence on the magnetic properties of in-situ prepared composites in terms of the molecular mechanism of oxidative polymerisation of aniline. That is, the molecular processes determining the molecular structure of oxidation products which are responsible for the physical and chemical properties of the products and their interaction with the surface of ferrite. This study is important from the standpoint of the synthesis of hybrid materials with reproducible electromagnetic properties.

2. Experimental

Ferrite particles were prepared by mechanical grinding of commercially available sintered 3000-NM MnZn ferrite cores. The main characteristics of bulk ferrite and its powder are listed in Table 1.

We prepared various composites of multidomain MnZn ferrite particles with PANI. Composites of the first type were obtained by mixing ferrite with PANI powder in the protonated emeraldine (MnZn/PANI*h*) and emeraldine base (MnZn/PANI*b*) forms. The PANI load in the *mixed* composites was varied from 30 to 80 vol.%. The second type of composites was synthesised by in-situ polymerisation of aniline in the presence of ferrite *(*in-situ MnZn–PANI*h*) [14,15,32]. Note that in this case most of the PANI (10 wt.%/27.7 vol.%) is bound in the coating (100-nm thick) of the particles, while free PANI (not bound to the ferrite surface) amounts to at most 3 wt.%. The processing of in-situ MnZn–PANI*h* composite by alkali converts the protonated emeraldine form with conductivity of 4 S cm^{-1} to a nonconducting state with conductivity of 10^{-7} S cm^{-1} *(*in-situ MnZn–PANI*b*). In order to measure the conductivity and the magnetic spectra, we compressed the *mixed* and in-situ type composites into pellets and toroids at 200 MPa.

The morphology of ferrite particles before and after coating with PANI, as well as the growth dynamics of a PANI film on the surface of MnZn single-crystal, were studied by the same methodology and equipment as described in [32].

The magnetic properties of composites were studied using the same experimental setup as in our previous work [32]. The magnetic spectra were analysed as a function of a DC magnetising field (H_{DC}) applied parallel to the AC magnetic field (H_{AC}) and temperature (from −30 °C up to 150 °C), followed by the fitting of the magnetic spectra with the use of the frequency dispersion formula [33]. All the characteristics of the composites are given in comparison with the properties of the original MnZn ferrite.

3. Results and discussion

3.1. Magnetic properties of MnZn ferrite and its composites with polyaniline

The magnetic properties of polymer bonded soft magnetic composites are determined by the demagnetising field, which reduces the applied magnetic field H_0 to the inner magnetic field H_i within a specimen: $\vec{H}_i = \vec{H}_0 - \hat{N}_M\vec{M}$, where $\vec{M}$ is the magnetisation vector, and $\hat{N}_M$ is the tensor of demagnetisation factors, i.e. a second-rank material tensor that determines the relationship between the magnetisation vector and the vector of the demagnetising field [34]. The $\hat{N}_M$ is the sum of the external N_{ex} and inner N_i demagnetisation factors. The external demagnetisation factor is determined by the geometrical shape of the sample. The inner demagnetisation factor in composites has its origin in the nonmagnetic interfaces between magnetic particles created by polymer. Therefore the inner demagnetising field caused by the poles on the surface of magnetic particles is given by $H_i = H_0 - J \times \frac{N_i}{\mu_0}$, where J is the polarisation and μ_0 is the permeability of vacuum. The inner demagnetisation factor is affected by magnetocrystalline anisotropy and magnetoelastic stresses due to the inverse magnetostrictive effect, as well as by the concentration, shape, size and distribution of the magnetic filler particles. While studying dynamic magnetisation processes in composite materials, the effect of N_{ex} can be avoided with the use of toroidal samples. However, the effect of N_i on μ should be considered, especially in order to control the ferromagnetic resonance frequency f_R of the magnetic composite material. It has been experimentally established that the inner demagnetisation factor in magnetic composites obtained by mixing magnetic particles with a polymer decreases with the increase of the filler concentration [29,35–38]. When the filler content C is above the percolation threshold C_P (C_P is about 30–40 vol.% for the majority of magnetic composites), the effect of N_i on f_R is negligible. Such a concentration dependence of N_i is explained as follows. At low concentrations, magnetic interaction between particles is weak, and the value of μ is determined by the polarisability of individual particles {$P = \chi/(1+N_k\chi)$, where χ is the magnetic susceptibility and ($k = x, y, z$) is the shape demagnetising factor of a particle}. The increase in the concentration of magnetic particles leads to the

Table 1
The main characteristics of sintered polycrystalline MnZn ferrite and its powder.

Sintered MnZn ferrite (data from manufacturer)	Fe_2O_3 (mol %)	53.75
	MnO (mol %)	25.10
	ZnO (mol %)	21.15
	Initial magnetic permeability μ_i	2700–3000
	Maximum magnetic permeability μ_{max}	3700–5200
	Saturation magnetisation M_s (kOe)	3.5
	Curie temperature T_C (°C)	200
	Conductivity σ_f ($S\,cm^{-1}$)	0.02
	Density ρ_f ($g\,cm^{-3}$)	4.8
MnZn ferrite powder (SEM image, Fig. 1 a)	Particle size distribution after sieving (μm)	40–80
	Mean particle size (μm)	60
	Grain size (μm)	5–20

fading of the magnetic pole on the surface of particles, which eventually leads to such a state that, above the percolation threshold, the magnetic flux becomes continuous, as in an ensemble of magnetically interacting particles. Nevertheless, as is shown in [37,38], N_i is different from zero even for $C = 100$ vol.% (i.e. for bulk ferromagnet). This is due to the fact that the value of N_i depends not only on P (and hence on the shape and concentration of particles), but also on the micromagnetic structure of the particles: the shape and distribution of crystallites, the number of grain boundaries, the disposition of pores, and internal stresses (Fig. 1).

3.1.1. Magnetostatic properties

Magnetisation curves of MnZn ferrite and its composites with PANI are reproduced in Fig. 2, which shows that the saturation magnetisation M_s in the samples is reached in fields of 4000 Oe. The original ferrite is characterised by high M_s and low coercivity H_c. In the composites, the M_s and the magnetic flux density B are lower (Fig. 2b). At the same time, in composites obtained by the in-situ polymerisation technique, the H_c is three times higher compared with that of the original ferrite, whereas the coercivity of mixed composites is not changed. The increase in coercivity indicates a decrease in the mobility of *dw*s in magnetic field.

It should be noted that H_c increases by another 30% under deprotonation of the PANI coating, whereas B decreases little. Along with change in the conductance, the deprotonation causes structural changes in PANI: the polymer loses a significant part of its mass in the form of the molecules of doping acid [39]. In this case, the volume of PANI decreases significantly, and PANI shows more compact morphology due to conformational changes of the polymer and electrostatic repulsion between polymer chains; hence, the PANI film shrinks [40]. Based on the results obtained, we can assume that a ferrite particle undergoes a compressive stress under the PANI coating, which affects the magnetisation processes in the MnZn ferrite.

It is known, that magnetoelastic effect has a great influence on magnetic properties of low-anisotropy MnZn ferrites in spite of their small magnetostrictive constant [41–44]. It was found out, that the compressive stresses produce the decrease in flux density and considerable change in the shape of the hysteresis loop, i.e. increase of coercive force, of a series of polycrystalline MnZn ferrites differing in chemical composition and porosity [45]. In [43] it was shown that the electromagnetic properties of low-anisotropy single-crystal MnZn ferrite significantly change under the application of tensile stress. Specifically, when stress increases above a critical level, as the stress-induced anisotropy exceeds the magnetocrystalline anisotropy, the low-frequency permeability decreases, while the f_R increases.

According to the theory [34,46,47], if a ferromagnet is subjected to an elastic stress before magnetisation, then, depending on the character of the deformation (stretching or compression), the certain redistribution of the magnetisation vector I_S of the domains will take place. The effect of the external stresses on the magnetic properties is determined by the sum of the magnetocrystalline anisotropy energy E_A and the magnetoelastic energy E_σ: $E = E_A + E_\sigma = \left(K + \frac{3}{2}\lambda_S\sigma_i\right)\sin^2\varphi$, where K is the magnetic anisotropy constant, λ_S is the magnetostriction constant, σ_i is the local (internal) stress, φ is the angle between the I_S and the easy axis of magnetisation [47]. According to numerous experimental data, the local stress σ_i is proportional to the external mechanical stresses σ_{ex}: $\sigma_i = \alpha\sigma_{ex}$, where α is a system parameter [48]. The parameter α depends on the elemental composition (the values of K and λ_S), the mechanical properties (elastic limit), and the

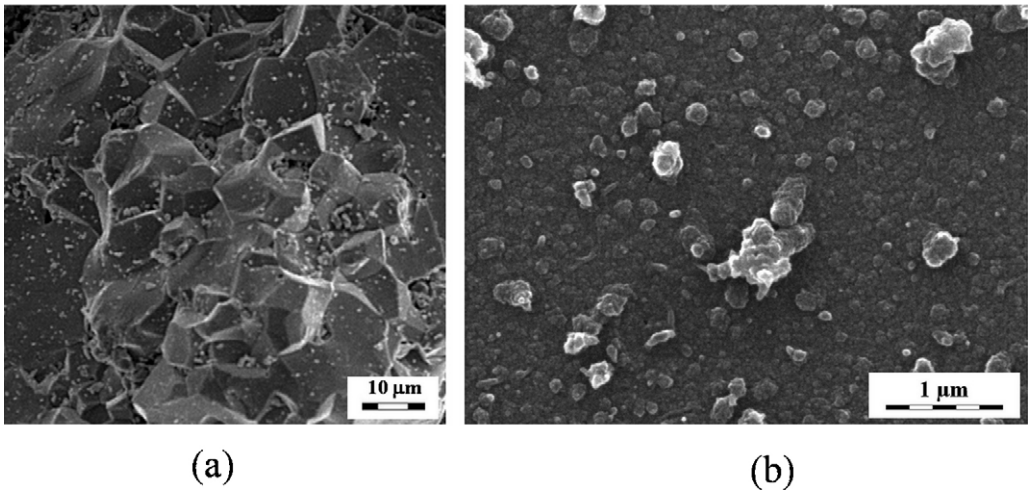

Fig. 1. SEM image of MnZn ferrite: (a) the surface of a ferrite particle, and (b) the surface of a ferrite particle coated with PANI.

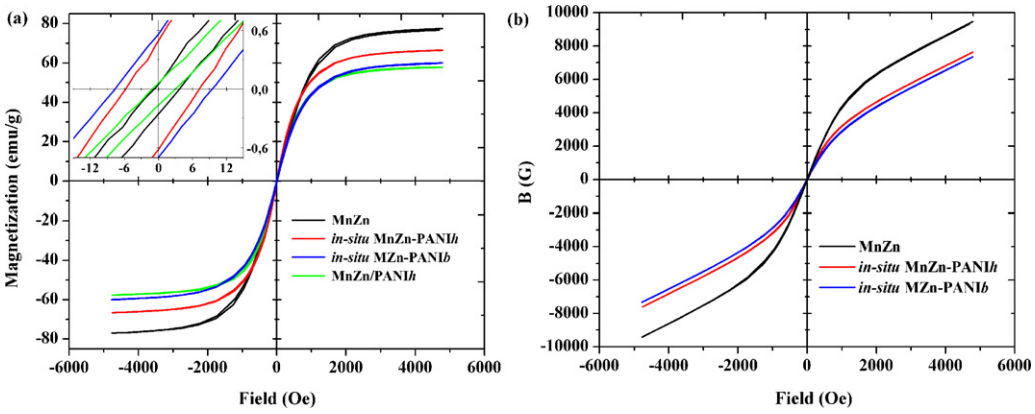

Fig. 2. Magnetisation curves of MnZn ferrite and its in-situ prepared and *mixed* composites with PANI: (a) M/H and (b) B/H.

micromagnetic structure of the ferrite. At high stresses, E_σ may be of the same order of magnitude as E_A or even greater. In this case, the direction of easy magnetisation is determined not only by the crystal structure of the ferromagnet, but also by the distribution of internal stresses in it.

Thus, we can draw the following conclusions. The PANI coating gives rise to elastic stresses in a MnZn ferrite particle and, consequently, induces a magnetostrictive anisotropy in it. Since the magnetocrystalline anisotropy of MnZn ferrite of the given composition is small, it is quite probable that the orientation of the vectors I_S in the domains and, hence, the processes of *dw* motion and *mr* are determined by the internal elastic stresses. In terms of demagnetising fields, the effect of elastic stresses on the magnetisation of in-situ composites manifests itself in the decreased internal magnetic field in composites due to the increased inner demagnetisation factor of the particles.

3.1.2. Dynamic magnetisation processes

The magnetic spectra of ferrites at radio frequencies contain two regions of frequency dispersion of permeability: the low-frequency region, which ranges from about 10 MHz to 10^3 MHz, and the high-frequency region, which roughly ranges from 500 MHz to 3×10^3 MHz [34,49]. The high-frequency region of magnetic dispersion of a ferrite is associated with the natural ferromagnetic resonance (NFR) in the effective magnetic anisotropy fields and demagnetising fields. The low-frequency region is determined in most cases by the *dw* motion (due to the rotation of magnetisation vectors in the *dw*s, which is determined by their high-frequency vibrations), rather than by the NFR. However, the *mr* may play a significant role in the low-frequency magnetisation in high-permeability and low-anisotropy MnZn ferrites. This is associated with the domain structure of such ferrites: the *dw* thickness is comparable with the domain size [50].

Just as bare ferrite, polymer composites filled with MnZn ferrite are characterised by magnetic spectrum with a single dispersion region. This applies to composites made of polymer–dielectrics [29,36] and of polymer–semiconductors, such as PANI [14–16,32]. However, there are a number of significant differences between the spectra of bare MnZn ferrites and of its composites. Specifically, for 3000-NM-type MnZn ferrite, these differences are: (1) ferrite has a magnetic spectrum of mixed relaxation–resonance type, whereas composites have a spectrum of relaxation type; (2) the complex-permeability dispersion region of ferrite extends from 10^5 Hz to 10^7 Hz, while that of its composites with PANI, from 10^7 Hz to 10^{10} Hz; and (3) ferrite has a much greater value of the low-frequency μ compared with that of composites and a considerably lower value of the high-frequency μ (Fig. 3).

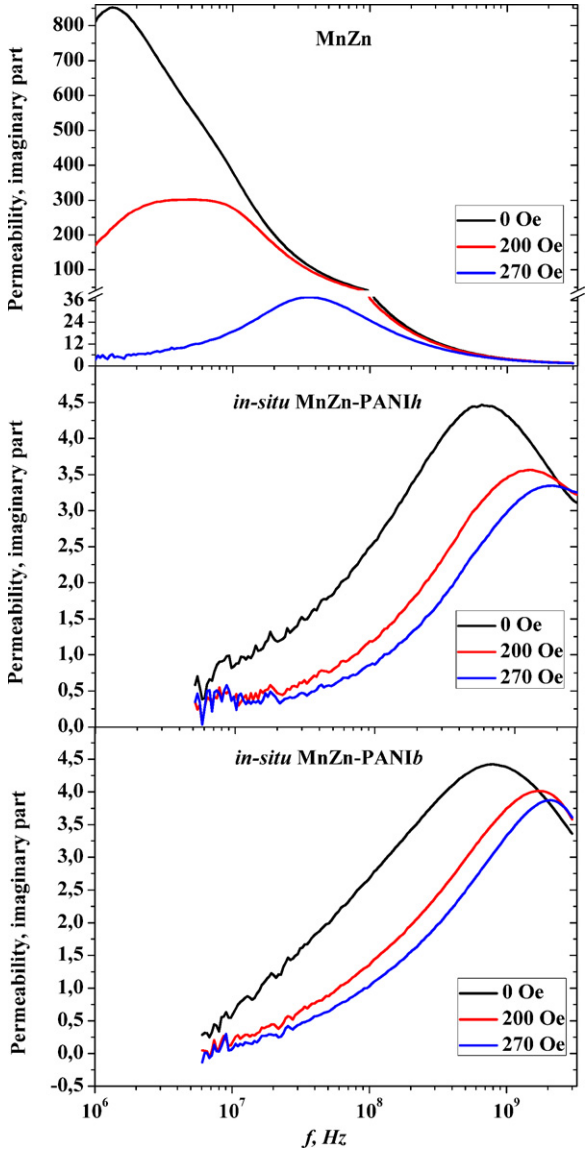

Fig. 3. Imaginary part of complex magnetic permeability for MnZn ferrite and its in-situ prepared composites in various DC external magnetic fields (H_{DC}).

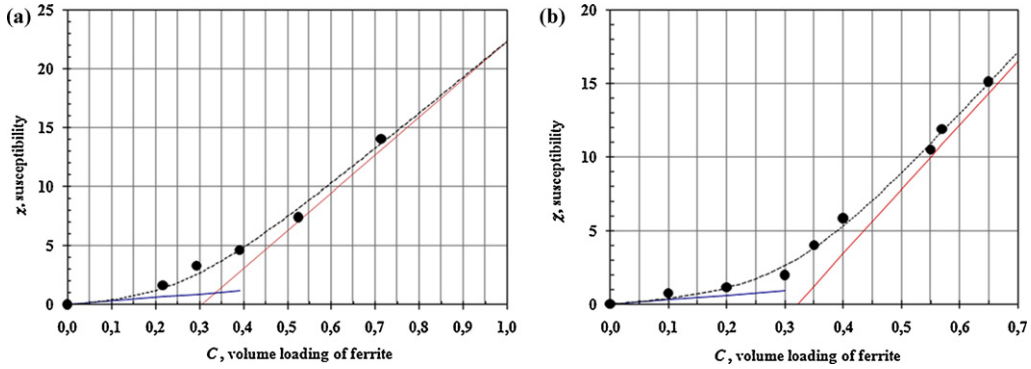

Fig. 4. The concentration dependence of real part of susceptibility of polymer composites of MnZn ferrite at 10 MHz: (a) composites prepared by mixture of ferrite powder with conducting form of PANI and (b) with polyurethane [29]. The experimental data is fitted by "mean-field" model [51].

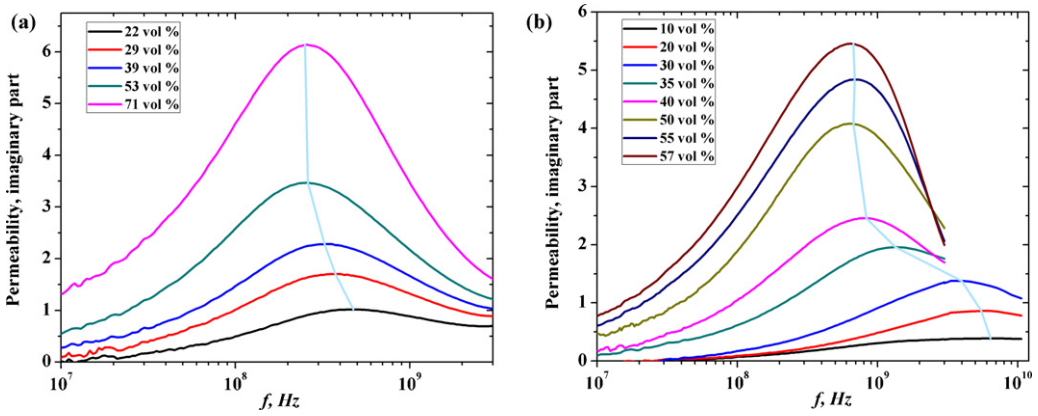

Fig. 5. Experimental variation of the imaginary part of the permeability of polymer composites of MnZn ferrite at the different volume concentration of ferrite: (a) composites prepared by mixture of MnZn ferrite powder with conducting form of PANI and (b) with polyurethane [29].

It should be noted that the magnetic spectra of the composites of MnZn ferrite mixed with PANI and with polymer–dielectrics exhibit similar behaviour. Both of them show nonlinear dependence of μ on the ferrite concentration in the polymer. The approximation of the experimental data by "mean-field" model [51] has shown that the value of percolation threshold is of about 30 vol.% (Fig. 4). Furthermore, for the ferrite concentration above 50 vol.%, f_R is virtually independent of C (Fig. 5). Thus, in high-filled mixed composites, one can practically neglect the effect of N_i on f_R.

The in-situ composites exhibit appreciably greater high-frequency shift of f_R compared with the composites obtained by mixing ferrite with PANI for the same filler-to-polymer ratio of 70 vol.%/30 vol.%. Moreover, in-situ MnZn–PANI*b* composites are characterised by appreciably higher values of f_R compared with in-situ MnZn–PANI*h*, in spite of the fact that these composites with "core–shell" like structure differ only in their conductivity and the elastic properties of the PANI coating (Fig. 6). To model such frequency shift using "coherent model" [52], the thickness of one of the coatings must be increased from actual value of 100–370 nm (Fig. 7). However in the case of in-situ composites both systems comprise the same particle size and the coating thickness. Therefore, this difference cannot be explained by the demagnetising field due to the presence of polymer gaps in the material, but is rather attributed to the enhanced value of the inner demagnetising factor of ferrite particles due to the magnetoelastic stresses induced by PANI coating. In fact, the PANI coating induces magnetic anisotropy

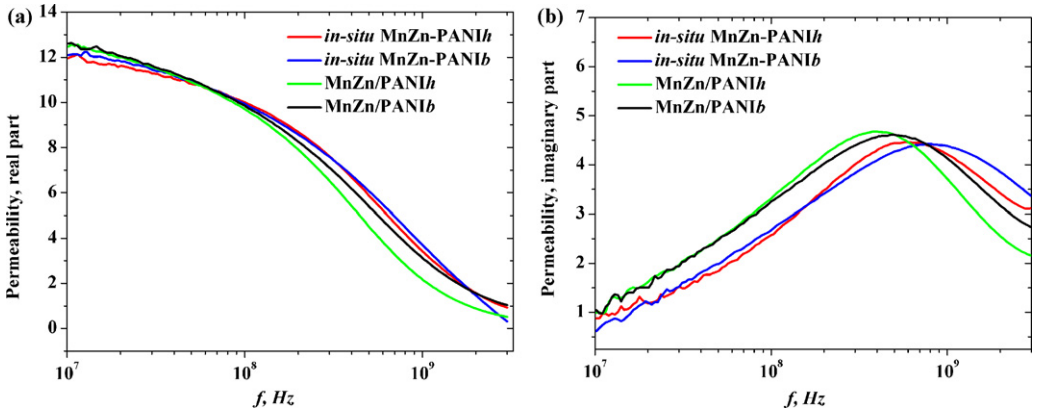

Fig. 6. Magnetic spectra of MnZn ferrite and its in-situ prepared and *mixed* composites with PANI. The concentration of PANI in all composites is 30 vol.%.

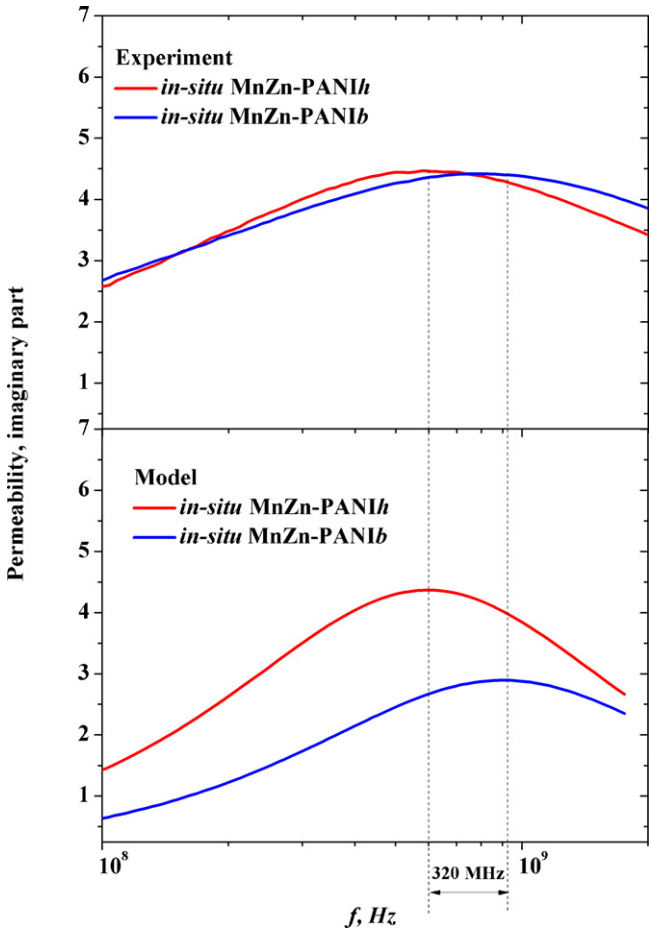

Fig. 7. Magnetic spectra of in-situ composites of MnZn ferrite: experimental results (top); approximation of experimental results by coherent model to fit resonance frequency (bottom).

(of the magnetostrictive nature) in MnZn ferrite because of its low magnetocrystalline anisotropy. This leads to a change in the magnetic state of the ferrite due to the reorientation of the vectors I_S in the domains with respect to the new directions of easy magnetisation defined by magnetoelastic stresses and should ultimately affect the contributions of *dw* motion and *mr* to μ.

In order to determine the contribution of *dw* motion and *mr* processes to μ, the following methodology has been implemented, i.e. frequency-field dependence of μ was approximated by the model described in [33]. This methodology is widely used in the study of the dynamic magnetisation processes in bare ferromagnetic materials [32,33,49,53,54], as well as in composite magnetic materials [32,33,53,54]. The applicability of this method arises from the fact that:

(1) The variation of H_{DC} allows one to determine the rebuilding of domain structure in ferrite, namely, to detect a transition of ferrite from a multidomain to the single-domain state. This is the beginning of NFR region where the magnetisation is determined only by the *mr*.

(2) The fitting of the magnetic spectra by the frequency dispersion formula allows one to determine the relative contributions of the *dw* and *mr* to μ and thus makes it possible to establish a correlation between magnetisation mechanisms and the processes of rebuilding of the domain structure of ferrite.

The results of fitting, as well as the main magnetic characteristics of in-situ prepared and mixed composites of MnZn ferrite with PANI are summarised in Tables 2 and 3 in comparison with the parameters of the original ferrite.

Table 2
Contribution of domain-wall motion and magnetisation rotation to complex magnetic permeability for manganese–zinc ferrite and its composites with polyaniline.

Sample name	Contribution of dw motion (%)		Contribution of mr (%)	
	H_{DC} 0 Oe	H_{DC} 270 Oe	H_{DC} 0 Oe	H_{DC} 270 Oe
MnZn	43	0.0	57	100
MnZn/PANI	39	22	61	78
In-situ MnZn–PANI	30	28	70	72

Table 3
Saturation magnetisation, coercivity and resonance frequency for manganese–zinc ferrite and its composites with polyaniline.

Sample name	Coercivity (Oe)	Saturation magnetisation (emu g^{-1})	Resonance frequency (MHz)
MnZn	2.2	77	1.3
MnZn/PANI*h*	2.2	59	400
MnZn/PANI*b*	2.2	58	450
In-situ MnZn–PANI*h*	6.5	67	580
In-situ MnZn–PANI*b*	8.6	60	900

The contribution of *dw* motion and *mr* to magnetisation processes in bulk MnZn ferrite is almost equal (*dw* = 43%, *mr* = 57%, Table 2). The complex-permeability dispersion region and the resonance frequency shift to higher frequencies with the application of an external magnetic field due to the suppression of domain structure (Fig. 8). It was found that for 3000-NM MnZn ferrite *dw* motion processes come to the end point when H_{DC} = 270 Oe, since the magnetisation process is determined only by the *mr* (*mr* = 100%, Table 2) marking the beginning of the NFR region. In the case of in-situ prepared and mixed MnZn–PANI composites high-frequency dispersion of μ is mainly determined by the *mr*, nevertheless, *dw* motion processes still persist up to the critical fields of $H_{DC} \geq 270$ Oe, where bare ferrite should be in the single-domain state. Moreover, in contrast to mixed composites, the *dw* contribution to μ in in-situ composites remains virtually unchanged up to very high values of H_{DC} (Table 2); thus, the "single-domain" state in coated ferrite is not reached.

Bare MnZn ferrite and its in-situ prepared composites also exhibit different thermomagnetic stability. In contrast to ferrite, which is characterised by nonlinear temperature dependence of μ, in-situ composites exhibit monotonic temperature dependence of μ, with the in-situ MnZn–PANI*b* composite being the least temperature dependent (Fig. 9). Such a significant change in the temperature dependence of μ of ferrite may be attributable to the reduced sensitivity of the ferrite to magnetostrictive strain [41].

Consequently, the features of magnetisation processes of in-situ MnZn–PANI composites in DC and AC magnetic fields, as well as the high thermomagnetic stability of in-situ prepared composites, provide evidence for the strong effect of the PANI film on the magnetic properties of composites. The coating of MnZn ferrite particles with PANI during in-situ polymerisation leads to the damping of *dw* motion in magnetic fields, which manifests itself in: (1) the increased H_c; (2) decreased low-frequency value of μ, which is associated with the contribution of *dw* motion; (3) the shift of the complex-permeability dispersion region to the ultra-high frequency (UHF) band; and (4) the increased thermomagnetic stability. In addition, in-situ MnZn–PANI*b* composite demonstrates the maximum shift of the resonance frequency due to the increase in the compressive stress generated by deprotonation of PANI coating (Table 3). These effects can be accounted for by the increased value of the inner demagnetisation factor of ferrite particles, which results from stress-induced magnetic anisotropy due to the pinning of *dw*s appearing on the surface of ferrite. What is the mechanism of pinning? Undoubtedly, it is related to the oxidative polymerisation

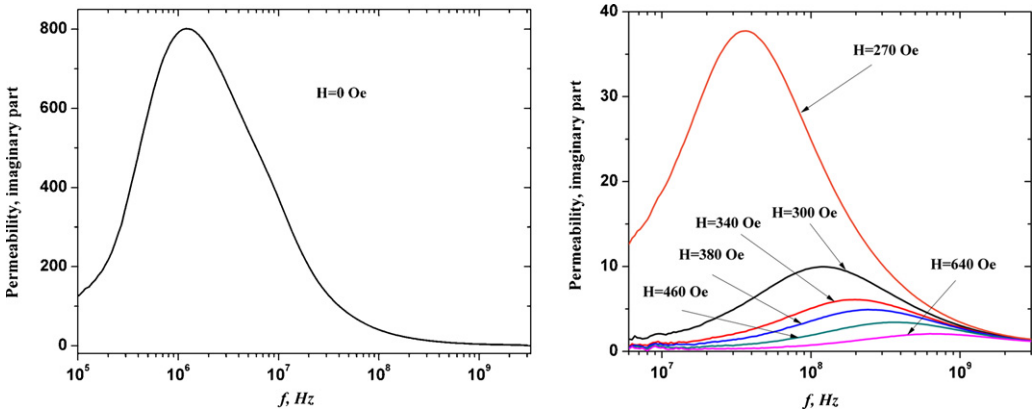

Fig. 8. Imaginary part of complex magnetic permeability for MnZn ferrite under an external DC magnetic field.

of aniline during the growth of a PANI film on the surface of a ferrite particle. To find out the effect of the PANI film on the magnetic properties of MnZn ferrite, we investigated the aniline polymerisation process in the presence of ferrite particles, as well as the morphology of the PANI film at different stages of polymerisation.

3.2. Growth mechanism of a PANI film on the surface of MnZn ferrite and related factors responsible for the change of the magnetic properties of in-situ prepared composites

3.2.1. The change in the course of oxidative polymerisation of aniline due to ferrite

The oxidative polymerisation of aniline is an exothermic process, where the course of the reaction is easily traced by the variation of the temperature of the polymerisation medium [13]. Fig. 10 shows the temperature profiles of aniline polymerisation without ferrite (curve 1) and in the presence of MnZn ferrite powder with a ferrite/aniline mass ratio of 10. To study the effect of the surface area of ferrite particles on the polymerisation, we used particles with a size of 200–250 μm (Fig. 10, curve 2) and 40–80 μm (Fig. 10, curve 3). MnZn ferrite is a chemically inert filler, as it is insoluble and does not change the composition of the polymerisation medium. Nevertheless, ferrite accelerates the polymerisation of aniline. Moreover, the larger the surface area of particles, the faster the oxidative polymerisation process. It is significant that the induction period of polymerisation decreases as the surface area increases, whereas the exothermic stage of the growth of polymer chains remains virtually unchanged. The acceleration of the oxidative polymerisation of aniline indicates that the reaction proceeds heterogeneously on the solid/liquid interface; i.e., the PANI film grows directly on the surface of ferrite particles.

It has generally been observed that the introduction of a substrate having a larger-surface area speeds up the oxidation of aniline. This phenomenon is observed not only in the case of ferrite, but also in fillers of other chemical nature, where, again, the acceleration of the reaction correlates with the surface area of the substrate. This confirms the general principles in the formation of an in-situ PANI film on a substrate. However, in the case of ferrite, the increase in the polymerisation rate is stronger than that in the case of, say, silica, which has a comparable specific surface area [55], or in the case of water-soluble polymers [56].

According to the mechanism of oxidative polymerisation of aniline [13], the initial stage of oxidation (induction period) is associated with the formation of aniline oligomers, which have a heterocyclic phenazine structure. The polymerisation rate is limited by the stage of bonding the first monomeric aniline molecule to phenazine-like oligomers. The further growth of polymer chains represents a very fast exothermic reaction. Thus, the reduction of the induction period of oxidation in the presence of ferrite implies that ferrite stimulates the propagation of PANI chains. This is associated with the effect of the microstructure of high-permeability, low-anisotropy MnZn ferrite on the oxidative polymerisation of aniline. The assumption is based on the AFM results, which show that a discontinuous PANI film is formed during the induction

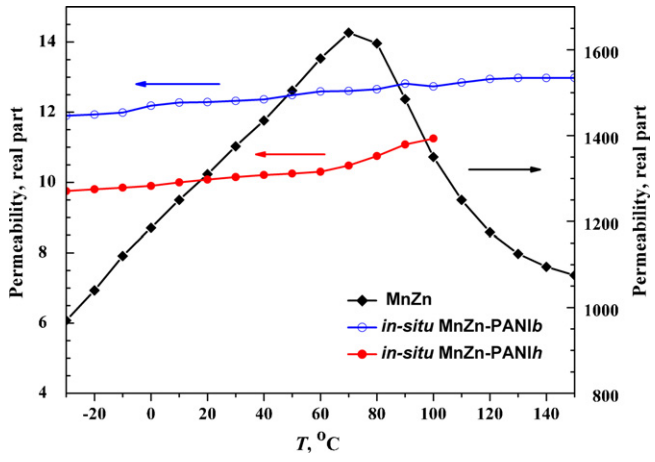

Fig. 9. Temperature dependence of the real part of complex permeability at 1 MHz for MnZn ferrite and its in-situ prepared composites.

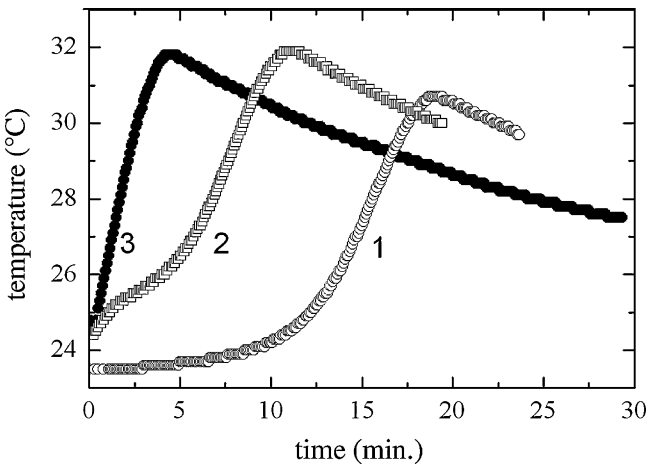

Fig. 10. Temperature profile in the oxidative polymerisation of aniline hydrochloride (0.2 mol L^{-1}) with ammonium peroxydisulphate (0.25 mol L^{-1}) in water: (1) without MnZn ferrite and in the presence of (2) 200–250 μm and (3) 40–80 μm MnZn ferrite particles.

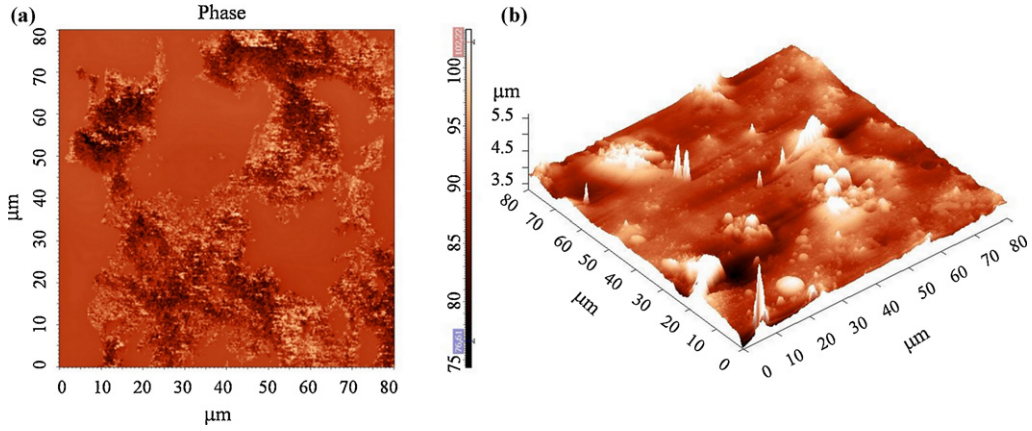

Fig. 11. Atomic force microscopy of the surface of MnZn ferrite coated with polyaniline by in-situ polymerisation: (a) initial stage of polymerisation (discontinuous polyaniline film with a "honeycomb" structure, phase contrast) and (b) final stage of polymerisation (continuous PANI film, 3D relief).

period, and a continuous polymer layer appears only at the end of polymerisation (Fig. 11). The honeycomb morphology of a discontinuous PANI film (Fig. 11a) largely corresponds to the grain pattern of the MnZn ferrite (Fig. 1a), where the concentration of *dw*s is high, as is shown in [57] by an example of high-permeability MnZn ferrite.

3.2.2. The mechanism of a PANI film growth on the surface of MnZn ferrite: effect of ferrite–polyaniline interaction

The acceleration of oxidative polymerisation of aniline, as well as the formation of a PANI film with a honeycomb structure on the ferrite surface during the induction period, correlates with the molecular mechanism of aniline oxidation. This allows us to suggest a scenario for the growth of a PANI film on the ferrite surface and interpret its effect on the magnetic properties of in-situ composites of MnZn ferrite.

According to the mechanism of oxidative polymerisation of aniline [13,58], the induction period of the oxidation is associated with the formation of aniline oligomers, which have a phenazine structure. Phenazine heterocycles have a flat molecular structure in the form of aromatic rings with high π-electron density. Molecules of this type exhibit a tendency to adsorption and self-assembly due to the π-electron interactions, whose energy is estimated to be tens of kcal mol^{-1} [59]. Under the conditions of oxidative polymerisation of aniline, the phenazine cycle is oxidised. In this case, a molecule becomes paramagnetic due to the formation of a stable cation-radical on a nitrogen atom. Since *dw*s are the source of an inhomogeneous magnetic field, the sorption of paramagnetic cation radicals can take place precisely near the *dw* appearing on the ferrite surface. The honeycomb morphology of the PANI film repeats the microstructure of the grain boundaries on the surface of the ferrite; this fact confirms that the specific sorption of paramagnetic nuclei takes place on the *dw*s. The hypothesis on the specific sorption of aniline oligomers on the *dw*s is proved by the data reported in the literature on the effect of a magnetic field, as well as magnetic dopants introduced into the polymerisation medium, on the aniline polymerisation [60–62].[1]

Phenazines serve as nuclei of future polymer chains. The polymer film growing in the region of sorption of phenazines represents an organised structure where individual PANI chains are linked by hydrogen bonds. The formation of such a structure near the region where *dw*s appear on the ferrite surface leads to the pinning of the *dw*s. Taking into account the 3-fold increase in the coercivity of PANI-coated ferrite and the persistence of the multidomain state in this ferrite even in high magnetic fields, we can assume that the *dw* pinning forces are strong enough to induce elastic stresses in a ferrite particle that stimulate the growth of the effective magnetic anisotropy. It is necessary to take into account that high-permeability MnZn ferrite is characterised by low values of the magnetic anisotropy energy and the magnetic dipolar interaction energy. Therefore, the domain structure of such ferrite, i.e. the domain size and the thickness of *dw*s, is determined by internal stresses. In this case, the magnetic anisotropy induced in a PANI-coated ferrite particle favours the reorientation of I_S in domains and *dw*s with respect to the new directions of easy magnetisation defined by internal stresses, which manifests itself in the increased thickness of *dw*s, thus hampering their motion in magnetic fields [63]. This mechanism does not operate in highly anisotropic ferrites. For instance, our investigations failed to reveal any influence of a PANI film on the magnetic properties of highly anisotropic hexagonal ferrites (Co_2Z, Co_2W, Ni_2W, Zn_2Co_xW, BaM, BaW). A significant effect of *dw* pinning and the related magnetoelastic stresses on the magnetic properties of in-situ prepared composites is also confirmed by the fact that the maximum variation in the coercivity and the maximum shift of the resonance frequency are exhibited by a nonconductive deprotonated form of the PANI film, which produces the maximum internal stresses in a ferrite particle.

4. Conclusions

We have investigated the magnetic properties of two types of MnZn ferrite–PANI composites that have the same composition but different structures due to different preparation methods. The composites obtained by the in-situ polymerisation method, in which ferrite particles are coated with PANI, differ from simply mixed composites by higher coercivity, higher resonance frequencies and higher thermomagnetic stability. These changes in the magnetic properties of polyaniline-coated ferrite are attributed to the increased value of the inner demagnetisation factor, which results from stress-induced magnetic anisotropy due to the pinning of *dw*s appearing on the surface of ferrite. The analysis of the structure of PANI films at different stages of polymerisation

[1] In references [60–62], the authors established that the polymerization rate of aniline oxidation increases under the application of a DC magnetic field and that a PANI film grows faster on a substrate as the field intensity increases from 0 to 8 kOe. They also revealed the effect of an external magnetic field of 7 kOe on the morphology, crystallinity, and the electric conductivity of a polymer film growing during electrochemical synthesis. The most effective field was the one applied parallel to the electrode surface; this field leads to a significant increase in the crystallinity of a sample and increased its electric conductivity from 10 to 50 S cm^{-1} [60].

shows that the film grows selectively in the regions where *dw*s appear on the surface. This is attributed to the selective sorption of paramagnetic phenazine nuclei on the *dw*s. The strong π-electron interaction between phenazine and ferrite gives rise to the growth of polymer chains in the place of sorption of nuclei. This leads to the *dw* pinning and, as a consequence, to the damping of *dw* motion in magnetic fields. The *dw* pinning forces are strong enough to induce elastic stresses in the particles of low-anisotropy MnZn ferrite that contribute to the increase in the effective magnetic anisotropy. The rise of stress-induced magnetic anisotropy is most pronounced in in-situ MnZn−PANI*b* composite due to the film shrinkage after deprotonation of PANI. Therefore it is characterised by the highest values of coercivity and resonance frequency, as well as by the highest thermomagnetic stability.

Acknowledgements

This article was produced with the support of Operational Program Research and Development for Innovations co-funded by the European Regional Development Fund (ERDF) and national budget of Czech Republic, within the framework of project Centre of Polymer Systems (reg. number: CZ.1.05/2.1.00/03.0111), the internal grant of TBU in Zlin (IGA/7/FT/11/D), as well as with the support of Russian Federation Programmes (RAS-P22 and 16.516.11.6034).

References

[1] T.A. Skotheim, J.R. Reynolds, Handbook of Conducting Polymers. Conjugated polymers: Processing and Applications, 3rd ed., CRC Press, Boca Raton, 2007.
[2] S.S. Umare, B.H. Shambharkar, R.S. Ningthoujam, Synthesis and characterization of polyaniline-Fe_3O_4 nanocomposite: electrical conductivity, magnetic, electrochemical studies, Synthetic Metals 160 (2010) 1815–1821.
[3] B.I. Podlovchenko, V.N. Andreev, Electrocatalysis on polymer-modified electrodes, Russian Chemical Reviews 71 (2002) 837–851.
[4] A.J. Dominis, G.M. Spinks, G.G. Wallace, Comparison of polyaniline primers prepared with different dopants for corrosion protection of steel, Progress in Organic Coatings 48 (2003) 43–49.
[5] A. Kalendova, I. Sapurina, J. Stejskal, D. Vesely, Anticorrosion properties of polyaniline-coated pigments in organic coatings, Corrosion Science 50 (2008) 3549–3560.
[6] V.E. Bochenkov, G.B. Sergeev, Nanomaterials for sensors, Russian Chemical Reviews 76 (2007) 1013–1022.
[7] A.A. Karyakin, M. Vuki, L.V. Lukachova, E.E. Karyakina, A.V. Orlov, G.P. Karpachova, J. Wang, Processible polyaniline as an advanced potentiometric pH transducer. Application to biosensors, Analytical Chemistry 71 (1999) 2534–2540.
[8] I. Sapurina, J. Stejskal, Ternary composites of multi-wall carbon nanotubes, polyaniline, and noble-metal nanoparticles for potential applications in electrocatalysis, Chemical Papers 63 (2009) 579–585.
[9] S. Sugimoto, T. Maeda, D. Book, T. Kagotani, K. Inomata, M. Homma, H. Ota, Y. Houjou, R. Sato, GHz microwave absorption of a fine alpha-Fe structure produced by the disproportionation of Sm_2Fe_{17} in hydrogen, Journal of Alloys Compound 330 (2002) 301–306.
[10] P. Xu, X.J. Han, J.J. Jiang, X.H. Wang, X.D. Li, A.H. Wen, Synthesis and characterization of novel coralloid Polyaniline/$BaFe_{12}O_{19}$ nanocomposites, Journal of Physical Chemistry C 111 (2007) 12603–12608.
[11] X.L. Dong, X.F. Zhang, H. Huang, F. Zuo, Enhanced microwave absorption in Ni/polyaniline nanocomposites by dual dielectric relaxations, Applied Physics Letters 92 (2008) 013127.
[12] A. Malinauskas, Chemical deposition of conducting polymers, Polymer 42 (2001) 3957–3972.
[13] I. Sapurina, J. Stejskal, The mechanism of the oxidative polymerization of aniline and the formation of supramolecular polyaniline structures, Polymer International 57 (2008) 1295–1325.
[14] N.E. Kazantseva, Y.I. Bespyatykh, I. Sapurina, J. Stejskal, J. Vilcakova, P. Saha, Magnetic materials based on manganese-zinc ferrite with surface-organized polyaniline coating, Journal of Magnetism and Magnetic Materials 301 (2006) 155–165.
[15] N.E. Kazantseva, J. Vilcakova, V. Kresalek, P. Saha, I. Sapurina, J. Stejskal, Magnetic behaviour of composites containing polyaniline-coated manganese-zinc ferrite, Journal of Magnetism and Magnetic Materials 269 (2004) 30–37.
[16] Y.I. Bespyatykh, N.E. Kazantseva, Electromagnetic properties of hybrid polymer composites, Journal of Communications Technology and Electronics 53 (2008) 143–154.
[17] O. Yavuz, M.K. Ram, M. Aldissi, P. Poddar, S. Hariharan, Synthesis and the physical properties of MnZn ferrite and NiMnZn ferrite-polyaniline nanocomposite particles, Journal of Materials Chemistry 15 (2005) 810–817.
[18] J. Jiang, L.H. Ai, L.C. Li, Synthesis and magnetic performance of polyaniline/Mn–Zn ferrite nanocomposites with intrinsic conductivity, Journal of Material Sciences 44 (2009) 1024–1028.
[19] L.C. Li, C. Xiang, X.X. Liang, B. Hao, $Zn_{0.6}Cu_{0.4}Cr_{0.5}Fe_{1.46}Sm_{0.04}O_4$ ferrite and its nanocomposites with polyaniline and polypyrrole: preparation and electromagnetic properties, Synthetic Metals 160 (2010) 28–34.
[20] S.P. Gairola, V. Verma, L. Kumar, M.A. Dar, S. Annapoorni, R.K. Kotnala, Enhanced microwave absorption properties in polyaniline and nano-ferrite composite in X-band, Synthetic Metals 160 (2010) 2315–2318.
[21] S. Bedanta, W. Kleemann, Supermagnetism, Journal of Physics D: Applied Physics 42 (2009) 013001.
[22] Y.X. Li, H.W. Zhang, Y.L. Liu, Q.Y. Wen, J. Li, Rod-shaped polyaniline-barium ferrite nanocomposite: preparation, characterization and properties, Nanotechnology 19 (2008) 105605.
[23] A.A Farghali, M. Moussa, M.H. Khedr, Synthesis and characterization of novel conductive and magnetic nano-composites, Journal of Alloys Compound 499 (2010) 98–103.
[24] P. Gomez-Romero, Hybrid organic–inorganic materials—in search of synergic activity, Advanced Materials 13 (2001) 163–174.
[25] X.G. Peng, Y. Zhang, J. Yang, B.S. Zou, L.Z. Xiao, T.J. Li, Formation of nanoparticulate Fe_2O_3-stearate multilayer through the langmuir-blodgett method, Journal of Physical Chemistry 96 (1992) 3412–3415.
[26] H. Kawaguchi, Functional polymer microspheres, Progress in Polymer Science 25 (2000) 1171–1210.
[27] T.C. Girija, M.V. Sangaranarayanan, Analysis of polyaniline-based nickel electrodes for electrochemical supercapacitors, Journal of Power Sources 156 (2006) 705–711.
[28] A. Ohlan, K. Singh, A. Chandra, S.K. Dhawan, Microwave absorption properties of conducting polymer composite with barium ferrite nanoparticles in 12.4–18 GHz, Applied Physics Letters 93 (2008) 053114.
[29] R. Moucka, A.V. Lopatin, N.E. Kazantseva, J. Vilcakova, P. Saha, Enhancement of magnetic losses in hybrid polymer composites with MnZn-ferrite and conductive fillers, Journal of Materials Science 42 (2007) 9480–9490.
[30] R. Moucka, J. Vilcakova, N.E. Kazantseva, A.V. Lopatin, P. Saha, The influence of interfaces on the dielectric properties of MnZn-based hybrid polymer composites, Journal of Applied Physics 104 (2008) 103718.
[31] R. Malik, S. Lamba, R.K. Kotnala, S. Annapoorni, Role of anisotropy and interactions in magnetic nanoparticle systems, European Physical Journal B 74 (2010) 75–80.
[32] V. Babayan, N.E. Kazantseva, R. Moucka, I. Sapurina, Y.M. Spivak, V.A. Moshnikov, Combined effect of demagnetizing field and induced magnetic anisotropy on the magnetic properties of manganese–zinc ferrite composites, Journal of Magnetism and Magnetic Materials 324 (2012) 161–172.
[33] T. Nakamura, T. Tsutaoka, K. Hatakeyama, Frequency dispersion of permeability in ferrite composite-materials, Journal of Magnetism and Magnetic Materials 138 (1994) 319–328.
[34] S.V. Vonsovskii, Magnetism, J. Wiley, New York, 1974.
[35] J.L. Mattei, M. Le Floc'h, Percolative behaviour and demagnetizing effects in disordered heterostructures, Journal of Magnetism and Magnetic Materials 257 (2003) 335–345.
[36] J.L. Mattei, M. Le Floc'h, Effects of the magnetic dilution on the ferrimagnetic resonance of disordered hetero structures, Journal of Magnetism and Magnetic Materials 264 (2003) 86–94.
[37] M. Anhalt, B. Weidenfeller, J.L. Mattei, Inner demagnetization factor in polymer-bonded soft magnetic composites, Journal of Magnetism and Magnetic Materials 320 (2008) E844–E848.
[38] M. Anhalt, B. Weidenfeller, Theoretical and experimental approach to characteristic magnetic measurement data of polymer bonded soft magnetic composites, Journal of Applied Physics 105 (2009) 113903.
[39] E.S. Matveeva, R.D. Calleja, V. Parkhutik, Equivalent circuit analysis of the electrical properties of conducting polymers: electrical relaxation mechanisms in polyaniline under dry and wet conditions, Journal of Non-Crystalline Solids 235 (1998) 772–780.
[40] P.R. Singh, S. Mahajan, S. Raiwadec, A.Q. Contractor, EC-AFM investigation of reversible volume changes with electrode potential in polyaniline, Journal of Electroanalytical Chemistry 625 (2009) 16–26.
[41] D. Stoppels, U. Enz, J.P.M. Damen, H.M.W. Booij, Stress dependence of the magnetic-permeability of MnZn ferrous ferrites, Journal of Magnetism and Magnetic Materials 20 (1980) 231–235.
[42] K. Aso, Mechanically induced anisotropy and its effect on magnetic-permeability in single-crystal ferrites, IEEE Transactions on Magnetics 14 (1978) 76–81.
[43] E.G. Visser, The stress dependence of the domain structure and the magnetic permeability of monocrystalline $MnZnFe^{II}$ ferrite, Journal of Magnetism and Magnetic Materials 26 (1982) 303–305.
[44] A. Bienkowski, Magnetoelastic Villari effect in Mn–Zn ferrites, Journal of Magnetism and Magnetic Materials 215 (2000) 231–233.
[45] A. Bienkowski, K. Rozniatowski, R. Szewczyk, Effects of stress and its dependence on microstructure in Mn–Zn ferrite for power applications, Journal of Magnetism and Magnetic Materials 254 (2003) 547–549.
[46] C. Kittel, Introduction to Solid State Physics, 8th ed., J. Wiley, New York, 2005.
[47] S. Chikazumi, Physics of Ferromagnetism, 2nd ed., Oxford University Press, New York, 1997.
[48] A. Chevalier, E. Le Guen, A.C. Tarot, B. Grisart, D. Souriou, P. Queffelec, A. Thakur, J.L. Mattei, Pressure dependence of the frequency permeability spectra of soft

ferrite composite materials: a method of measuring the natural ferromagnetic resonance frequency, IEEE Transactions on Magnetics 47 (2011) 4132–4134.
[49] A.G. Gurevich, G.A. Melkov, Magnetization Oscillations and Waves, CRC Press, Boca Raton, 1996.
[50] M. Kornetzki, E. Moser, E. Ross, Mangan–zink–ferrite mit spontaner isopermschleife, Naturwissenschaften 47 (1960) 274.
[51] M. Le Floc'h, J.L. Mattei, P. Laurent, O. Minot, A.M. Konn, A physical model for heterogeneous magnetic materials, Journal of Magnetism and Magnetic Materials 140 (1995) 2191–2192.
[52] E.G. Visser, M.T. Johnson, A novel interpretation of the complex permeability in polycrystalline ferrites, Journal of Magnetism and Magnetic Materials 101 (1991) 143–147.
[53] T. Tsutaoka, T. Kasagi, K. Hatakeyama, Magnetic field effect on the complex permeability for a Mn–Zn ferrite and its composite materials, Journal of the European Ceramic Society 19 (1999) 1531–1535.
[54] T. Tsutaoka, Frequency dispersion of complex permeability in Mn–Zn and Ni–Zn spinel ferrites and their composite materials, Journal of Applied Physics 93 (2003) 2789–2796.
[55] J. Stejskal, M. Trchova, S. Fedorova, I. Sapurina, J. Zemek, Surface polymerization of aniline on silica gel, Langmuir 19 (2003) 3013–3018.
[56] J. Stejskal, I. Sapurina, On the origin of colloidal particles in the dispersion polymerization of aniline, Journal of Colloid and Interface Science 274 (2004) 489–495.
[57] T. Kasahara, D. Shindo, H. Yoshikawa, T. Sato, K. Kondo, In situ observations of domain structures and magnetic flux distributions in Mn–Zn and Ni–Zn ferrites by Lorentz microscopy and electron holography, Journal of Electron Microscopy 56 (2007) 7–16.
[58] I.Y. Sapurina, J. Stejskal, The effect of pH on the oxidative polymerization of aniline and the morphology and properties of products, Russian Chemical Reviews 79 (2010) 1123–1143.
[59] F.J.M. Hoeben, P. Jonkheijm, E.W. Meijer, A. Schenning, About supramolecular assemblies of pi-conjugated systems, Chemical Reviews 105 (2005) 1491–1546.
[60] L.T. Cai, S.B. Yao, S.M. Zhou, Effects of the magnetic field on the polyaniline film studied by in situ conductivity measurements and X-ray diffraction, Journal of Electroanalytical Chemistry 421 (1997) 45–48.
[61] L.T. Cai, S.B. Yao, S.M. Zhou, Improved conductivity and electrical properties of polyaniline in the presence of rare-earth cations and magnetic field, Synthetic Metals 88 (1997) 205–208.
[62] L. Ma, J. Yan, M.Y. Gan, W. Qiu, L. He, J.F. Li, Application of QCM technique in the kinetic study of polyaniline film formation in the presence of a constant (0.4 T) magnetic field, Polymer Testing 27 (2008) 683–687.
[63] S. Krupicka, P. Novak, Oxide spinels, in: E.P. Wohlfarth (Ed.), Ferromagnetic Materials, vol. 3, North-Holland, Amsterdam, 1982, pp. 189–304.

PAPER III

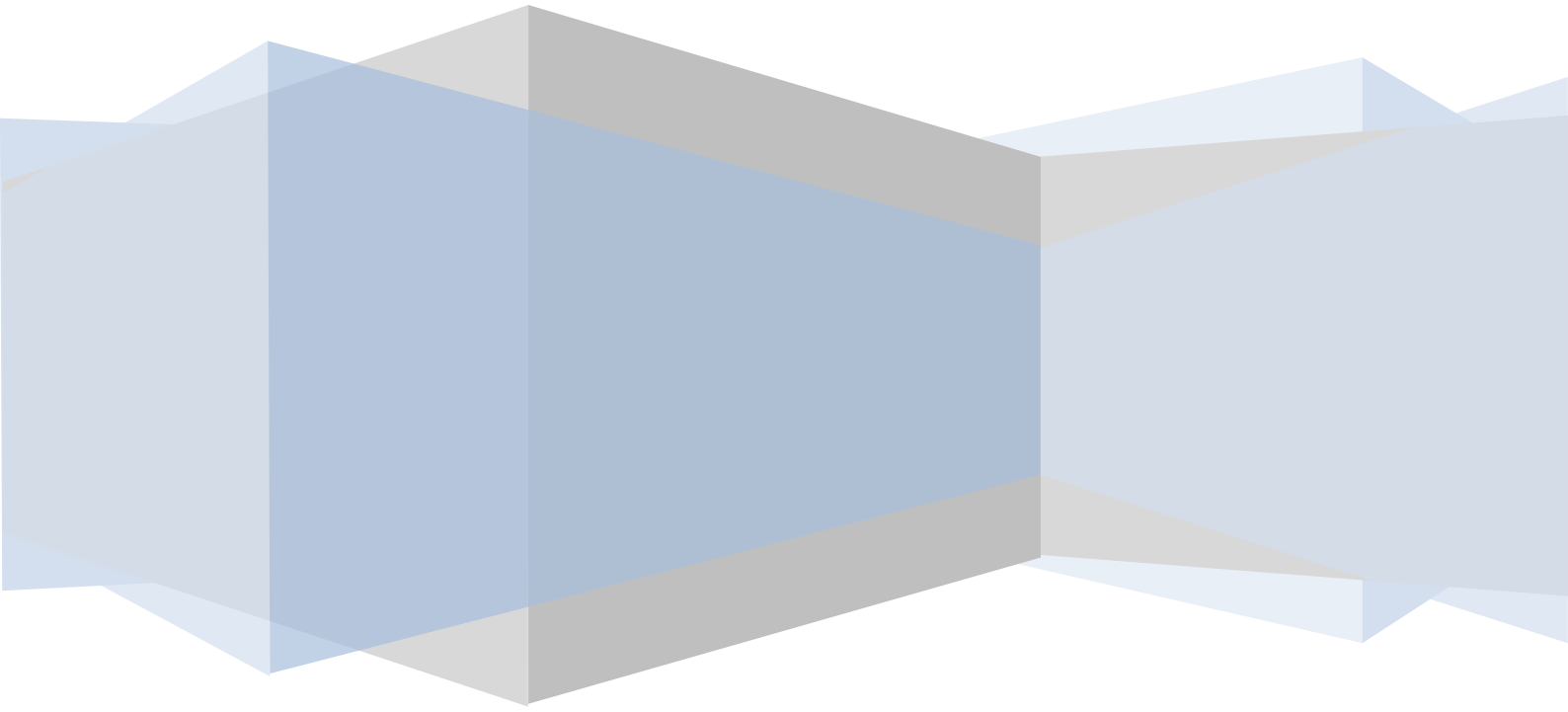

Increasing the high-frequency magnetic permeability of MnZn ferrite in polyaniline composites by incorporating silver

V. Babayan[a], N. E. Kazantseva[a,b*], I. Sapurina[c], R. Moučka[a,b], J. Stejskal[d], P. Sáha[a,b]

[a] *Centre of Polymer Systems, University Institute, Tomas Bata University in Zlin, Nad Ovcirnou 3685, 760 01 Zlin, Czech Republic*

[b] *Polymer Centre, Faculty of Technology, Tomas Bata University in Zlin, T. G. Masaryk Sq. 5555, 760 01 Zlin, Czech Republic*

[c] *Institute of Macromolecular Compounds, Russian Academy of Sciences, St. Petersburg 199004, Russia*

[d] *Institute of Macromolecular Chemistry, Academy of Sciences of the Czech Republic, 162 06 Prague 6, Czech Republic*

Elsevier Editorial System(tm) for Journal of Magnetism and Magnetic Materials
Manuscript Number: MAGMA-D-12-00986R1

Corresponding author: Dr. Natalia E. Kazantseva, Polymer Centre, Faculty of Technology, Tomas Bata University in Zlin, T. G. Masaryk Sq. 275, 762 72 Zlin, Czech Republic. Tel.: +420-576-038-114, fax: +420-576-031-444. *E-mail address:* nekazan@yahoo.com (N. Kazantseva).

Abstract: A hybrid composite containing 73 vol. % of MnZn ferrite, 21 vol. % of polyaniline, and 6 vol. % of silver is obtained by oxidative polymerization of aniline with silver nitrate in the presence of ferrite powder. The hybrid composite contains ferrite particles with a size of 40–80 micrometres coated by an inhomogeneous layer of polyaniline in the conducting emeraldine form. Silver in the form of nano- and submicrometre -size particles is localized both on the surface of ferrite particles and in the bulk of polyaniline coating. The electrical and magnetic properties of the hybrid composite are investigated and compared with the properties of a composite with 71 vol. % of MnZn ferrite coated by a conducting polyaniline layer (29 vol. %). The hybrid composite containing silver exhibits an increase in the real and imaginary parts of the complex permeability in the radio-frequency band by more than one and a half times compared with those of the MnZn ferrite–polyaniline composite. The high-frequency permittivity of both composites is determined by the properties of core–shell structure: electric properties of shell and its uniformity.

Keywords: Ferrite; polyaniline; silver; core-shell particles; hybrid composite; complex magnetic permeability; complex dielectric permittivity.

1. Introduction

At present, considerable effort is being devoted to the development of high-efficiency radio-absorbing materials (RAMs) for the frequency range of 0.6–1 GHz, which is the operating band of many radio electronic systems, including mobile communication systems. RAMs with high values of the real (μ') and imaginary (μ'') parts of the complex permeability (μ) are more advantageous. As a rule, modern RAMs are composites in which magnetic particles (most often, ferrites and Fe-based alloys) are dispersed in a polymer matrix. The effective value of μ, as well as the characteristic resonance frequencies (f_R) of magnetic composites, are determined by the demagnetizing fields. Therefore, μ and f_R depend on the type of the magnetic filler and its concentration in the polymer matrix. Moreover, the size and the shape of the filler particles, as well as the properties of the polymer and a method of obtaining a magnetic composite, are also important [1]. The increase of the intrinsic permeability (μ_i) of the filler guarantees the increase of μ of the composite by only a few units [2]. The increase of the filler particle size increases the magnetic losses, though μ' increases insignificantly [3, 4]. A significant increase in μ can be achieved with the use of flake-shape filler particles, because they are characterized by a low value of the shape demagnetization factor and allow for the formation of magnetically textured composites [5-7]. The permeability μ of composites with high filling factor ($C \geq 0.5$) is nearly independent of the demagnetizing fields and the shape factor [8-10]. However, in this case, eddy current effect appears in magnetic spectrum. Especially, it is concerning composites filled with electrically-conductive magnetic particles [11].

At the moment, several methods have been proposed to improve the high-frequency permeability dispersion of polymer magnetic composites. The heat-treatment of metal particles increases the contact resistance between

them in composite and thus suppresses the eddy currents effect [11].

Table 1. The main characteristics of sintered polycrystalline 3000–NM MnZn ferrite and its powder.

Sintered MnZn ferrite (data from manufacturer)	Initial magnetic permeability, μ_i	2700–3000
	Maximum magnetic permeability, μ_{max}	3700–5200
	Saturation field, H_s (kOe)	3.5
	Saturation magnetization, M_S (emu g^{-1})	97
	Curie temperature, T_C (K)	473
	Conductivity, σ_f (S cm^{-1})	0.02
	Density, ρ_f (g cm^{-3})	4.8
MnZn ferrite powder (own data)	Particle-size distribution after sieving (μm)	40–80
	Mean particle size (μm)	60
	Grain size (μm)	5–20
	Coercivity (Oe)	2.2
	Saturation magnetization (emu g^{-1})	77
	Saturation field H_s (kOe)	3.5–4
	Remanence (emu g^{-1})	0.15

In the ferrite-filled composites, the μ can be increased due to the use of a mixture of fillers or multicomponent particles with «magnetic core – conducting shell» structure. In the first case, the desired effect is achieved by combining ferrites of different composition [12, 13], ferrites and electrically-conductive magnetic particles [14, 15], and MnZn ferrite with electrically- conductive non-magnetic particles [3]. An increase in the value of μ in the composites containing ferrites mixed with electrically-conductive fillers is observed when conducting filler is distributed between the particles of the main magnetic phase in the bulk of the composite [1]. It was shown that the presence of electric contact between magnetic particles in composite increases μ [16]. This effect, as was explained in [16], is attributed to the increased concentration of magnetic flux in the material. In the contrast to composites with mixed fillers, the composites with multicomponent particles exhibit not only a variation in the absolute value of μ but, in many cases, a shift in f_R to higher frequencies. In [17], by an example of ferrite particles with conducting coating, it is shown that the effect of coating on the frequency dependence of μ of an ensemble of such particles can be explained from the viewpoint of electromagnetic shielding. A thin conducting coating partially shields a microwave field induced by AC magnetization of a ferrite particle. This leads to the increase in the energy of the dipole field and, hence, to a shift of the ferromagnetic resonance frequency of a uniformly magnetized particle. Depending on the relation between the thickness and the skin depth of a conducting overlayer, as well as on the characteristic radius of a ferrite particle, the conducting overlayer manifests itself in the shift of the ferromagnetic resonance frequency and/or in the enhanced magnetic losses in the system.

At present, two methods are used for the synthesis of multicomponent particles with «magnetic core–conducting shell» structure. The *first method* consists in the metallization of magnetic particles by electrolysis plating process [18, 19]. The main problem of the metallization method is to obtain a uniform metal coating of thickness no greater than the skin-depth which, for the most conducting metals amounts to a few micrometres in the ultra-high frequency band. The *second method* is based on the surface modification of ferrite particles by electrically conducting polymers, such as polyaniline (PANI) and polypyrrole, by the method of oxidative polymerization of a monomer in the presence of magnetic particles [20-22]. A polymer coating of required thickness and morphology can be obtained by controlled synthesis methods [23]; the conductivity however, is not higher than ten S cm^{-1}; therefore, these polymers have a rather weak effect on the μ of composites with multicomponent particles [1]. There exists a method for increasing the effective conductivity of the polymer coatings by incorporating nanoparticles of noble metals into PANI and PPy [24].

In this paper, we propose a method for obtaining a hybrid composite material in which multidomain particles of MnZn ferrite are coated by a polyaniline in the electrically conducting emeraldine form, that contains nanosized silver particles (MnZn–PANI/Ag). We investigate the magnetic and electrical properties of this hybrid composite and compare them with the properties of MnZn ferrite composites with polyaniline (MnZn–PANI) and with polyaniline and silver (PANI/Ag). We discuss the role of silver in the variation of electric transport in PANI/Ag and in the significant increase in the μ of MnZn–PANI /Ag.

2. Experimental

2.1 Materials and sample preparation

Ferrite particles were prepared by mechanical grinding of commercially available sintered 3000-NM MnZn ferrite cores (Ferropribor, Russia). The main characteristics of bulk ferrite and its powder are listed in Table 1. The MnZn–PANI/Ag hybrid composite is obtained by oxidation of aniline in the presence of MnZn ferrite powder. As an oxidant, we used silver nitrate. The oxidative polymerization was carried out at a stoichiometric mole ratio of [Ag^+]/[aniline] = 2.5, which corresponds to the reaction scheme shown in Fig. 1. The initial mass of aniline was 10 wt. % of the mass of the ferrite powder immersed in the reaction mixture, the concentration of aniline was 0.2 M. The reaction was carried out in a 1 M aqueous solution of nitric acid at room temperature. The PANI/Ag composite was obtained under the same experimental conditions as the MnZn–PANI/Ag composite but in the absence of ferrite [24]. According to the stoichiometry of the reaction, the content of silver should be 69 wt.% of the PANI/Ag

composite. Thermogravimetric analysis yields from 69 % to 70 % mass fraction of silver, which is in good agreement with theory.

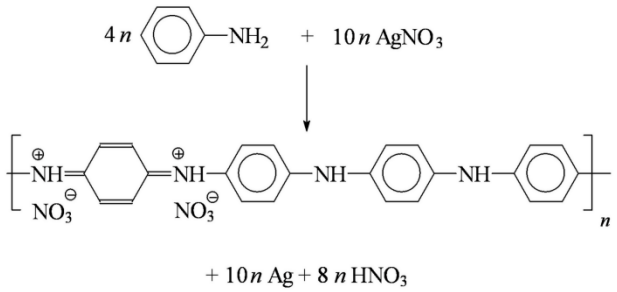

Fig. 1. Oxidation of aniline with silver nitrate in acidic medium.

Numerous experiments confirm that metal–polymer PANI–Ag composites prepared by the method in-situ polymerization of aniline with silver nitrate have constant composition and contain 70 wt.% of silver. Thus, at monomer loading of 10 wt.% and full conversion of the monomer, the MnZn–PANI/Ag should contain 33 wt.% of PANI–Ag. The degree of conversion is determined by the mass increment of the material during the reaction and is controlled by weighing the composite dried out to a constant weight [25]. In the current work, the degree of conversion was incomplete and amounted to 20–21 wt.% of PANI–Ag in the composite. The weight fractions of the ingredients were as follows: MnZn = 79–80 wt.%, Ag = 15 wt.%, and PANI = 6 wt.%. The volume fractions of the components in MnZn–PANI/Ag composite were calculated based on the density of the materials (ρ_{MnZn} = 4.8 g cm^{-3}, ρ_{Ag} = 10.5 g cm^{-3} and ρ_{PANI} = 1.3 g cm^{-3}) which yielded the following results: 73 vol.% of MnZn ferrite, 21 vol.% of polyaniline, and 6 vol.% of silver.

The MnZn–PANI composite was synthesized by the method described in [20]. The oxidation of aniline hydrochloride (0.2 M) with ammonium peroxydisulfate (0.25 M) was carried out at room temperature in an aqueous medium in the presence of ferrite powder. 10 wt.% of aniline hydrochloride with respect to the mass of MnZn ferrite were used.

2.3. Characterization

The magnetization curves of the samples in the form of powders were measured on a VSM 7407 Vibrating Sample Magnetometer (Lake Shore) at room temperature in air. The amplitude and the frequency of vibration were 1.5 mm and 82 Hz, respectively.

The complex magnetic permeability and dielectric permittivity spectra of materials were studied in the frequency range from 1 MHz to 3 GHz by the impedance method using an Agilent E4991A Impedance/Material Analyzer.

The conductivity was measured by a four-point van der Pauw method, using a Keithley 6517A as a current meter and a Multimeter Keithley 2410 as a source and voltmeter. To obtain the temperature dependence of conductivity, we measured the latter at a series of temperature points ranging from 233 K to 313 K with a step of ten degree with the use of an Espec SU 271 temperature chamber (Japan).

In order to measure the conductivity, the dielectric and magnetic spectra, polyaniline-coated ferrite particles were compressed into pellets and toroids at 200 MPa. The thickness of the toroidal samples with an inner diameter of 3.1 mm and an outer diameter of 8 mm was controlled to be less than 2 mm to avoid the skin effect.

The morphology of the samples was assessed using a JEOL JXA 733 Scanning Electron Microscope, a ZEISS Gemini Supra High Resolution Scanning Electron Microscope, and a JEOL 1200 Transmission Electron Microscope.

The UV–visible spectra of PANI dissolved in NMP were taken using an SF-56 spectrophotometer (LOMO, Russia) with a spectral range of 190–1100 nm.

3. Results and discussion

3.1. Composition and morphology of MnZn–PANI, PANI/Ag, and MnZn–PANI /Ag composites

3.1.1. MnZn–PANI

The oxidation of aniline hydrochloride with ammonium peroxydisulfate with a mole ratio of [oxidant]/[monomer] ≤ 1.25 yields PANI. By-products of the synthesis are ammonium sulfate and sulfuric acid, which are well soluble in water and easily washed away from the insoluble polymer [26]; therefore, PANI obtained under the action of peroxydisulfate does not contain other reaction products. Ammonium peroxydisulfate is a strong oxidizing agent with oxidation potential of +2.0 V; therefore, it completes the polymerization process within a few minutes at currently used 0.2 M concentration of aniline. In the presence of MnZn ferrite, the synthesis is speeded up still further, the acceleration being the greater, the greater the specific area of particles [10]. This fact indicates that a polymer layer grows directly on the surface of the ferrite particles. The sorption of intermediate aniline oligomers occurs predominantly where domain walls appear on the surface of the ferrite, and the initial PANI layer has a cellular structure with a cell size corresponding to the domain size [10, 22]. The further growth of polymer leads to the complete encapsulation of ferrite particles by a thin (about 100 nm) layer of PANI with electric conductivity of a few S cm^{-1}. The properties of nanostructured MnZn–PANI composite differ considerably from those of a mixed composite of the same quantitative composition. MnZn–PANI exhibits enhanced coercivity, high thermal stability of μ, and a shift in the resonance frequency to a high-frequency region compared with that of MnZn ferrite and its mixed composite with PANI. The magnetic properties of MnZn–PANI are attributed to the effect of induced magnetic anisotropy produced by magnetoelastic

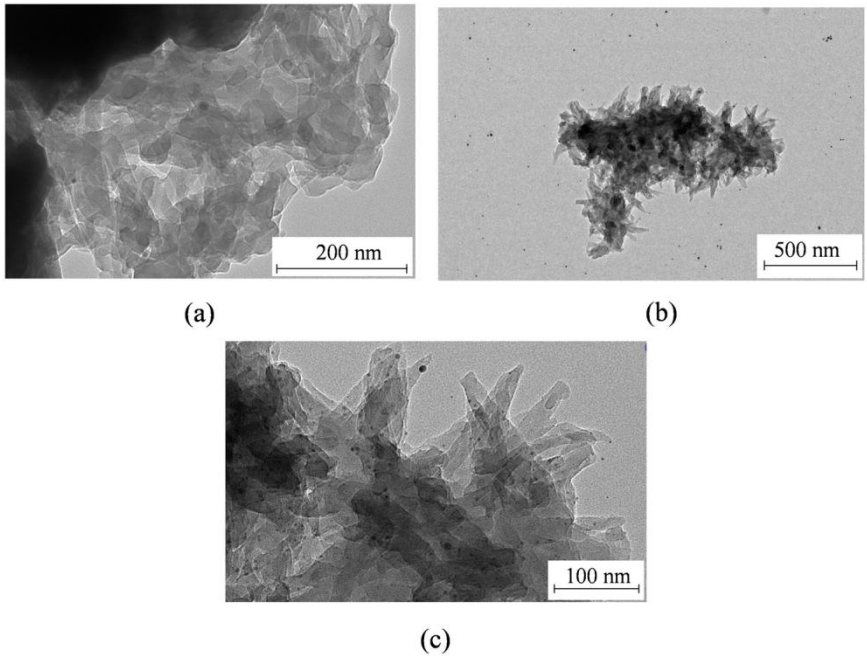

Fig. 2. Transmission electron microscope images of MnZn–PANI/Ag (a) and PANI/Ag (b, c).

stresses in ferrite particles due to the polyaniline coating [10, 22].

3.1.2. PANI/Ag

The synthesis of PANI/Ag occurs as a result of oxidation of aniline by silver nitrate; in this case, silver cations are reduced to metal, and the products of the reaction contain inclusions of metallic silver. As it was described above, the concentration of Ag in PANI/Ag composite is about 70 wt.% (~22 vol.%). Silver is dispersed in the polyaniline matrix in the form of spherical nanoparticles with a size ranging from 10 to ~ 60 nm (Fig. 2).

The final product of aniline oxidation in an acid medium (1 M nitric acid) is PANI. This is indicated by the characteristic absorption band at 630 nm in the UV spectra of the PANI/Ag (Fig. 3). Nevertheless, this is not only the presence of silver that makes the PANI/Ag composite different from the PANI obtained under the action of ammonium peroxydisulfate. The change in the nature of the oxidant leads to the change in the composition and morphology of polyaniline [25].

A silver cation is a weak oxidant having the oxidation potential of +0.80 V; therefore, oxidation in the presence of silver cations proceeds slower and is delayed at the stage of formation of aniline oligomers. At the initial stage of synthesis, within the first 100 h, the products of polymerization do not contain a polaron absorption band, which points to the oligomeric character of these products (Fig. 3, curve 1). The products of polymerization exhibit the characteristic spectrum of PANI only after 100 h of polymerization (Fig. 3, curve 2). Further, the mass of oxidation products increases faster and reaches a 30 % of yield in 300 h. As the conversion increases, the amount of PANI also increases; at the same time, silver particles become larger and agglomerate into clusters (Fig. 2b). The size of silver particle clusters ranges in a wide interval and reaches a value of several micrometers. The use of a weak oxidizer also changes the morphology of PANI itself. Under the accumulation of oligomers, which can be self-organized into one-dimensional columns, polyaniline is organized into a fiber-like structure, which makes it different from the granular morphology of PANI formed in the presence of ammonium peroxydisulfate.

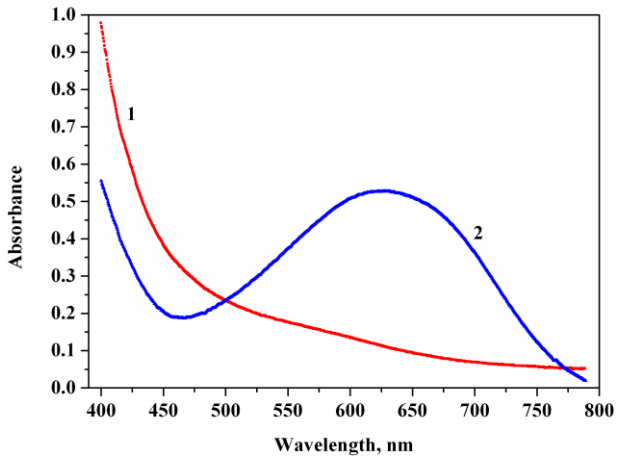

Fig. 3. The UV–visible spectra of the organic part of MnZn–PANI/Ag composite extracted by *N*-methylpyrrolidone; (1) up to 40 h of oxidation of aniline by silver nitrate in the presence of MnZn ferrite powder and (2) after 100 h of synthesis.

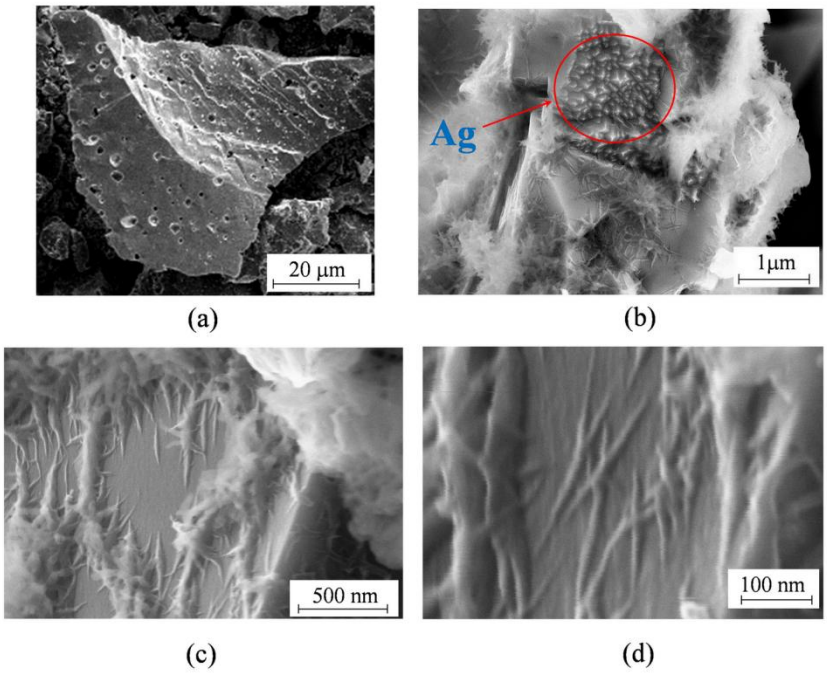

Fig. 4. Scanning electron microphotographs of a MnZn-ferrite particle (a), and high-resolution scanning electron microphotographs of a multicomponent MnZn–PANI/Ag particle after 100 hours of synthesis (b, c, d).

3.1.3. MnZn–PANI/Ag

The MnZn–PANI/Ag hybrid composite was obtained by oxidation of aniline by silver nitrate in the presence of ferrite powder in the reaction medium. In the presence of ferrite, the polymerization of aniline under the action of silver nitrate is accelerated in exactly the same way as it does in the presence of ammonium peroxydisulfate. The products of polymerization display the characteristic spectrum of PANI (an absorption band at 600 nm in the spectra of PANI base). They are formed as early as after 40 h, rather than 100 h, and the PANI yield after 300 h amounts to 45 wt. %.

Figure 4 presents the microphotographs of a MnZn ferrite particle (a) and of a multicomponent MnZn–PANI/Ag particle (b, c, d) collected after 100 h of synthesis. A ferrite particle has a morphology characteristic of particles obtained by grinding ferrite ceramic in a ball mill: irregular shape and clear-cut faces and surface with defects in the form of craters with diameter of up to 1 micrometre. During polymerization of aniline, a particle becomes coated by a discontinuous layer of PANI/Ag, and a considerable part of the ferrite surface remains free. On the surface of the ferrite, micrometre-sized rhombic cells are formed. Such a morphology of coating is similar to that of a PANI film that is formed on the ferrite surface at the initial stages of oxidative polymerization of aniline in the presence of ammonium peroxydisulfate [10, 22]. Just as in the case of oxidation by ammonium peroxydisulfate, it is reasonable to attribute this fact to the predominant sorption of paramagnetic oligomers of aniline and the formation of a polymer layer in regions where domain walls appear on the surface of the ferrite [10, 22]. Near the ferrite surface, the structure of the polymer coating is dense, whereas, away from the ferrite surface, it becomes looser.

High-resolution scanning electron micrographs show that, in the presence of ferrite, polyaniline reproduces the fiber-like morphology of the PANI/Ag composite (Fig. 4). The diameter and the length of the fibers amount to tens and hundreds of nanometers, respectively. The silver particles have two localization areas. Firstly, they are dispersed over the polymer matrix and, just as in the case of the PANI/Ag composite, they have a spherical shape and range in size from tens to hundreds of nanometers. As the conversion increases, the silver particles agglomerate into larger clusters that consist of many individual particles. Another localization area of silver is the surface of ferrite particles. The droplets of metal form areas that are concentrated at the defects of the ferrite (Fig. 4 b).

3.2. Electrical conductivity and dielectric properties

The highest conductivity (from 90 to 500 S cm^{-1}) is exhibited by the PANI/Ag composite (Table 2). The DC conductivity of PANI/Ag samples varies from sample to sample (for samples obtained in the same synthesis procedure), rather than from synthesis to synthesis. We made such a conclusion by measuring samples in three experimental series. The MnZn–PANI and MnZn–PANI/Ag composites exhibit much lower conductivity, which is attributed to the fact that

Table 2. Electric conductivity of PANI and its composites PANI/Ag, MnZn–PANI and MnZn–PANI/Ag at room temperature.

Sample	PANI	PANI/Ag	MnZn–PANI	MnZn–PANI/Ag
σ_{DC} (S cm^{-1})	2	90-500	0.008	0.002

conductivity in this case is determined by the conductivity of the ferrite, which amounts to 71–73 % of the composite volume, respectively.

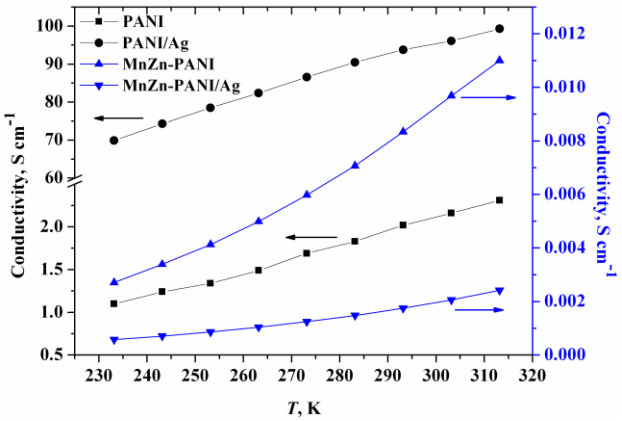

Fig. 5. DC conductivity of the samples of PANI, PANI/Ag (σ_{RDC} ~ 90 S cm^{-1}), MnZn–PANI/Ag, and MnZn–PANI as a function of temperature.

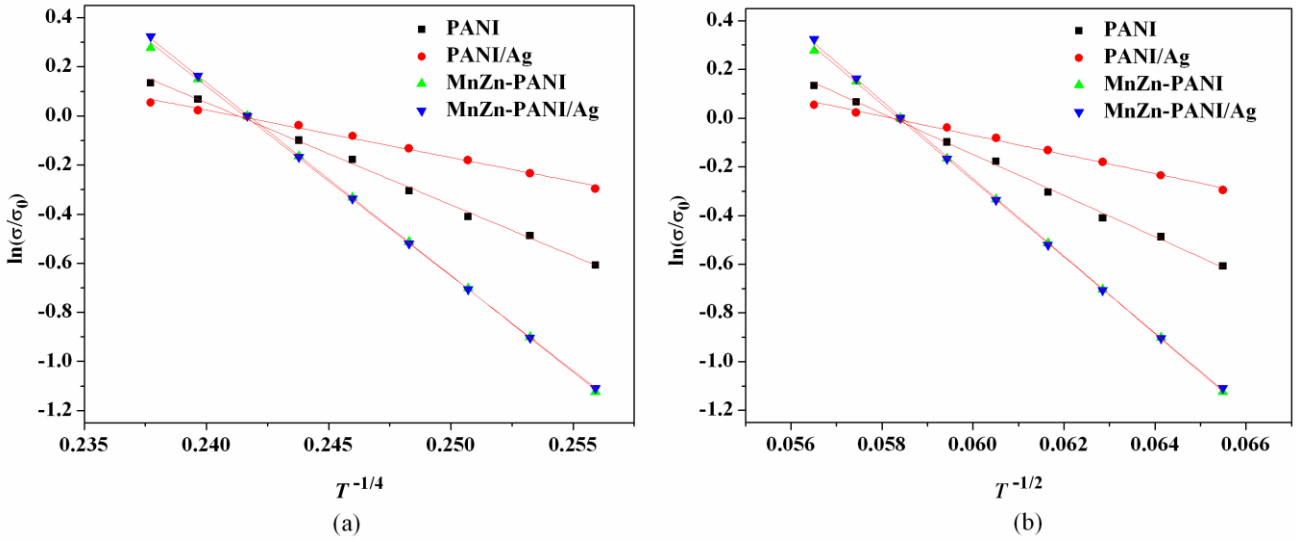

Fig. 6. The temperature dependence of conductivity in the coordinates ln (σ/σ_0) ~ $(1/T)^{1/4}$ and ln (σ/σ_0) ~ $(1/T)^{1/2}$ for PANI, PANI/Ag, MnZn–PANI/Ag and MnZn–PANI.

Figure 5 demonstrates the temperature dependence of the DC conductivity (σ_{DC}) of PANI and its composites with ferrite (MnZn–PANI, MnZn–PANI/Ag), as well as of low-conductivity (**σ_{RDC}** ~ 90 S cm^{-1}**)** samples of PANI/Ag. All the materials show positive temperature conductivity factor, which points to the semiconducting nature of charge transport due to the semiconducting properties of polyaniline and MnZn ferrite. Silver obviously does not participate in the conduction.

The approximation of the experimental functions $\sigma_{DC}(T)$ in the coordinates ln (σ/σ_0) ~ $(1/T)^{1/4}$ and ln (σ/σ_0) ~ $(1/T)^{1/2}$ (Fig. 6) shows good agreement with Mott law, which describes the charge transport in disordered media in terms of the variable-range hopping [27]: $\sigma = \sigma_0 \exp\left[-(T_0/T)^{\frac{1}{d+1}}\right]$, where $T_0 = \gamma_p \alpha^3 / N_F$, α is the localization radius, N_F is the density of states at the Fermi level, γ_p is a numerical coefficient, and d is the dimensionality of the system. The slope of the curves ln (σ/σ_0) ~ $(1/T)^{(d+1)}$ shows that PANI/Ag has the highest density of states at the Fermi level, which is responsible for its high conductivity. The temperature dependences of σ_{DC} of the MnZn–PANI/Ag and MnZn–PANI are imposed onto each other, which indicate that the σ_{DC} of these composites is determined by the conductivity of ferrite.

At the same time, a number of samples of PANI/Ag with conductivity of σ_{RDC} ~ 500 S cm^{-1} exhibit non-monotonic behavior of $\sigma_{DC}(T)$ with metallic type of conductivity below 290 K and semiconductor type above 290 K (Fig. 7). Similar temperature dependence of conductivity in the composites of polyaniline with silver was also observed [28, 29].

The instability of conductivity in the PANI/Ag composite and non-monotonic behavior of $\sigma_{DC}(T)$ observed in a number of samples is associated with the inhomogeneity of distribution of silver. The average concentration of silver in PANI/Ag is 22 vol.%, which corresponds approximately to the percolation threshold. Thus, the PANI/Ag composite composition is near the metal–insulator transition point, and its electrical properties are determined not only by the average content

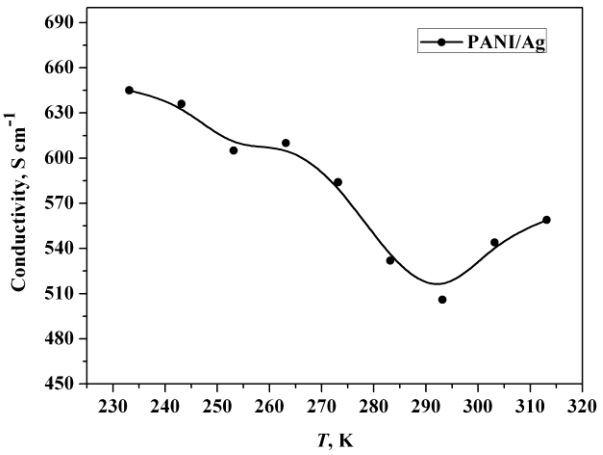

Fig. 7. DC conductivity of high-conductivity samples of PANI/Ag (σ_{RDC} ~500 S cm^{-1}).

of silver, but also by the distribution of conducting particles in the polymer matrix.

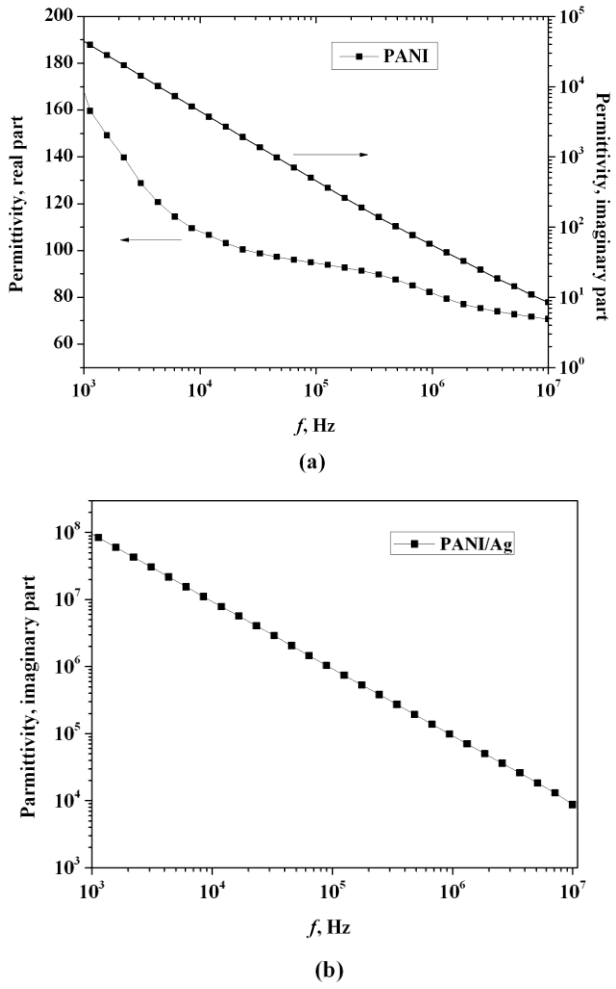

Fig. 8. Frequency dependence of the real and imaginary parts of the complex permittivity of PANI (a) and PANI/Ag (b).

One of characteristic features of composites near the metal–insulator threshold is a transition from insulating to conducting state under an electric field [30]. Figure 8 demonstrates the frequency dependence of the complex dielectric permittivity (ε) for PANI and the imaginary part of permittivity (ε'') for PANI/Ag. The values of the real part of permittivity (ε') of PANI/Ag cannot be measured by the impedance method; this, along with much higher value of ε'' of PANI/Ag compared to ε'' of PANI, indicates that PANI/Ag is in the percolated state and thus demonstrates the metallic type conductivity.

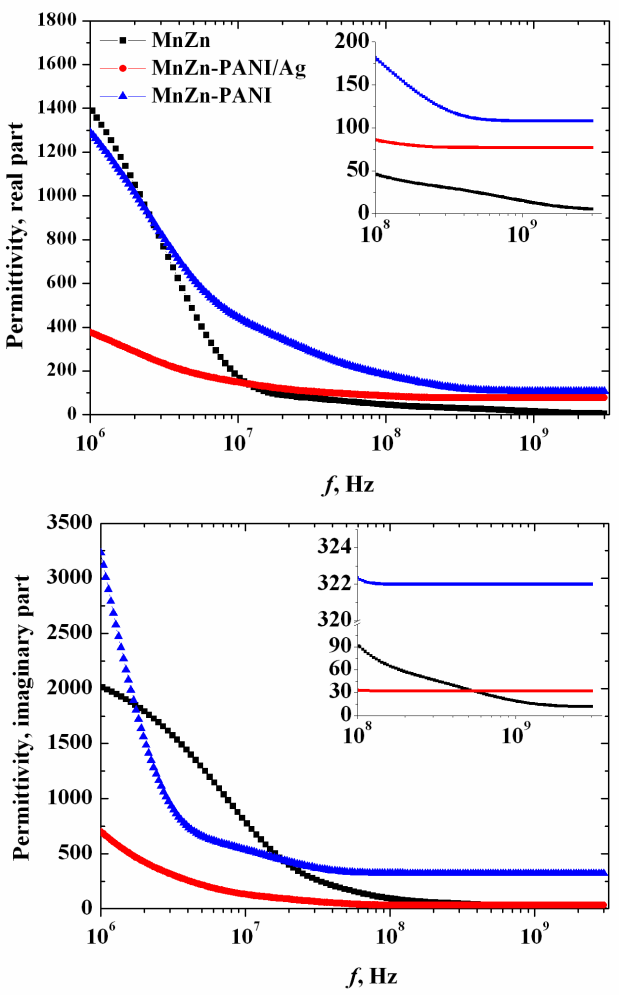

Fig. 9. Dielectric spectra of MnZn ferrite and its composites MnZn–PANI and MnZn–PANI/Ag.

The conducting coating of ferrite particles increases the ε' of the MnZn–PANI and MnZn–PANI/Ag composites (Fig. 9). This is caused by the displacement of charge carriers contained in PANI and PANI/Ag overlayers through the variable range hopping mechanism. The absolute value of ε depends on the density of charge carriers and their mobility, which is higher in MnZn–PANI compared to that in

Table 3. The main magnetostatic and dynamic characteristics of MnZn ferrite and of MnZn–PANI and MnZn–PANI/Ag composites.

Sample	Coercivity (Oe)	Saturation magnetization (emu g^{-1})	Remanence (emu g^{-1})	Resonance frequency f_R (MHz)	Static permeability μ'	Maximum of magnetic losses μ''_{max}
MnZn	2.2	77	0.15	1.3	1800/10^4 Hz	850
MnZn–PANI	6.5	67	0.55	580	11.7/10^6 Hz	4.5
MnZn–PANI/Ag	6.6	67	0.37	520	19.6/10^6 Hz	7.5

MnZn–PANI/Ag due to the uniformity of the conducting PANI coating on the surface of ferrite particles.

3.3. Magnetic properties

Figure 10 demonstrates the magnetization curves of MnZn ferrite and its composites: MnZn–PANI/Ag and MnZn–PANI. The numerical values of the saturation magnetization M_S, the coercivity H_C, and the remanent magnetization M_R for all these materials are shown in Table 3.

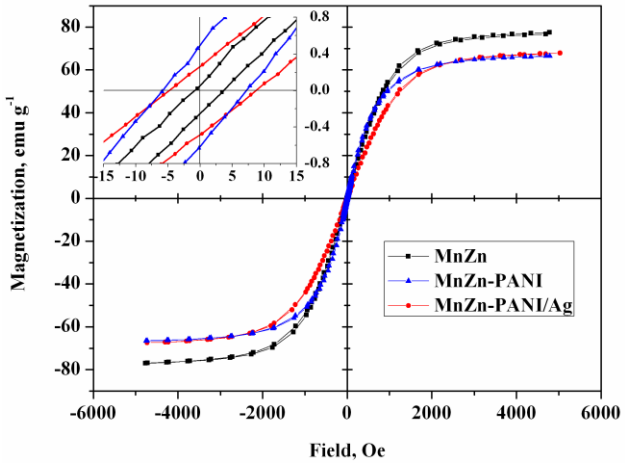

Fig. 10. Magnetization curves of MnZn ferrite and its composites MnZn–PANI and MnZn–PANI/Ag.

The saturation magnetization M_S of the composites is lower, while the H_C and M_R are higher than those of the ferrite. The increased values of the coercivity and the remanent magnetization of MnZn–PANI and MnZn–PANI/Ag composites cannot be explained solely by the effect of the demagnetization fields due to the non-magnetic component. According to our previous results [10, 22], the main contribution to the coercivity of the MnZn-PANI composite is made by the deceleration of domain-wall motion due to the polyaniline coating grown in a region where domain walls appear on the surface. The increase in the coercivity of MnZn-PANI/Ag is likely to be attributed to the same phenomenon, because the polymerization is significantly speeded up in the presence of ferrite, while the polyaniline coating exhibits a similar cellular character of distribution on the surface of ferrite.

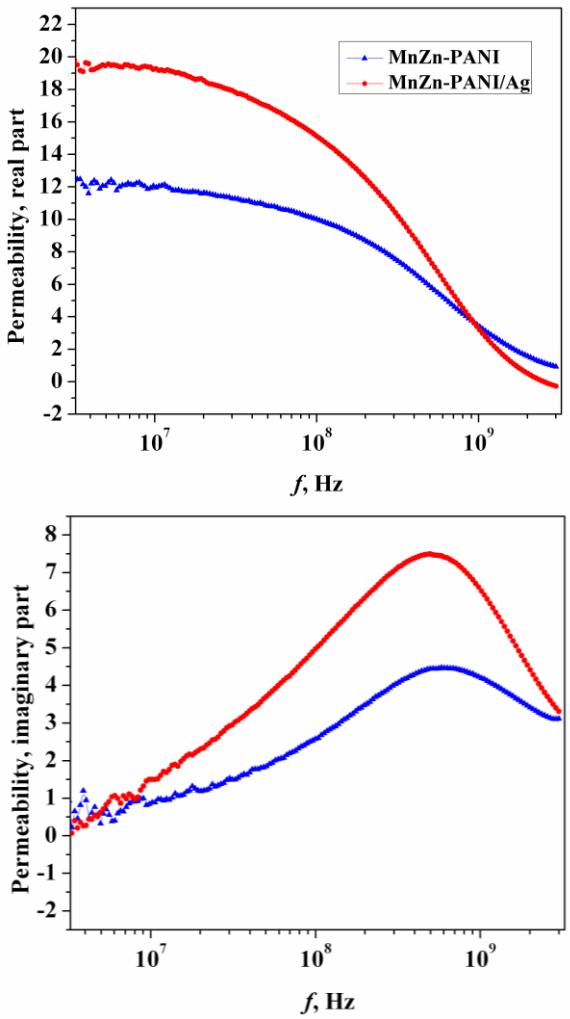

Fig. 11. Magnetic spectra of MnZn–PANI and MnZn–PANI/Ag composites.

The magnetostatic parameters of the MnZn–PANI/Ag and MnZn–PANI composites nearly coincide; however,

the values of μ of these composites are strongly different. Figure 11 demonstrates the magnetic spectra of composites in the frequency range from 10^6 to 3×10^9 Hz. The composites show small difference in f_R (Table 3); however, the magnetic losses of MnZn-PANI/Ag are one and a half times higher than those of MnZn–PANI. Moreover, MnZn–PANI/Ag exhibits one and a half times higher values of μ' in the frequency range $10^6 - 10^8$ Hz.

It is clear that the increase in μ is not related to the magnetic properties of PANI/Ag, which, just as PANI alone, exhibits linear dependence of magnetization on the external magnetic field, as it is characteristic of diamagnetic materials (Fig. 12). Moreover, the difference between the values of magnetic permeability of MnZn–PANI/Ag and MnZn–PANI is not associated with the shielding effect due to relatively high conductivity of PANI. The calculation of skin depth in radio-frequency band (Fig. 13) revealed that skin effect starts to manifest itself for MnZn–PANI at frequencies above 700 MHz, and, in MnZn–PANI/Ag, above 1.75 GHz, when the skin depth becomes comparable with the sample thickness (the sample thickness in the experiments ranged from 1.5 to 1.7 mm). Thus, we can assume that, below 700 MHz, i.e. in the region of ferromagnetic resonance frequencies of the composites, the effect of electromagnetic shielding on the magnetic permeability is negligible.

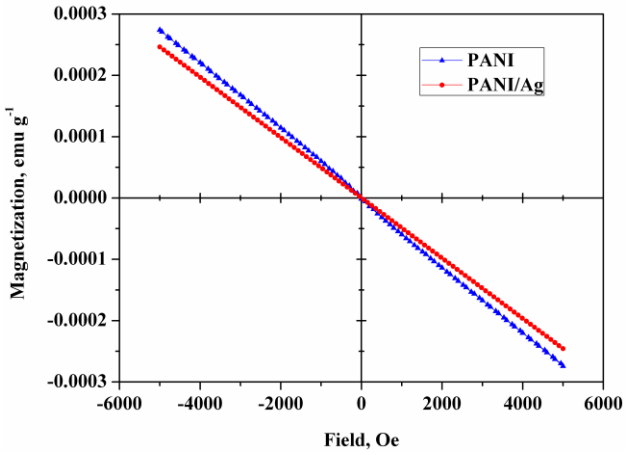

Fig. 12. Magnetization of PANI and PANI/Ag as a function of a DC magnetic field.

The increased value of the effective μ of the hybrid MnZn–PANI/Ag composite, especially the value of μ', points to the increased value of the effective internal magnetic field in this composite. Certainly, this is associated with the increased magnetic interaction between individual ferrite particles in the MnZn–PANI/Ag. The question is what is responsible for the increased magnetic interaction between particles in the composite.

A review of the literature has shown that the presence of silver often leads to the increase in μ of various magnetic materials. For example, the addition of 4.5 wt. % of Ag to hexaferrites with the structure of Co_2Z increased both μ' and μ'' in the high-frequency range (1–8 GHz) [31]. In [32, 33], the authors showed that, in the microwave band, both components μ' and μ'' of polymer composites filled with core–shell particles of nickel core, and silver shell are greater than those of a composite filled with nickel particles alone. However, these authors have not offered any explanation for the increased value of μ.

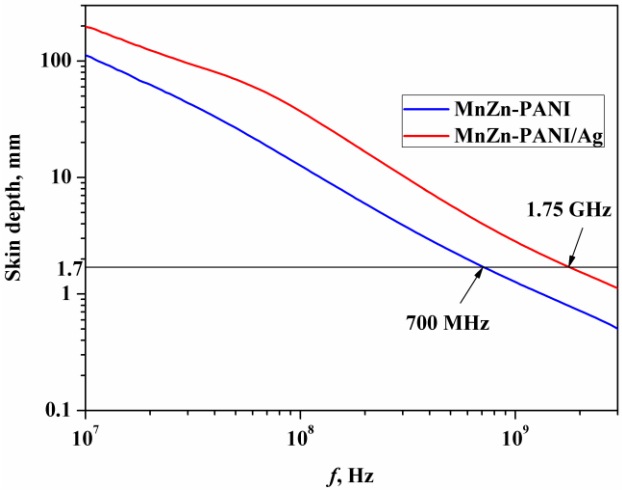

Fig. 13. Skin depth of MnZn–PANI and MnZn–PANI/Ag in radio-frequency band.

At the moment, the experimental data are not sufficient to explain unambiguously the reason for the increase in μ of a MnZn–PANI/Ag. In our opinion, one of possible reasons for the high values of μ is the surface phenomena near the MnZn–PANI/Ag interface. Such interfaces are characterized by the relation of charge-carrier transport in the conductor and the spin ordering of the magnetic phase [34, 35]. The charge transport in a PANI/Ag film under a high-frequency electromagnetic field may result in an increase in the exchange interaction between magnetic atoms in the surface layer of the MnZn ferrite due to the electron exchange between these atoms in the PANI/Ag film. The growth of exchange energy in a thin surface layer of ferrite leads to the increase in the energy of domain walls and, accordingly, to the decrease in the number of domains in a particle. Consequently, the decrease in the number of domains enhances the magnetic interaction between particles and increases the μ. More definite conclusions about the observed phenomenon require a more detailed experimental and theoretical analysis.

4. Conclusions

(1) The high-frequency magnetic permeability of a hybrid composite of MnZn ferrite with polyaniline significantly increases by the incorporation of silver nanoparticles into polyaniline.

(2) The conducting coating of ferrite particles increases the permittivity of the MnZn–PANI and MnZn–PANI/Ag composites but does not shield a radio-frequency field induced by the AC magnetization of a ferrite particle in the frequency range lying below 700 MHz, where the ferromagnetic resonance occurs.

(3) The increased permeability of MnZn–PANI/Ag is not related to the magnetic properties of PANI/Ag; the latter exhibits linear dependence of magnetization on the external magnetic field, which is characteristic of diamagnetic materials.

(4) We assume that the increased permeability of MnZn–PANI/Ag composite is attributed to the increased exchange interaction between magnetic atoms in the surface layer of the MnZn ferrite due to the electron exchange between these atoms in the PANI/Ag film.

Acknowledgments

This article was produced with the support of Operational Program Research and Development for Innovations co-funded by the European Regional Development Fund (ERDF) and national budget of Czech Republic, within the framework of project Centre of Polymer Systems (CZ.1.05/2.1.00/03.0111). The financial support of Czech Grant Agency (202/09/1626) and Program P1 of Russian Academy of Sciences is also appreciated. The authors are grateful to Prof. M. E. Kompan for the helpful discussion during the preparation of the manuscript.

References

[1] N. E. Kazantseva, Magnetic particle-filled polymer microcomposites, in: Sabu Tomas et al. (Eds.), Polymer Composites, vol. 1, Willey-VCH, Weinheim, 2012, pp. 613–669.

[2] Y. Pittini-Yamada, E.A. Perigo, Y. de Hazan, S. Nakahara, Permeability of hybrid soft magnetic composites, Acta Mater., 59 (2011) 4291–4302.

[3] R. Moucka, A.V. Lopatin, N.E. Kazantseva, J. Vilcakova, P. Saha, Enhancement of magnetic losses in hybrid polymer composites with MnZn-ferrite and conductive fillers, J. Mater. Sci., 42 (2007) 9480–9490.

[4] M. Anhalt, Systematic investigation of particle size dependence of magnetic properties in soft magnetic composites, J. Magn. Magn. Mater., 320 (2008) E366–E369.

[5] N.E. Kazantseva, A.T. Ponomarenko, V.G. Shevchenko, C. Klason, Magnetically textured composite materials as elements of electromagnetic wave absorbers, Electromagnetics, 20 (2000) 453–466.

[6] G.Q. Lin, Z.W. Li, L.F. Chen, Y.P. Wu, C.K. Ong, Influence of demagnetizing field on the permeability of soft magnetic composites, J. Magn. Magn. Mater., 305 (2006) 291–295.

[7] Z.W. Li, Z.H. Yang, R.F. Huang, L.B. Kong, Greatly enhanced permeability and expanded bandwidth for spinel ferrite composites with flaky fillers, IEEE Trans. Microw. Theory Tech., 58 (2010) 2794–2799.

[8] J.L. Mattei, M. Le Floc'h, Percolative behaviour and demagnetizing effects in disordered heterostructures, J. Magn. Magn. Mater., 257 (2003) 335–345.

[9] M. Anhalt, B. Weidenfeller, J.L. Mattei, Inner demagnetization factor in polymer-bonded soft magnetic composites, J. Magn. Magn. Mater., 320 (2008) E844–E848.

[10] V. Babayan, N.E. Kazantseva, I. Sapurina, R. Moucka, J. Vilcakova, J. Stejskal, Magnetoactive feature of in-situ polymerised polyaniline film developed on the surface of manganese-zinc ferrite, Appl. Surf. Sci., 258 (2012) 7707–7716.

[11] T. Kasagi, S. Suenaga, T. Tsutaoka, K. Hatakeyama, High frequency permeability of ferromagnetic metal composite materials, J. Magn. Magn. Mater., 310 (2007) 2566–2568.

[12] T.J. Fiske, H. Gokturk, D.M. Kalyon, Enhancement of the relative magnetic permeability of polymeric composites with hybrid particulate fillers, J. Appl. Polym. Sci., 65 (1997) 1371–1377.

[13] Y. Shen, Z.X. Yue, M. Li, C.W. Nan, Enhanced initial permeability and dielectric constant in a double-percolating $Ni_{0.3}Zn_{0.7}Fe_{1.95}O_4$-Ni-polymer composite, Adv. Funct. Mater., 15 (2005) 1100–1103.

[14] T. Kasagi, T. Tsutaoka, K. Hatakeyama, Complex permeability of permalloy-ferrite hybrid composite materials, J. Magn. Magn. Mater., 272 (2004) 2224–2226.

[15] B.W. Li, Y. Shen, Z.X. Yue, C.W. Nan, High-frequency magnetic and dielectric properties of a three-phase composite of nickel, Co_2Z ferrite, and polymer, J. Appl. Phys., 99 (2006) 123909.

[16] B. Drnovsek, V.B. Bregar, M. Pavlin, Numerical study of effective permeability of soft-magnetic composites with conductive inclusions, J. Appl. Phys., 105 (2009) 07D546.

[17] Y.I. Bespyatykh, N.E. Kazantseva, Electromagnetic properties of hybrid polymer composites, J. Commun. Technol. Electron., 53 (2008) 143–154.

[18] V.I. Ponomarenko, V.N. Berzhanskiy, V.N. Zhuravlev, Y.D. Pershina, Permittivity and permeability of a synthetic dielectric with metal-plated ferrite particles at microwave frequencies, Sov. J. Comm. Tech. Electron., 36 (1991) 133–136.

[19] X.F. Pan, H.G. Shen, J.X. Qiu, M.Y. Gu, Preparation, complex permittivity and permeability of the electroless Ni-P deposited strontium ferrite powder, Mater. Chem. Phys., 101 (2007) 505–508.

[20] N.E. Kazantseva, J. Vilcakova, V. Kresalek, P. Saha, I. Sapurina, J. Stejskal, Magnetic behaviour of composites containing polyaniline-coated manganese-

zinc ferrite, J. Magn. Magn. Mater., 269 (2004) 30–37.
[21] N.E. Kazantseva, Y.I. Bespyatykh, I. Sapurina, J. Stejskal, J. Vilcakova, P. Saha, Magnetic materials based on manganese-zinc ferrite with surface-organized polyaniline coating, J. Magn. Magn. Mater., 301 (2006) 155–165.
[22] V. Babayan, N.E. Kazantseva, R. Moucka, I. Sapurina, Y.M. Spivak, V.A. Moshnikov, Combined effect of demagnetizing field and induced magnetic anisotropy on the magnetic properties of manganese-zinc ferrite composites, J. Magn. Magn. Mater., 324 (2012) 161–172.
[23] I. Sapurina, J. Stejskal, The mechanism of the oxidative polymerization of aniline and the formation of supramolecular polyaniline structures, Polym. Int., 57 (2008) 1295–1325.
[24] N.V. Blinova, J. Stejskal, M. Trchová, I. Sapurina, G. Ćirić-Marjanović, The oxidation of aniline with silver nitrate to polyaniline-silver composites, Polymer, 50 (2009) 50–56.
[25] I.Yu. Sapurina, J. Stejskal, Oxidation of aniline with strong and weak oxidants, Russ. J. Gen. Chem., 82 (2012) 256–275.
[26] J. Stejskal, R.G. Gilbert, Polyaniline. Preparation of a conducting polymer (IUPAC technical report), Pure Appl. Chem., 74 (2002) 857–867.
[27] N.F. Mott, Conduction in non-crystalline materials. 3. Localized states in a pseudogap and near extremities of conduction and valence bands, Philos. Mag., 19 (1969) 835.
[28] C.Y. Lee, H.G. Song, K.S. Jang, E.J. Oh, A.J. Epstein, J. Joo, Electromagnetic interference shielding efficiency of polyaniline mixtures and multilayer films, Synth. Met., 102 (1999) 1346–1349.
[29] P. Bober, J. Stejskal, M. Trchová, J. Prokeš, Polyaniline-silver composites prepared by the oxidation of aniline with mixed oxidants, silver nitrate and ammonium peroxydisulfate: The control of silver content, Polymer, 52 (2011) 5947–5952.
[30] L.V. Lutsev, M.N. Kopytin, A.V. Sitnikov, O.V. Stognei, Properties of nanogranular metal-dielectric composites in strong electric fields and the cluster electronic states, Phys. Solid State, 47 (2005) 2169–2179.
[31] D. Lisjak, M. Drofenik, Thermal stability of (Co,Cu)Z-hexaferrite and its compatibility with Ag at 900 degrees C, J. Am. Ceram. Soc., 90 (2007) 3517–3521.
[32] C.C. Lee, D.H. Chen, Ag nanoshell-induced dual-frequency electromagnetic wave absorption of Ni nanoparticles, Appl. Phys. Lett., 90 (2007) 193102.
[33] C.C. Lee, Y.Y. Cheng, H.Y. Chang, D.H. Chen, Synthesis and electromagnetic wave absorption property of Ni-Ag alloy nanoparticles, J. Alloy. Compd., 480 (2009) 674–680.
[34] Y.H. Chu, L.W. Martin, M.B. Holcomb, M. Gajek, S.J. Han, Q. He, N. Balke, C.H. Yang, D. Lee, W. Hu, Q. Zhan, P.L. Yang, A. Fraile-Rodriguez, A. Scholl, S.X. Wang, R. Ramesh, Electric-field control of local ferromagnetism using a magnetoelectric multiferroic, Nat. Mater., 7 (2008) 478–482.
[35] A.N. Lachinov, N.V. Vorob'eva, V.M. Kornilov, B.A. Loginov, V.A. Bespalov, On the role of spin polarization of electrons in the effect of giant injection magnetoresistance in the Ni-polymer-Cu system, Phys. Solid State, 50 (2008) 1502–1505.

PAPER IV

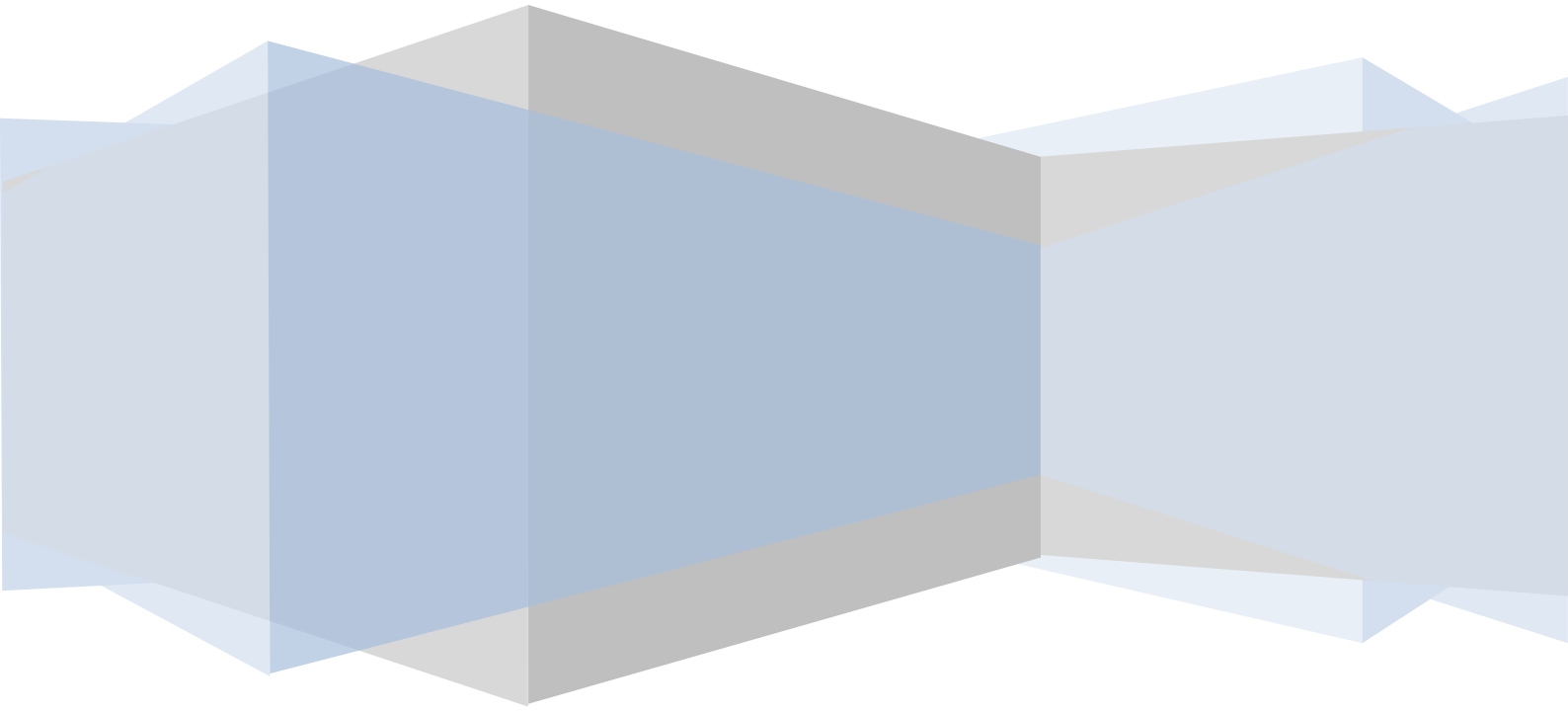

ISSN 1063-7834, Physics of the Solid State, 2012, Vol. 54, No. 12, pp. 2412–2418. © Pleiades Publishing, Ltd., 2012.
Original Russian Text © M.E. Kompan, I.Yu. Sapurina, V. Babayan, N.E. Kazantseva, 2012, published in Fizika Tverdogo Tela, 2012, Vol. 54, No. 12, pp. 2275–2281.

MAGNETISM

Electrically Conductive Polyaniline—A Molecular Magnet with the Possibility of Chemically Controlling the Magnetic Properties

M. E. Kompan[a, *], I. Yu. Sapurina[b], V. Babayan[c], and N. E. Kazantseva[c, d]

[a] *Ioffe Physical-Technical Institute, Russian Academy of Sciences, Politekhnicheskaya ul. 26, St. Petersburg, 194021 Russia*
** e-mail: kompan@mail.ioffe.ru*

[b] *Institute of Macromolecular Compounds, Russian Academy of Sciences, Bol'shoi pr. 31, St. Petersburg, 199004 Russia*

[c] *Centre of Polymer Systems, Tomas Bata University in Zlin, nam. T. G. Masaryka 5555, Zlin, 760 01 Czech Republic*

[d] *Fryazino Branch of the Kotelnikov Institute of Radio Engineering and Electronics, Russian Academy of Sciences, pl. Vvedenskogo 1, Fryazino, Moscow oblast, 141190 Russia*

Received May 14, 2012

Abstract—Different forms of an electrically conductive polymer, an organic semiconductor, namely, polyaniline, have been synthesized and characterized. The magnetization curves of the obtained forms have been analyzed. It has been found that, in the oxidized form, the material exhibits a magnetic hysteresis at room temperature. For polyaniline without a special doping with magnetic additives, this result has been obtained for the first time. The possibility of controlling the magnetic properties of the material by means of chemical treatment at the post-polymerization stage has been demonstrated.

DOI: 10.1134/S1063783412120190

1. INTRODUCTION

Organic magnets (or molecular magnets) ceased to be exotic at the end of the last century. A wide range of high-spin organic materials based on charge-transfer complexes [1] and nitric oxide radicals [2] has been synthesized. Aromatic amines have also been used as structural units of organic magnetic materials [3]. In recent years, the magnetic properties of high-molecular polyconjugated compounds—electrically conductive polymers, have been intensively investigated. It has been shown that representatives of this class, such as polyaniline, polypyrrole, and polythiophene, undergo a strong spin–spin interaction and hold much promise for the use in the design and fabrication of high-molecular organic magnets [4]. The development of materials of this type is not only maintained by interest expressed in fundamental problems of magnetism but also is a part of the general process of searching for new materials with an unusual combination of properties that open up new opportunities for engineering and technology [5]. The object of investigation in this work was an organic semiconductor, namely, polyaniline, which belongs to high-molecular aromatic amines.

2. GENERAL CHARACTERISTICS OF THE OBJECT OF INVESTIGATION

The polymer chain of the electrically conductive polyaniline (PANI) consists of regularly alternating benzene rings and nitrogen-containing groups (Fig. 1). This structure of the polymer chain ensured polyconjugation (regular alternation of single and double bonds). The polymer chain forms a zigzag lying in the same plane, so that the π-electron clouds overlap above and below the chain plane.

Charge carriers in this polymer are generated during its oxidation. The oxidation centers of PANI are nitrogen atoms that have a long electron pair not involved in chemical valence bonds. During the oxidation, i.e., the removal of one of the electrons, a positive charge arises in the polymer chain. The removal of an electron of the pair means the formation of an unpaired spin. It is the existence of such spins in the material that leads to unusual magnetic properties of PANI. The concentration of oxidized nitrogen atoms in PANI can vary from zero (which corresponds to the reduced leucoemeraldine form) to almost unity (the highest degree of oxidation—pernigraniline). The most stable form of PANI is emeraldine where every second nitrogen atom is oxidized (Fig. 1).

A positive charge that is generated during oxidation in the polymer backbone should be compensated (or, in chemical terms, stabilized) by a counterion. The best stabilizers of charge carriers in PANI are strong acids. The anion of the acid is coupled through the Coulomb interaction to the electron hole formed during the oxidation (i.e., upon the removal of an electron). The interaction of PANI with the acid is a reversible process and is referred to as protonation.

The removal of the stabilizing acid (deprotonation) leads to a decrease in the electrical conductivity and the concentration of unpaired spins. The processes of oxidation–reduction and protonation–deprotonation of PANI are reversible. This creates a wide variety of forms of polymers with different properties.

In this work, we have investigated the magnetic properties of PANI subjected to different chemical treatments at the post-polymerization stage, which was in different states of oxidation and protonation.

3. SAMPLE PREPARATION AND EXPERIMENTAL TECHNIQUE

3.1. Materials

In the preparation of samples, much attention was given to the purity of initial reactants and careful synthesis and subsequent procedures in order to prevent samples from being contaminated by magnetic impurities and to exclude changes in the morphology of the material. This is particularly important in the study of weak magnetism of unknown nature. In our opinion, a comparative study of the same initial material, whose magnetic properties change under chemical treatment without introducing impurities and without changing the morphology of the material, is most reliable.

In this work, we used Fluka reagents of the highest reagent grade, which contained impurity ions of magnetic metals in amounts no more that 1 mg/kg. In the synthesis of PANI and its post-polymerization treatment, metal utensils and appliances were not used. The samples were stored and transported in a sealed plastic bag.

3.2. Synthesis of PANI

Polyaniline was synthesized by oxidative polymerization of aniline [6]. Equal volumes of solutions of aniline (0.2 M) in sulfuric acid (0.2 M) and ammonium peroxodisulfate (0.25 M) in water were mixed at room temperature. The exothermic reaction accompanied by a change in color of the reaction mixture with the formation of a thick black-green precipitate of the polymer proceeded in a reaction flask for 10 min.

The main product of the polymerization was the protonated emeraldine form of PANI. By-products of the synthesis, ammonium sulfate and sulfuric acid, as well as small amounts of aniline oligomers, were removed by repeated washing of the precipitate in acidic aqueous media and methanol. The yield of the polymer was 95–98%. In what follows, this material will be referred to as sample *A*.

The deprotonated and oxidized (to pernigraniline) forms of PANI (hereinafter, sample *B* and sample *C*, respectively) were synthesized from the initial protonated emeraldine (sample *A*) by means of its chemical

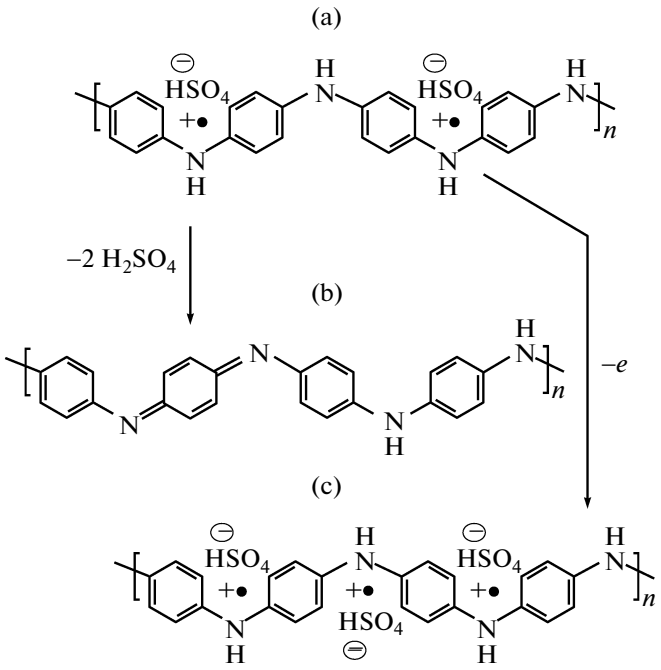

Fig. 1. Structural formulas of different forms of polyaniline: (*A*) protonated emeraldine form containing half of the oxidized nitrogen atoms; (*B*) deprotonated emeraldine with the lowest concentration of spins; and (*C*) protonated pernigraniline form of PANI, where more than half of the nitrogen atoms are in the oxidized state. Closed circles represent the unpaired electrons not involved in the covalent bonds. The plus sign means the presence of an effective positive charge (hole) localized on the nitrogen atom as a result of oxidation.

treatment. Figure 1 shows the structural formulas of samples *A*, *B*, and *C*.

The deprotonated emeraldine was prepared by alkaline neutralization of sulfuric acid bound with the polymer. For this purpose, the protonated form of PANI was treated with a 1 M aqueous ammonia solution, then washed with water, and dried under vacuum at a temperature of +60°C.

The oxidation of emeraldine to pernigraniline was carried out by the oxidation of a powder of the protonated emeraldine with a 0.5 M aqueous solution of ammonium persulfate in a 1 M sulfuric acid, followed by washing with a 1 M sulfuric acid solution and drying the sample under vacuum.

It can be seen from the structural formulas presented in Fig. 1 that the initial form is intermediate in the content of spins, the deprotonated emeraldine form, ideally, does not contain unpaired spins, and the oxidized pernigraniline form, on the contrary, contains a larger number of unpaired spins than the initial form.

This is also confirmed by the results of other authors. The study of different forms of PANI by the methods of EPR analysis with an organic spin-density standard showed that the content of unpaired spins

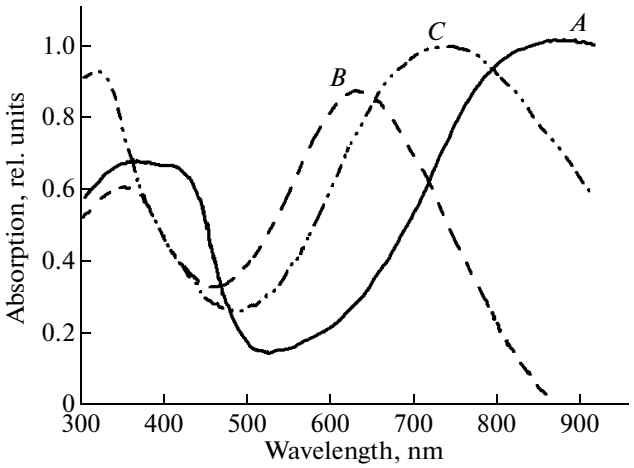

Fig. 2. Absorption spectra of the studied PANI forms in the visible region: (*A*) protonated emeraldine form, (*B*) deprotonated emeraldine, and (*C*) protonated pernigraniline.

depends on the degree of oxidation and protonation of the polymer [7].

The emeraldine form of PANI, which is doped to a level of 20%, has an electrical conductivity of 10^{-2} S/cm and contains 10^{20} spins/g. Upon further doping and with an increase in the electrical conductivity of the sample, spins have not been detected. The deprotonated emeraldine form contains 10^{16} spins/g, which at least four orders of magnitude smaller than that in the case of the protonated form. The content of unpaired spins in pernigraniline has not been determined experimentally, because the sample exhibits a high electrical conductivity.

4. CHARACTERIZATION OF THE MATERIALS UNDER INVESTIGATION

(1) The absorption spectra of the samples in the visible region were obtained for PANI thin films deposited on cover glasses by in situ polymerization [6]. The films were deposited on transparent substrates simultaneously with the synthesis of a powdered precipitate. Then, the films on glasses were subjected to the same chemical treatment as the samples of the PANI precipitate; consequently, the materials of the precipitate and films were identical. The absorption measurements were performed on a Specord M40 spectrometer.

The absorption spectra of different forms of PANI are presented in Fig. 2. These spectra contain the known bands of π–π^* transitions of the benzene rings in the range 300–380 nm, as well as the charge-transfer band of the cation radical center. In the spectrum of the protonated emeraldine, the maximum of this band is located at wavelengths exceeding 800 nm. The identification of the bands was performed in [8]. Upon deprotonation and oxidation, the band located in the range 600–900 nm (cation radical absorption) is shifted toward the high-frequency region. The spectroscopic data indicate the localization of charge carriers and agree with the results of the investigation of the electrical conductivity of the samples.

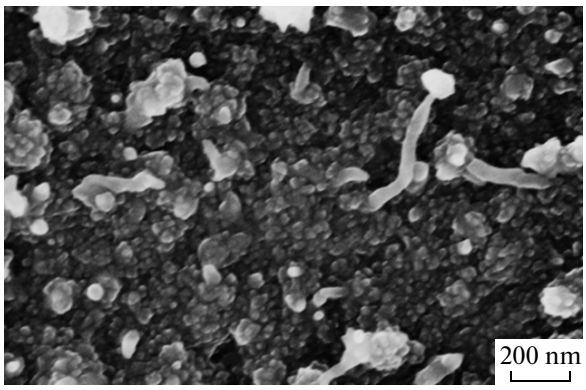

Fig. 3. Morphology of the protonated emeraldine form of PANI.

(2) The electrical conductivity of the materials was measured by the four-point probe method. The maximum electrical conductivity is observed in the protonated emeraldine. At room temperature, the electrical conductivity of the sample is equal to 5 S/cm. The electrical conductivity of the deprotonated emeraldine sample is nine orders of magnitude lower (3×10^{-9} S/cm). The oxidation of emeraldine and the transformation into the protonated pernigraniline form also decrease the electrical conductivity. The electrical conductivity of the samples measured by the four-point probe method is 6.4×10^{-4} S/cm.

(3) The morphology of the material at the microscopic level was determined using scanning electron microscopy. Figure 3 shows the micrograph of the emeraldine form of PANI immediately after the synthesis. The polymer has a granular structure that is typical of PANI. It consists of spherical granular particles approximately 30 nm in diameter with rare fiber inclusions of the same diameter. The particles are similar to each other and have a narrow size distribution. The post-polymerization methods used to transform PANI into other forms do not change the morphology of the polymer, which remains granular in all variants of chemical treatment.

Thus, the preliminary spectral and conductance investigations have demonstrated that, by means of simple chemical procedures, the initial material—the protonated emeraldine form of PANI—was transformed into the other two forms. The chemical treatment excluded the introduction of magnetic ions into the material and did not lead to a change in the morphology of the samples.

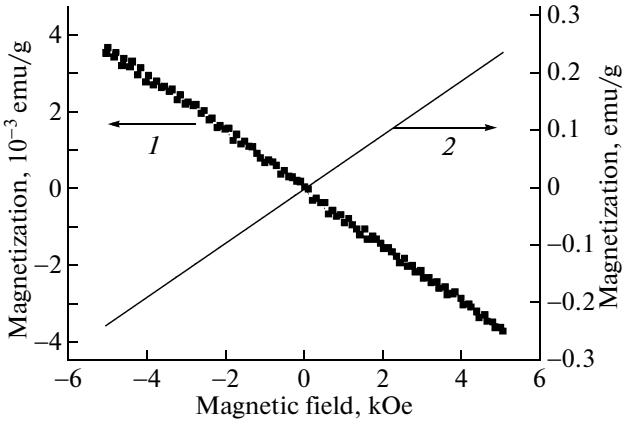

Fig. 4. Dependence of the magnetization on the external magnetic field for test materials: (*1*) diamagnetic NaCl and (*2*) paramagnetic $FeCl_2$.

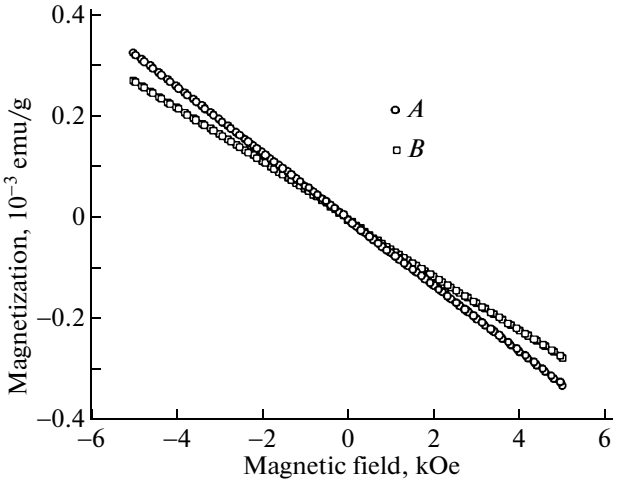

Fig. 5. Magnetization curves of diamagnetic samples of polyaniline (samples *A* and *B*).

5. MAGNETIZATION MEASUREMENTS

The magnetization curves for powdered polymer samples were measured on a Lake Shore VSM 7407 vibrating-sample magnetometer in magnetic fields up to 6 kG. The measurements were carried out at a frequency of 82 Hz, and the vibration amplitude was 1.5 mm.

For testing the operation of the setup, the magnetization was measured for well-known materials, namely, diamagnetic NaCl and paramagnetic $FeCl_2$. The results of these measurements are presented in Fig. 4.

It can be seen from this figure that both dependences—for the diamagnetic material and the paramagnet—are linear and pass through the origin of the coordinates, as should be expected for similar materials. The numerical values of the susceptibility of these materials are obtained from the slope of the straight lines and correspond to the tabular values.

6. MAGNETIC CHARACTERISTICS OF DIFFERENT FORMS OF PANI

The measured dependences of the magnetization M on the external magnetic field H are shown in Figs. 5 and 6. In magnetic fields above 1 kG, all samples have the dependence $M = M(H)$, which is characteristic of diamagnetic materials. The main differences in the samples are observed in magnetic fields below 1 kG.

The samples of the protonated (*A*) and deprotonated (*B*) emeraldine in weak magnetic fields have a negative static susceptibility, which is characteristic of diamagnetic materials.

Sample *C* (protonated pernigraniline) in weak magnetic fields is characterized by a magnetization hysteresis and a positive sign of the susceptibility (Fig. 6). The hysteresis region is shown on an enlarged scale in the inset to Fig. 6. It is usually assumed that this behavior of the magnetization corresponds to a ferromagnetic (or ferrimagnetic) material. In magnetic fields above 1 kG, as was already mentioned, the behavior of sample *C* corresponds to a diamagnetic material.

7. DISCUSSION OF THE RESULTS

The experimental results obtained in this work raise questions for which thus far there are only tentative answers. It is even more difficult to offer a general picture of the phenomena and interactions that were revealed in the experiment.

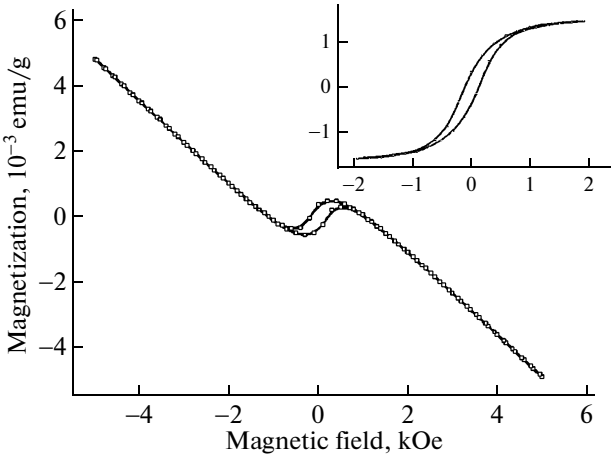

Fig. 6. Hysteretic behavior of the magnetization curve of sample *C*. The inset shows, on an enlarged scale, the hysteresis part of the magnetization curve in weak magnetic fields ($H < 2$ kOe), where the field-linear (diamagnetic) component is subtracted from the experimentally obtained dependence.

7.1. Diamagnetic Forms of PANI

The dependences of the magnetization on the external magnetic field for two of the studied materials have a diamagnetic character over the entire magnetic field range. These dependences are linear and have a negative slope (Fig. 5). The experimental dependences also exhibit small nonlinearities, the nature of which requires further investigation.

The diamagnetic response observed for sample *B* is beyond question. This modification of the material with the lowest spin content (ideally spinless) is obtained from the spin-containing form (sample *A*). An explanation is required by the diamagnetic character of the magnetization curve of sample *A* containing half of the oxidized nitrogen atoms and, therefore, a significant fraction of unpaired spins.

This character of the magnetization curve of sample *A* can be explained as follows. In the vast majority of cases, the filled electron shells exhibit diamagnetism. In the presence of unpaired spins, the sample becomes paramagnetic. The absolute values of the magnetic susceptibilities of paramagnets are usually one to two orders of magnitude greater than those of diamagnetic materials. Hence, in the case of the coexistence of these mechanisms, the contribution from paramagnetism, as a rule, considerably exceeds the contribution from diamagnetism and, consequently, is decisive; therefore, the magnetic susceptibility should change sign.

In the case of PANI, the main contribution to the diamagnetism is provided by benzene rings that make up the polymer backbone. Benzene rings, as well as naphthalene, anthracene, and other planar aromatic molecules, have an abnormally large diamagnetic susceptibility, which, on the average, is two orders of magnitude greater than the diamagnetic susceptibility of other materials. The corresponding values are given in the physical reference books. The reason for this anomaly is well known: in aromatic molecules under the action of an external magnetic field, there appear circular electric currents that are similar to Meissner currents in superconductors. It is this effect of the anomalous diamagnetism of aromatic molecules that is a consequence of the superconductivity of electrons on the intramolecular level, which exists up to temperatures above room temperature.

The abnormally high diamagnetism of benzene rings is responsible for the fact that the resulting susceptibility of high-spin samples of the *A* type is diamagnetic. For sample *A*, the paramagnetic contribution is smaller in magnitude than the contribution from the diamagnetic fragments of the polymer chain. The susceptibility of this form of PANI is the result of a partial compensation of the diamagnetism by a weaker paramagnetism. In turn, the susceptibility of sample *B* is largely determined by the diamagnetic mechanism, and, therefore, the dependence of the magnetization on the external magnetic field for sample *B* has a greater slope.

7.2. Manifestation of the Magnetically Ordered State

The hysteretic behavior of the magnetization of PANI was reliably observed in our experiments for the samples subjected to oxidation treatment. Since the majority of the molecular magnets synthesized so far exhibit magnetic properties at substantially lower temperatures [9], the observation of a magnetic hysteresis at room temperature is not trivial. It should be noted that, based on our data, the ferromagnetism and ferrimagnetism cannot be separated. Further, we will analyze the arguments of other authors.

There are published studies in which the hysteresis in the magnetization curve was obtained for the PANI doped with magnetic ions or radicals. For example, in [10], the ferromagnetism at room temperature was achieved in the PANI doped with a nickel salt. In [11], PANI was chemically bound to the TCNQ molecules forming stable high-spin radicals. This made it possible to reveal pronounced magnetic properties of the material at room temperature. The authors of [11] classified the obtained material as a ferrimagnet.

A direct comparison of our results with the results of other authors cannot be made because of the already mentioned diversity of PAMI. However, since the mechanism of magnetism of this material has not yet moved beyond the discussion at a qualitative level [1, 12], the assumption of the possible mechanisms of magnetic interactions, including those published by other authors, should be discussed.

If we consider the object—polyaniline—as one-dimensional chains of spins (unpaired electrons on the nitrogen atoms), the answer to this question is known. Ferromagnetism in this object cannot occur, regardless of the specific mechanism and the force of interaction between the spins, because the ordered state, in principle, cannot exist in one-dimensional systems [13].

Here, however, we note that a strict prohibition on the ordering in a one-dimensional system applies to the ideal infinite one-dimensional object, whereas a prohibition on a specific object can be illegal. We list the morphological factors that, in our opinion, can provide the lifting of the prohibition in our case. First of all, the real material consists of many chains of finite length, which are overlapped with each other and the interaction between which is not infinitesimal. This is enough to the above prohibition could not be propagated automatically to the test material.

Another mechanism that could also ensure the removal of the prohibition on ferromagnetism in a chain polymer was proposed in [14], where the authors considered the branching of chains and the formation of two-dimensional clusters due to this branching.

An even more important factor can be the existence of granular clusters with a dense quasicrystalline core.

This structure of PANI grains was revealed using high-resolution transmission electron microscopy in [15] (Fig. 7). The existence of granules in effect means that the test material is voluminous, and the observation of the ferromagnetism in it does not contradict the existing ideas.

An analysis of the quasicrystalline structure of the cluster cores could also provide an answer to the other questions. In particular, this can be one of the factors responsible for the smallness of the ferromagnetic component of the magnetic moment (which is determined from the amplitude of the hysteresis) as compared to the diamagnetic moment of the material. This relationship can be easily explained by the smallness of the mass of matter in the quasicrystalline cores as compared to the material as a whole.

The large distance between the localized spins is a factor that should hinder the emergence of magnetism. If we assume that, in PANI, elementary magnetic moments (spins) belong to unpaired electrons of the nitrogen atoms, the distance between them in the polymer chain should be more than 1 nm, which, at least, excludes a direct exchange interaction. At the same time, in the quasicrystalline regions, the nitrogen atoms of the adjacent chains are located at distances considerably shorter than the distances between the nearest neighbor nitrogen atoms of the same polymer chain. In [16], the author performed a detailed X-ray diffraction analysis of the crystalline forms of PANI and calculated the unit cell parameters. It was shown that the distance between the nitrogen atoms of the adjacent chains is 0.6 nm. This can also favor an enhancement of the exchange interaction between the magnetic moments.

In [12], it was suggested that the ferromagnetism of PANI can be provided by the concentration (kinetic) mechanism of the interaction between the magnetic moments. The idea of this mechanism goes back to the work by Vonsovskii et al. [17] and further was developed by Nagaev (see, for example, [18]). However, the experimental investigations carried out by Afanas'ev et al. [19] on the material with even more pronounced magnetic properties showed the smallness of the effect and, consequently, the failure of this mechanism for ferromagnetism at room temperature.

In the already mentioned work [11], the authors considered the exchange interaction between spins localized on the nitrogen atoms through the electron density of the benzene rings and pointed out that, in the material, there occur both the ferromagnetic and antiferromagnetic interactions. The authors of [11] believe that, in a particular material which they examined, there are nonequivalent oppositely directed magnetic sublattices, so that this material—the derivative of PANI—is a ferromagnet.

Similar ideas about the behavior of the magnetic moments in PANI were advanced in [20]. Among the other assumptions, the author of this work make a suggestion that the magnetic moments interact in undeformed parts of chains, so that there arise groups of electrons with different total moments other than the spin of a single electron.

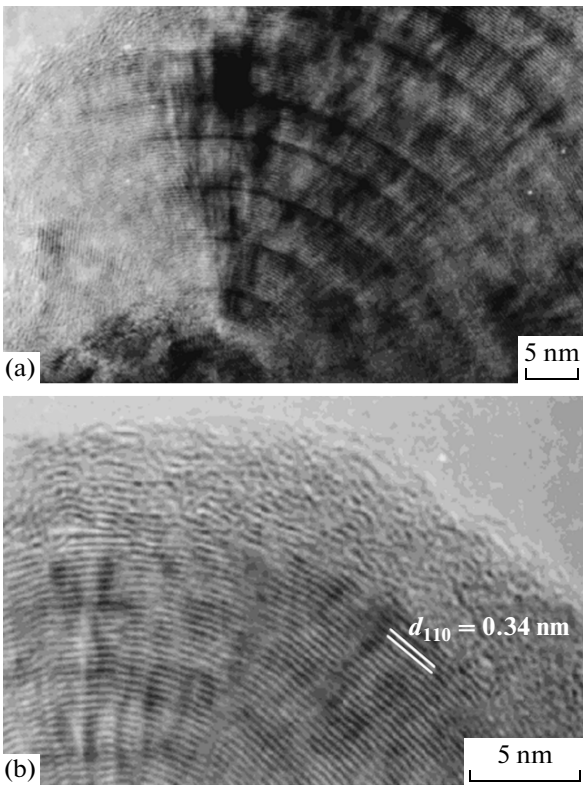

Fig. 7. Crystal structure of the central region of PANI granules (high-resolution scanning electron microscopy data). Reproduced from [15] with permission from ACS Publications.

Quite possibly, the assumption that, in different regions of the polymer chains, there exist exchange constants with positive and negative signs contains the key to the explanation of the magnetic behavior of PANI. Real polymers are not ideal straight line chains with fixed angles between the bonds and units. The deformation of the chains, which is associated with the type of supramolecular structure, has almost never been controlled by researchers. In turn, the variations in angles and distances can change values and even signs of the exchange integrals in some parts of the polymer chain. It is this change in the supramolecular structure that can be responsible for frequently encountered discrepancies between the results of different authors or for the changes in the magnetic properties of one of the PANI derivatives with time, which were revealed by the authors of [11]. In light of this suggestion, the magnetism of PANI most likely is not provided by a particular type of magnetism: the real material is a heterogeneous medium consisting of regions with different properties (from ferromagnetism to diamagnetism).

8. CONCLUSIONS

In this paper, we have demonstrated the possibility of controlling the magnetic properties of electrically conductive polyaniline by means of chemical treatment of the polymeric material. The character of the actions that change the magnetic properties of the material is not related to the introduction of magnetic additives, which proves the inherent character of the magnetism of polyaniline. In one of the three studied forms (the highest oxidation state—pernigraniline), it is characterized by a magnetically ordered state at room temperature. The revealed change in the magnetic properties is in qualitative agreement with the existing concepts of the nature and structure of this material.

At the same time, only hypothetical assumptions can be made regarding the mechanisms responsible for the magnetism of polyaniline. A much greater number of parameters needed to characterize the polymeric material as compared to conventional solid objects (for example, conformational characteristics of polymer chains) opens, in our opinion, the possibilities for much speculation and requires further investigation.

ACKNOWLEDGMENTS

This study was supported by the Ministry of Education and Science of the Russian Federation (state contract no. 16.516.6034), the Presidium of the Russian Academy of Sciences within the framework of the Basic Research Program no. 1, the Polymer Research Center (Czech Republic) (project CZ.1.05/2.1.00/03.0111), and the joint program of the State Budget of the Czech Republic and the European Regional Development Fund (ERDF).

REFERENCES

1. P. M. Allemand, K. C. Khemani, A. Koch, F. Wudl, K. Holezer, S. Donovan, G. Gruner, and J. D. Thompson, Science (Washington) **253**, 301 (1991).
2. R. Chialelli, M. A. Novak, A. Rassat, and J. L. Tholence, Nature (London) **363**, 147 (1993).
3. M. M. Wienk and R. A. J. Janssen, J. Am. Chem. Soc. **119**, 4492 (1997).
4. A. Ito, K. Ota, K. Tanaka, and T. Yamabe, Macromolecules **28**, 5618 (1995).
5. *Handbook of Conducting Polymers. Conjugated Polymers: Theory, Synthesis, Properties, and Characterization*, Ed. by T. A. Skotheim and J. R. Reynolds (CRC Press, Boca Raton, Florida, United States, 2007), p. 1238.
6. J. Stejskal, I. Sapurina, J. Prokes, and J. Zemek, Synth. Met. **105**, 195 (1999).
7. X.-L. Wei and A. J. Epstein, Synth. Met. **84** 791 (1997).
8. A. A. Nekrasov, V. F. Ivanov, and A. V. Vannikov, J. Electroanal. Chem. **482** (1), 11, (2000).
9. O. R. Nascimento, A. J. A. Oliveira Pereira, E. C. Correa, and L. Walmsley, J. Phys.: Condens. Matter **20**, 035215 (2008).
10. Y. Zhang, C. Zhu, and J. Kan, J. Appl. Polym. Sci. **109**, 3024 (2008).
11. N. A. Zaidi, S. R. Giblin, I. Terry, and A. P. Monkman, Polymer **45**, 5683 (2004).
12. G. I. Zvereva, B. Z. Lubentsov, A. P. Moravskii, O. A. Bochkova, V. N. Spektor, and A. A. Ovchinnikov, Dokl. Chem. **354** (4–6), 140 (1997).
13. L. D. Landau and E. M. Lifshitz, *Course of Theoretical Physics*, Vol. 5: *Statistical Physics: Part 1*, 2nd ed. (Nauka, Moscow, 1964; Butterworth–Heinemann, Oxford, 1968), p. 564.
14. N. Spitseris, R. E. Ward, and T. Y. Mayer, Macromolecules **31**, 3158 (1998).
15. L. Mezoralles, S. Folch, and P. Colomban, Macromolecules **32**, 8504 (1999).
16. J. P. Pouget, M. E. Jozefowicz, A. J. Epstein, X. Tang, and A. G. MacDiarmid, Macromolecules **24**, 779 (1991).
17. S. V. Vonsovskii, A. A. Samokhvalov, and A. A. Berdyshev, Helv. Phys. Acta **43**, 9 (1970).
18. E. L. Nagaev, Sov. Phys.—Usp. **18** (11) 863 (1975).
19. M. M. Afanas'ev, M. E. Kompan, and I. A. Merkulov, Sov. Phys. JETP **71** (6), 1086 (1976).
20. A. B. Kulikov and M. N. Shishlov, Russ. Chem. Bull. **59** (5), 912 (2010).